METAL TRANSPORT AND IMMOBILIZATION AT MINE TAILINGS IMPOUNDMENTS

MEND Associate Project PA-2

This work was done on behalf of MEND and sponsored by the Waterloo Centre for Groundwater Research, and Ontario Mineral Development Agreement (MDA), and Placer Dome Canada Inc.

March 1997

METAL TRANSPORT AND IMMOBILIZATION AT MINE TAILINGS IMPOUNDMENTS

FINAL REPORT

J.W. Molson, D.W. Blowes, E.O. Frind, J. G. Bain, M.D.Wunderly
Waterloo Centre for Groundwater Research
University of Waterloo

March 26, 1997

Ontario Mineral Development Agreement (MDA) (Cost-Shared 44/56)

PWGSC file No. 006SQ.23440-4-1263
Contract No. 23440-4-1263/01-SQ

Financial Codes 206-172-000000-307105-0468
WRI Award No. 2377701 Acct. No. 652-8433

Table of Contents

page

List of Figures

page

List of Tables

page

Executive Summary

A new simulation model, MINTOX, has been developed to provide a useful tool for predicting the behaviour of kinetic sulphide mineral oxidation within mine tailings impoundments, and for simulating the subsequent speciation and transport of oxidation products through the tailings and into downstream aquifers. MINTOX includes the major reaction sequences known to control the hydrogeochemistry at many base metal tailings sites. These processes include diffusion of oxygen into the unsaturated zone, diffusion of oxygen into the sulphide mineral grains, sulphide mineral oxidation, acid generation and release of iron, sulphate and heavy metals. Furthermore, the model can simulate the advective-dispersive transport of the mobilized species, accounting for equilibrium speciation and reactive processes including solid mineral dissolution and precipitation.

MINTOX has been tested in both one-dimensional and two-dimensional modes against observed field data from the Nordic Main tailings impoundment near Elliot Lake Ontario (Wunderly et al. 1995, 1996). Simulated depth profiles of selected species, including oxygen and pyrite content, agreed well with observed data, with discrepancies in other phases due primarily to the assumption of local geochemical equilibrium. The two-dimensional simulations of the Elliot Lake site showed reaction sequences and concentration levels consistent with observed or inferred behaviour. MINTOX has also been applied to simulate the geochemical processes occurring at the Nickel Rim tailings impoundment and has provided new insights into processes governing acid generation and neutralization.

Methods to control the rate of sulphide mineral oxidation, and the impact of AMD include reducing the rate of oxygen diffusion into the tailings using a moisture-retaining surface cover, and adding limestone to increase the buffer capacity. MINTOX has simulated the beneficial effects of these types of remediation measures at both the Elliot Lake and Nickel Rim sites. Simulations showed for example, that an increase in moisture content from background levels to

saturation effectively restricted the oxidation process. Since most oxidation occurs within 10 years of deposition however, covers appear best suited if emplaced immediately following tailings deposition.

Additional simulations for both the Elliot Lake and Nickel Rim sites were completed to address the effects of adding limestone to the tailings. At Elliot Lake, the results showed significant reductions in heavy metal concentrations as higher pH favours the precipitation of minerals which removes the aqueous species from solution. At Nickel Rim, higher pH and sulphate concentrations were also observed.

A 1D sensitivity analysis based on the Nickel Rim site showed significant variation with diffusion coefficients, fraction of sulphide mineral, initial grain size, and carbonate buffer mineralogy. The simulations suggested a need for determining the influence of spatial variation of physical and chemical properties on AMD evolution, and incorporating uncertainty in the interpretation of results.

SOMMAIRE

Un nouveau modèle de simulation, MINTOX, a été développé pour servir d'outil pour la prévision du comportement durant l'oxydation cinétique des minéraux sulfurés à l'intérieur des parcs à résidus et la simulation de la différenciation ultérieure des espèces et le transport des produits d'oxydation à travers les résidus et dans les formations aquifères d'aval. MINTOX inclut les principales séquences réactionnelles qui influencent l'hydrogéochimie des parcs à résidus de maints métaux de base. Ces processus incluent la diffusion de l'oxygène dans la zone non saturée, la diffusion de l'oxygène dans les grains de minéraux sulfurés, l'oxydation des minéraux sulfurés, la production d'acides et la libération de fer, de sulfates et de métaux lourds. En outre, le modèle peut simuler le transport par advection-dispersion des espèces mobilisées en tenant compte des espèces formées à l'équilibre et de processus de réaction comme la dissolution et la précipitation des minéraux solides.

MINTOX a fait l'objet d'essais comparatifs, tant en mode unidimensionnel qu'en mode bidimensionnel, avec les données recueillies sur le terrain au parc à résidus “Nordic Main” situé près d'Elliot Lake en Ontario (Wunderly *et al*. 1995, 1996). Les profils de concentration simulés des espèces choisies (entre autres, la teneur en oxygène et en pyrite) concordaient bien avec les données observées; les écarts trouvés dans d'autres phases ont été expliqués principalement en faisant l'hypothèse d'équilibres géochimiques locaux. Les simulations bidimensionnelles du site d'Elliot Lake ont montré des séquences réactionnelles et des teneurs qui correspondaient au comportement observé ou déduit. MINTOX a aussi été appliqué pour la simulation des processus géochimiques qui surviennent au parc à résidus Nickel Rim, ce qui a permis une nouvelle compréhension des processus qui régissent la production et la neutralisation des acides.

Les méthodes de limitation de la vitesse d'oxydation des minéraux sulfurés et des répercussions du DMA incluent la réduction de la vitesse de diffusion de l'oxygène dans les résidus au moyen d'une couverture de surface pour retenir l'humidité et l'addition de calcaire pour augmenter le pouvoir tampon. MINTOX a simulé les effets bénéfiques de ces types de mesures d'assainissement aux sites d'Elliot Lake et de Nickel Rim. Les simulations ont montré, par exemple, que le passage du degré d'humidité de fond à la teneur de saturation ralentit efficacement le processus d'oxydation. Cependant, comme la majorité de l'oxydation a lieu dans les 10 premières années qui suivent la mise en place des residus, la construction d'une couverture semble plus appropriée si elle est faite immédiatement après le dépôt des résidus.

D'autres simulations ont été complétées pour les sites d'Elliot Lake et de Nickel Rim de façon à tenir compte des effets de l'addition de calcaire aux résidus. À Elliot Lake, les résultats ont montré des réductions significatives des concentrations de métaux lourds, car une augmentation du pH favorise la précipitation des minéraux qui éliminent les espèces aqueuses de la solution. À Nickel Rim, des augmentations du pH et des concentrations de sulfates ont aussi été observées.

Une analyse de sensibilité unidimensionnelle au site de Nickel Rim a montré une variation

significative des coefficients de diffusion, de la fraction de minéral sulfuré, de la granulométrie initiale et du pouvoir tampon en carbonates des minéraux. Les simulations semblent indiquer un besoin de déterminer l'effet de la variation spatiale des propriétés physiques et chimiques sur l'évolution du DMA et l'incorporation de l'incertitude dans l'interprétation des résultats.

Introduction

Acid mine drainage (AMD), which is often characterized by low pH and high dissolved concentrations of heavy metals, poses a potentially serious threat to Canada's water resources. The scale of the problem is highlighted in the estimation by Feasby and Jones (1994) that about 7 billion tonnes of metal-mine and industrial mineral tailings exist in Canada for which remediation costs range from $2 to $5 billion.

The characteristics of AMD can vary widely, depending on several factors including tailings mineralogy, grain size, degree of saturation and presence of buffering minerals. The oxidation processes are generally kinetically controlled and the oxidation products can react with tailings and aquifer waters through redox, ion-exchange and mineral precipitation/dissolution reactions. Furthermore, tailings impoundments can be several square kilometres in area and exhibit a large spatial variability in properties.

Quantitative prediction of AMD water quality can therefore be quite difficult and subject to much uncertainty. Indeed, we are in many respects still defining conceptual models of AMD generation, models which would greatly benefit from quantitative analysis. Numerical simulation models can potentially offer significant insight into such processes, and can help evaluate the effectiveness of proposed remediation measures.

This report outlines the development of a new simulation tool with which the generation and evolution of AMD can be quantitatively evaluated. The new model, MINTOX, can simulate the diffusion of oxygen into a tailings impoundment, the subsequent kinetic oxidation of sulphide minerals, the speciation and reactions of the oxidation products, and their transport within and downgradient from the source.

The development of the MINTOX model began with MINTRAN, a 2D multicomponent reactive transport model (Walter et al., 1994a). MINTRAN is based on a coupling of two primary modules: PLUME2D, a 2D advective-dispersive mass transport model for a single component, and MINTEQA2, an equilibrium geochemical speciation code (Allison et al., 1990).

Wunderly et al. (1996) developed a 1D model, PYROX, to simulate oxygen diffusion coupled with kinetic sulphide mineral oxidation within a partially saturated porous medium. Finally, the PYROX model was coupled to MINTRAN to form MINTOX.

Further developments related to these models (outside the scope of the current contract) include MINHEAT/3D, a 3D version of MINTRAN coupled with heat transport and temperature-dependent reactions (Molson et al., 1994), and a new version of MINTOX developed for application to large overburden spoil piles in Germany (Gerke et al., 1997). A fully coupled, 3-phase kinetic reactive transport model is currently under development (Mayer, 1996).

MINTOX is applied here to two field-scale tailings sites: first, to a simplified analogue of the Nordic impoundment near Elliot lake, and secondly to the Nickel Rim impoundment near Sudbury. The Elliot Lake example introduces the oxidation source as a boundary condition and illustrates how heavy metals can become immobilized in carbonate-bearing tailings. The MINTOX application to Nickel Rim incorporates the kinetic oxidation process and provides graphic insight into the geochemical evolution of acid mine drainage. Finally, a sensitivity analysis based on the Nickel Rim site examines the influence of the major parameters controlling the sulphide oxidation process.

Theoretical Development

MINTOX solves the coupled processes of sulphide mineral oxidation, equilibrium geochemical speciation and advective-dispersive mass transport within a porous medium. Sulphide oxidation is treated as a kinetic process since it is slow relative to typical groundwater flow rates while geochemical speciation can be considered an equilibrium process since, for the reactions considered in this study, they are relatively fast compared to flow rates. A more detailed account of the modelling approach can be found in Walter et al. (1994a,b) and Wunderly et al. (1996).

Advective Dispersive Multicomponent Transport

We begin by considering the transport of N_c aqueous components by advection and dispersion. The partial differential equation expressing mass continuity in the overall system and governing the advective-dispersive transport of the aqueous part of component k is (Bear, 1972):

$$\frac{\partial C_k}{\partial t} - \frac{\partial}{\partial x_i}\left(D_{ij}\frac{\partial C_k}{\partial x_j}\right) + \frac{\partial}{\partial x_i}\left(v_i C_k\right) - R_k = 0 \qquad k = 1, \ldots, N_c \qquad (1)$$

where x_i are the cartesian coordinates (L), t is time (T), v_i are the vector components of the average fluid velocity (L/T), D_{ij} represents the hydrodynamic dispersion tensor (L^2/T), which depends on the longitudinal and transverse dispersivities α_L and α_T (L) (for definition see Bear, 1972), and R_k is the chemical source/sink term (M/M/T) representing the changes in aqueous component concentrations.

The solid-phase part of component k (see eq. 1), which remains stationary, is also governed by mass conservation. The equation is:

$$\frac{\partial S_k}{\partial t} - R_k^S = 0 \qquad k = 1, \ldots, N_c \tag{2}$$

where R_k^S represents the change in solid component concentration (M/M/T) due to precipitation/dissolution and sorption/desorption reactions.

The boundary conditions for each aqueous component *k* are either of the Dirichlet type, with specified concentrations along the boundary, or the Cauchy type, with specified mass flux along the boundary. A complete set of boundary conditions and initial conditions are required for each aqueous component, and an initial condition is required for each solid phase component. The formulation of the physical boundary conditions is discussed by Huyakorn and Pinder (1983).

The above equations are incorporated in the proven 2D advective-dispersive transport model PLUME2D, which was previously applied to simulate reactive transport with two aqueous components (Frind et al., 1990). This model serves as the physical transport module for MINTOX. The groundwater flow velocity field (v_i in equation (1)), assumed to be at steady state, can be obtained from any standard flow model, provided the grid and boundary conditions are compatible. Alternatively, a uniform flow field may be specified within MINTOX; further details can be found in the user guide provided in Appendix B.

Geochemical Speciation

The transport equation (1) is written for N_c aqueous components which are defined as the minimum number of species that uniquely describe the chemical system (Mangold and Tsang, 1991). We assume a representative elementary volume (REV) that is isolated from the rest of the system and within which the total mass of the chemical substances remains constant during speciation.

Each component can exist in either the aqueous phase or the solid phase. Assuming N_c components, the total component concentration T_k (M/M) of component k can be defined as the sum of the aqueous-phase part C_k and the solid-phase part S_k of the concentration of component k:

$$T_k = C_k + S_k \qquad k = 1, \ldots N_c \tag{3}$$

For clarity, we will refer to C_k as the aqueous component concentration (moles/1000g H_2O) and to S_k as the solid concentration (moles/1000g H_2O) of component k. Assuming dilute concentrations, we can consider 1000g to equal 1L of water. In the case of the aqueous components, the unit of concentration is molality, while in the case of the solid component, it represents moles of solid per litre of water.

The component mass remains constant, regardless of the distribution between chemical species in both the aqueous and solid phases. The aqueous and solid phases of component k are related to the corresponding n_a aqueous and n_s solid-phase species through the stoichiometric mass balance equations:

$$S_k = \sum_{l=1}^{n_s} b_{lk}\, s_l \qquad k = 1, \ldots N_c \tag{4}$$

$$C_k = \sum_{l=1}^{n_a} a_{lk}\, c_l \qquad k = 1, \ldots N_c \tag{5}$$

where c_l is the concentration of species l in the aqueous phase, s_l is the concentration of species l in the solid phase, a_{lk} is the stoichiometric coefficient of component k in aqueous species l, and b_{lk} is the stoichiometric coefficient of component k in solid species l.

The distribution of the species included in the component concentrations is determined by nonlinear mass-action equations, with one equation for each chemical species. The mass-action equation for the aqueous-phase component is of the form:

$$Kc_l = \chi_l \prod_{k=1}^{N_c} \chi_k^{-a_{lk}} \qquad l = 1, \ldots, n_a \qquad (6)$$

where Kc_l is the equilibrium formation constant for species l, χ_k is the activity of component k (moles/1000g H_2O), and χ_l is the activity of species l (moles/1000g H_2O).

The activities χ_l in equation (6) are related to the species concentrations c_l in (4) through the individual ion activity coefficients γ_l by the approximation

$$\chi_l = \gamma_l c_l \qquad (7)$$

The activity coefficients γ_l can be calculated using an empirical equation, for example the extended Debye-Hückel equation (Stumm and Morgan, 1981).

Geochemical equilibrium speciation in MINTOX is performed using the model MINTEQA2 (Allison et al., 1990), which is a based on the earlier model MINTEQ (Felmy et al. 1983). MINTEQA2 includes a comprehensive set of chemical reactions including chemical speciation, acid-base reactions, mineral precipitation-dissolution, oxidation-reduction, and adsorption reactions. The ion-association equilibrium-constant approach, which is valid for ionic strengths of 0 - 0.5, is used to represent the geochemical reactions. The ion-association model involves the three sets of quantities discussed above: the masses of aqueous species and complexes, the equilibrium constants relating these complexes in solution, and the individual ion-activity coefficients for each species. The nonlinear algebraic equations (4) to (7) linking these quantities are solved for the individual ion activities, which are in turn used to calculate the

component concentrations at equilibrium. Activity coefficients are calculated using the WATEQ, extended Debeye-Hückel, or Davies equations. The Newton-Raphson iterative technique is used for the numerical solution. Below, we will briefly review the important reaction types most relevant to the simulation of AMD.

Redox and Acid/Base Reactions

MINTEQA2 allows the oxidation-reduction potential to be either specified by fixing the solution pe value, or calculated using the activities of electroactive species in differing redox states through the Nernst equation:

$$E_h = E^0 + \frac{RT}{nF} \ln\left(\frac{\chi_{ox}}{\chi_{red}}\right) \quad (8)$$

where E_h is the solution potential relative to the standard hydrogen electrode, E° is the standard potential for the reaction, R is the universal gas constant, T is temperature (Kelvin), n designates electron equivalents transferred, F is the Faraday constant, and χ_{red} and χ_{ox} are the activities of the reduced and oxidized species, respectively. The E_h is related to the pe through

$$\text{pe} = \frac{nF}{RT} E_h \quad (9)$$

Use of the Nernst equation requires that the initial distribution of the specified redox couples be known before the chemical equilibrium problem is solved. This distribution can be determined from the initial solution component chemistry and the solution pe. MINTEQA2 permits selection of redox couples that are maintained in equilibrium with the pe while keeping other electroactive species independent of the pe. Thus, the multivalent species can be reacted with their respective solid mineral phases without requiring interactions with other multivalent species.

Mineral Precipitation and Dissolution

Mineral precipitation and dissolution reactions can play controlling roles in the evolution of acid mine drainage by buffering low-pH tailings waters and by attenuating heavy metals. These types of reactions are described by mass-action equations for a solid and the reacting ions. The general form of the dissolution reaction of a solid is:

$$A_aB_{b(s)} \leftrightharpoons aA_{(aq)} + bB_{(aq)} \qquad (10)$$

where *(aq)* refers to the aqueous phase and *(s)* to the solid phase. This reaction is described by a solubility product of the form:

$$\frac{[A]^a[B]^b}{[A_aB_b]} = K_{sp} \qquad (11)$$

where the left hand side is the ion activity product, *I.A.P.* ($[A_aB_b]$=1 for a pure solid), and the right hand side, K_{sp}, is the solubility product which is an equilibrium constant specific to a solid. At equilibrium, K_{sp} and *I.A.P.* are equal. When a system is not at equilibrium, the degree of disequilibrium can be expressed through the saturation index (*S.I.*):

$$S.I. = \log\left(\frac{I.A.P.}{K_{sp}}\right) \qquad (12)$$

When *S.I.* > 0, the solution is supersaturated with respect to that solid phase which will tend to precipitate; when *S.I.* = 0 the mineral and the solution are in equilibrium; and when *S.I.* < 0, the solution is undersaturated with respect to the solid which will tend to dissolve.

The solid phases in MINTEQA2 may be classified according to three types: (a) solids that are in infinite supply (reacted to equilibrium), (b) solids in finite supply, where the initial mass of solid must be specified (moles of solid per litre of pore water), and (c) possible solids that may precipitate if the solution becomes supersaturated. Within an individual chemical simulation, the designation may switch between the last two solid types. Switching solid types is well suited to the coupled geochemical-reaction, solute-transport problems common to AMD where sharp changes in solid-phase concentrations can occur.

The selection of thermodynamically stable solids from the array of solids allowed to precipitate or dissolve is calculated by treating the *S.I.* (eq. 12) as an inequality. Each solid is ranked for its tendency to precipitate by dividing the *S.I.* by the number of ions in the precipitation reaction. After ranking, the solid with the highest value is allowed to precipitate. All of the remaining solids are then ranked again and sequentially precipitated or dissolved until all of the solids considered are undersaturated. If the mass of a previously precipitated solid becomes negative, that solid is allowed to dissolve and the solution procedure continues.

Numerical Solution Approach: Coupled Transport/Chemistry

The two steps of the coupled transport/chemistry processes can be visualized as a physical step, where the aqueous components are advected and dispersed through space and time without reacting, and a chemical step, where the components react instantaneously without being transported. The approach is similar to that used in mixing-cell models (Schulz and Reardon, 1983; Appelo and Willemsen, 1987). A review of different approaches of solving coupled reactive transport systems is provided by Steefel and MacQuarrie (1996). Fully coupled solution approaches, for example, are becoming more common because they often show improved convergence behaviour for more difficult problems. High demands on memory requirements, however, can impede their application to large scale systems.

Assuming local equilibrium over the REV, the chemical step restores the chemical equilibrium that has been perturbed through the transport step, but does not affect the transport step itself. The physical-chemical coupling is therefore linear, although the chemical reactions themselves remain nonlinear. The chemical equilibration would logically be allowed to take place at the end of the time step, at time ($t + \Delta t$).

With this concept, the coupled two-step algorithm takes the form:

- Step 1 (physical):

$$\frac{\left(C_k^{phys} - C_k^{n}\right)}{\Delta t} = L\left(C_k\right)^{n+1/2} \qquad k = 1, ..., N_c \qquad (13)$$

- Step 2 (chemical):

$$\left(C_k^{n+1} - C_k^{phys}\right)\delta(t+\Delta t) = R_k^{equil}\,\delta(t+\Delta t) \qquad k = 1, ..., N_c \qquad (14)$$

where C_k^{phys} is the concentration at the end of the physical step, where n and $n+1$ represent the

old and new time levels, respectively, Δt is the time step and L is the spatial difference operator. Adding (13) and (14) and integrating over the time step results in

$$\left(C_k^{n+1} - C_k^n\right) = \left(L\left(C_k\right)^{n+1/2}\right) \Delta t + R_k^{equil} \qquad k = 1, \ldots, N_c \qquad (15)$$

Equation (15) is the time-discretized form of (1) with the reactions taking place at the end of the time step. The unequilibrated set of values C_k^{phys} in (13) are supplied to the chemical routine, which equilibrates the system individually for each nodal point and returns directly the set of equilibrated values C_k^{n+1} (14).

Walter et al. (1994) outline a second, iterative coupling approach to solve (1), however they found the sequential approach to be more computationally efficient with comparable accuracy. In the mine tailings simulations presented here using MINTOX, we will use the sequential approach exclusively, although the iterative approach is still supported in the model.

The physical transport step of equation (13) is solved using a standard Galerkin finite element technique (Hyakorn and Pinder, 1983), combined with the Leismann time weighting scheme (Leismann and Frind, 1989). The Leismann scheme produces a symmetric coefficient matrix for the transport equation while achieving second-order accuracy in time. Deformable rectangular elements are used with mass lumping and linear basis functions. An efficient conjugate-gradient solver (Schmid and Braess, 1988) is used to solve the final matrix equations.

Oxygen Diffusion

The conceptual model for sulphide mineral oxidation can be considered a two-step process where oxygen first diffuses through a shallow, unsaturated zone within the tailings, then diffuses through an oxidation shell surrounding a spherical sulphide grain (Figure 1).

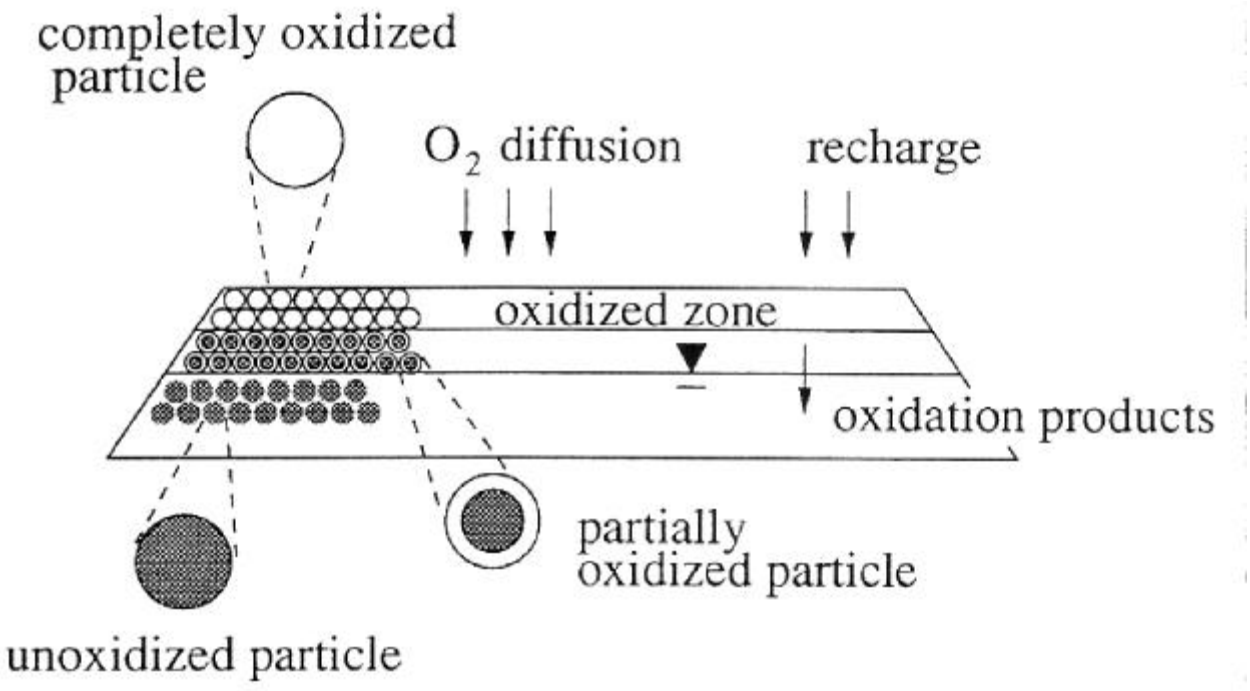

Figure 1. Conceptual model of oxygen diffusion and grain oxidation (after Wunderly et al., 1996).

The first step, bulk oxygen diffusion through the tailings, is considered a 1D process. This approach is justified on the basis of the large areal extent of typical tailings impoundments which reduces the influence any 2D or 3D effects occurring near lateral boundaries.

The equation describing oxygen diffusion through the unsaturated tailings can be written as

$$\frac{\partial U_A}{\partial t} = D_1 \frac{\partial^2 U_A}{\partial z^2} - q(z,t) \qquad (16)$$

where U_A is the concentration of oxygen in the air filled pore space (kg/m^3), D_1 is the diffusion coefficient of oxygen within the tailings (m^2/s), q(z,t) is a sink term representing oxygen consumption during sulphide mineral oxidation (kg/m^3s), t is time and z is the vertical coordinate direction.

The bulk diffusion coefficient of oxygen within the tailings (D_1) is calculated using (Reardon and Moddle, 1985)

$$D_1 = 3.98 \times 10^{-9} \cdot \left[\frac{\theta_A - 0.05}{0.95}\right] \cdot T^{1.5} \qquad (17)$$

where θ_A is the air-filled porosity of the tailings within the unsaturated zone and T is the temperature in Kelvin, with D_1 given in m^2/s.

In deriving an expression for the O_2 sink term q(z,t), we assume that all particles are spherical and surrounded by a thin, immobile water film (Figure 2) and, because the rate of unreacted core shrinkage is much slower than the O_2 diffusion rate within the particle (Levenspiel, 1972), we can also assume a stationary reaction front. With a further assumption that the consumption of O_2 at the oxidation site within the grain is instantaneous, we let the O_2 concentration here be zero.

To derive an expression for the consumption term in (1), we first relate the change in oxygen mass (M_U) to the oxygen concentration gradient within a spherical particle using

$$\frac{dM_U}{dt} = 4\pi r^2 D_2 \frac{dU}{dr} \qquad (18)$$

where dU/dr is the oxygen concentration gradient within the oxidation layer, D_2 is the oxygen

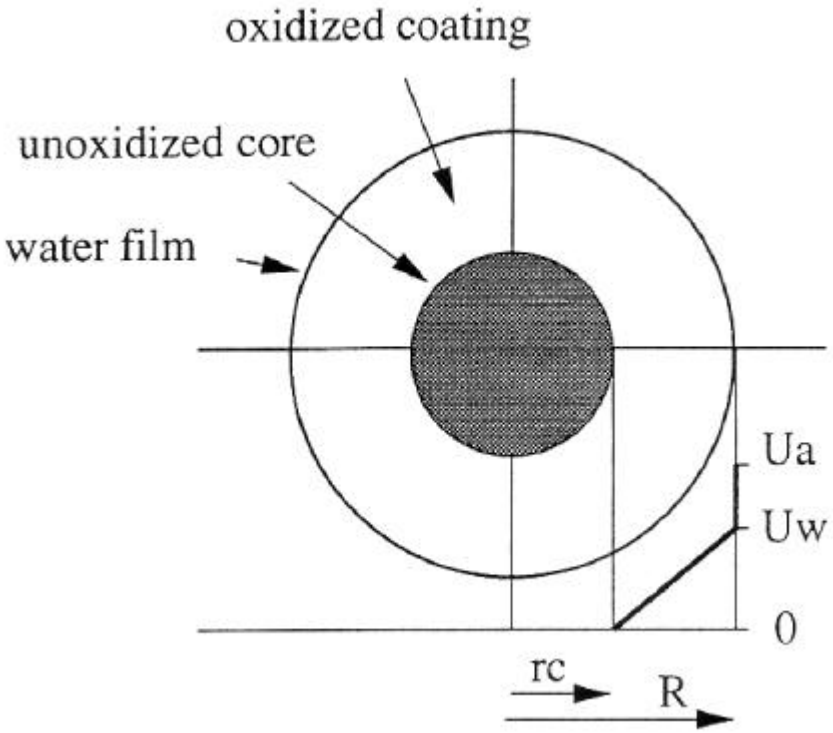

Figure 2. Detail showing parameters relating to mineral grain oxidation (after Wunderly et al., 1996).

diffusion coefficient within the grain, and r is the radius. Equation (18) can be integrated (from $R \rightarrow r_c$, $U_W \rightarrow 0$) over the oxidized shell to obtain

$$\frac{dM_U}{dt} = 4\pi D_2 \left(\frac{R r_c}{R - r_c} \right) U_w \qquad (19)$$

where R is the bulk grain radius, r_c is the unreacted core radius, and U_w is the oxygen

concentration within the outer water film. Equation (19) represents the change in oxygen mass for a single particle; multiplying by the number of particles per volume of porous medium ($(1-\theta)/(4/3\ \pi R^3)$) gives an expression for the oxygen consumption term:

$$q(z,t) = \frac{\partial U_A}{\partial t} = D_2 \cdot \frac{3(1-\theta)}{R^3}\left[\frac{Rr_c}{R-r_c}\right] U_w \qquad (20)$$

The equilibrium concentration of oxygen within the water film, U_w, can be related to the air phase oxygen concentration, U_A, through Henry's Law where $U_w=(1/H)\cdot U_A$ and H is Henry's constant (H=26.3 @10°C).

Core Shrinkage

As oxygen diffuses into the grain and oxidizes the sulphide mineral, the radius of the unoxidized core will shrink. This radius change can be derived by using the change in oxygen mass, derived in (19) and relating it to a volume change of the sulphur minerals within the unreacted core according to

$$\frac{dM_U}{dt} = \epsilon \frac{dM_S}{dt} = \epsilon \cdot \left(\frac{\rho_b}{1-\theta}\right) \cdot f_s \cdot \left(4\pi r_c^2\right) \cdot dr_c/dt \qquad (21)$$

where ϵ is the ratio of the mass of oxygen consumed to the mass of sulphur oxidized ($\epsilon = M_U/M_S$), where M_S is the mass of sulphur oxidized, ρ_b is the bulk density of the tailings and f_s is the mass fraction of sulphur within the tailings solids. The ratio ϵ can be obtained by considering the stoichiometry of the oxidation reaction. The oxidation of pyrite, for example, can be expressed using

$$FeS_2 + H_2O + 7/2O_2 \leftrightharpoons FeSO_4 + H_2SO_4 \qquad (22)$$

from which a mass ratio of ϵ=1.75 can be derived. Combining equations (19) and (21), an expression is derived for the change in radius of the unreacted core which can be written as

$$\frac{dr_c}{dt} = -\frac{(1-\theta)\cdot D_2}{\epsilon\rho_b \cdot f_s \cdot r_c^2}\left(\frac{Rr_c}{R-r_c}\right) \cdot \frac{U_A}{H} \qquad (23)$$

which can be solved for r_c using Newton-Raphson iteration.

Oxidation Reaction Products

Equation (23), coupled with (16), can be used to calculate the change in radius of the unoxidized core Δr_c=dr/dt, from which the number of moles of oxidized sulphur mineral per volume of tailings ($\Delta m_{Sul,}$ moles/m^{3}s) can be found from

$$\Delta m_{Sul} = \frac{\Delta M_S}{MW_S} = \left(\frac{\rho_s \cdot \Delta r_c^3}{R^3 \cdot MW_S}\right) \qquad (24)$$

where ρ_S is the density of sulphur, and MW_S is the molecular weight of sulphur. Knowing the quantity of sulphur consumed, we can compute the corresponding amounts of H^+, SO_4^{2-}, Fe^{2+} and Fe^{3+} released based on the following reaction stoichiometry:

$$FeS_2 + H_2O + 7/2O_2 \Rightarrow Fe^{2+} + 2SO_4^{2-} + 2H^+ \qquad (25)$$

$$FeS_2 + 1/2H_2O + 15/4O_2 \Rightarrow Fe^{3+} + 2SO_4^{2-} + H^+ \qquad (26)$$

The reaction path, either (25) or (26), is determined by the existing O_2 concentration and pH. The Fe^{2+} in (25) may be oxidized according to:

$$Fe^{2+} + 1/4O_2 + H^+ \Rightarrow Fe^{3+} + 1/2H_2O \qquad (27)$$

which consumes additional oxygen. From the mass action expression for (27), and replacing pO_2 with the oxygen concentration in the pore water (U_W), we can write

$$\left(\frac{Fe^{2+}}{Fe^{TOT}}\right) = 1/(K_{eq} \cdot (U_W)^{1/4} \cdot 10^{-pH} + 1) \qquad (28)$$

where K_{eq} is the equilibrium constant for (27), and

$$Fe^{TOT} = Fe^{2+} + Fe^{3+} \qquad (29)$$

An iterative approach is adopted for solution of the four coupled equations, (16), (23), (28) and (29), from which the unknowns U_A, r_c, Fe(II) and Fe^{TOT} can be determined. The following stepwise procedure is used in MINTOX (Wunderly et al., 1996):

1) Solve (16) for $\{U_A^{k+1}\}^{n+1}$ with an initial condition, or most recent value, of $\{r_c^k\}^n$ and $\{U_A^k\}^n$, where k represents the iteration level, and (n) and (n+1) represent the old and new time levels respectively.
2) Solve (23) for r_c using the Newton-Raphson method.
3) Solve (28) for the ratio (Fe^{2+}/Fe^{TOT}) using pH from the solution returned from MINTEQA2.
4) Solve for the new ratio of oxygen to sulphur (ϵ) according to (25) or (26) and the result from step 3.

5) Repeat steps 1-4 until convergence is attained.

6) Go to the next diffusion time step (which is usually less than the transport time step), and repeat steps 1-5.

Following convergence, the computed changes in aqueous concentrations of H^+, SO_4^{2-}, Fe^{2+} and Fe^{3+} are used to update the nodal chemistry throughout the grid. MINTEQA2 is then used to speciate the new chemistry, which completes step 2 of the two-step sequential operation (equation 14). Further information on the program structure and input requirements are provided in Appendix C.

Accuracy Criteria

As a minimum requirement for the control of numerical dispersion, the spatial and temporal discretization should satisfy the grid Peclet (*Pe*) and Courant (*Co*) criteria (Daus et al., 1985). These criteria are defined using:

$$Pe = \frac{v\Delta L}{D} \leq 2 \tag{30}$$

$$Co = \frac{v\,\Delta t}{\Delta L} \leq \frac{Pe}{2} \tag{31}$$

where v and D are the velocity and dispersion coefficient in the principal (flow) direction, respectively, ΔL is the effective element length in the flow direction, and Δt is the time step. Equation (30) is used to constrain the spatial discretization ΔL, while eq. (31) is used to constrain the time step.

Walter et al. (1994) also define an equivalent reactive mass ratio for component k (ρ_k) as:

$$\rho_k = \frac{R_k}{C_k^{phys}} = \frac{C_k^{n+1} - C_k^{phys}}{C_k^{phys}} \tag{32}$$

and give the condition that $\rho_k \geq -1$. An upper limit was not defined but would be dependent on the ability of the speciation model MINTEQA2 to equilibrate a disturbed system.

Model Evaluation

The parent model MINTRAN, on which MINTOX is based, has been proven in several tests including nonlinear ion exchange and a comparison against a 1D mixing cell model (Walter et al., 1994). The evaluation included a comparison of the sequential and iterative coupling approaches which both agreed well with PHREEQM, a mixing cell model developed by Appelo and Willemsen (1987). Because the sequential approach was over 3 times more computationally efficient than the iterative method, the sequential approach was adopted as the standard.

MINTRAN has also been successfully applied to simulate a realistic field case involving heavy metal transport and evolution of AMD from the Nordic tailings impoundment near Elliot Lake, Ontario (Walter et al., 1994). Their simulations included the coupled transport of 14 aqueous components together with 10 solid phase minerals. The evolution of AMD was simulated with MINTRAN over a 72-year period assuming a surface boundary source characterized by low-pH and elevated concentrations of Fe(II), SO_4^{2-}, Al, Pb and Cr.

The simulations showed how mobile heavy metals can be significantly attenuated through precipitation of carbonate and hydroxide mineral phases. By completing a scenario in which the source was removed after 12 years to simulate the effect of surface flooding, it was shown that heavy metals could remain effectively immobilized, reducing the impact of AMD on downgradient water resources.

The 1D oxygen diffusion and sulphide oxidation model (PYROX) was tested against the existing model of Davis et al. (1986) with results showing excellent agreement after 1 year (Figure 3). Further model evaluation tests can be found in Wunderly et al. (1996).

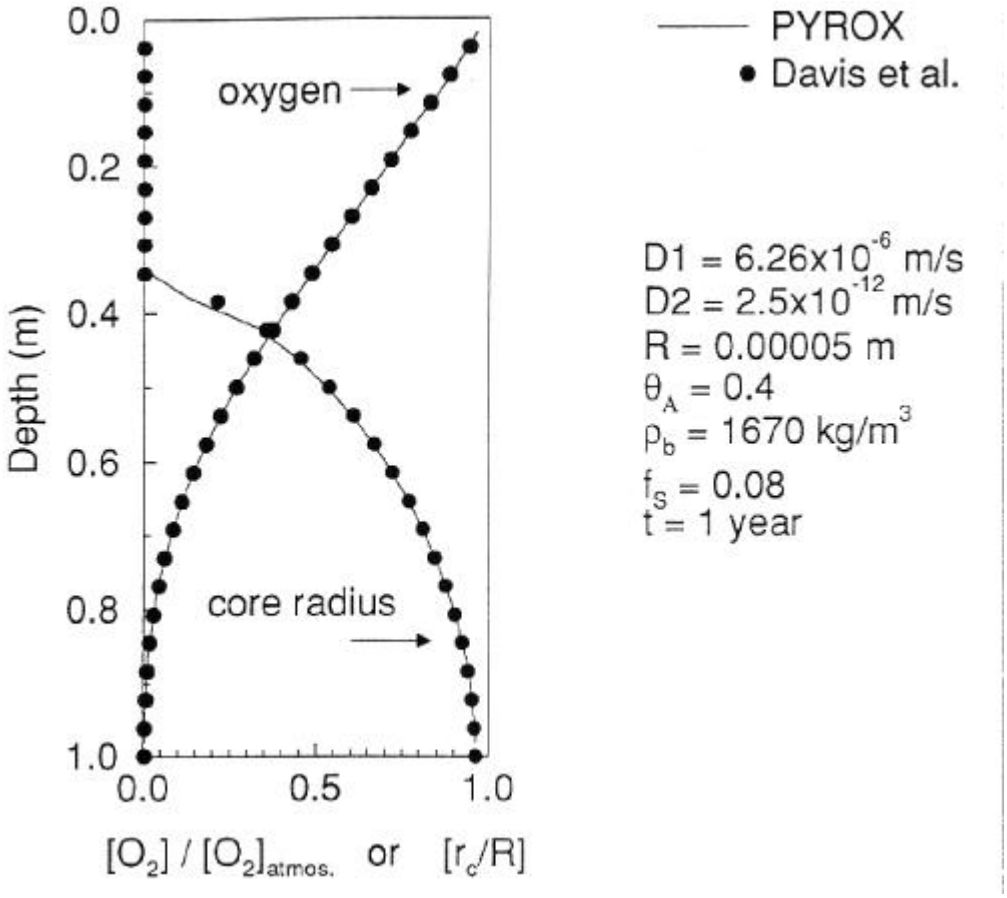

Figure 3. Profiles of oxygen concentration and unreacted core radius obtained from PYROX, and from the model by Davis et al. (1986).

Modelling the Evolution of Acid Mine Drainage

MINTOX can incorporate sources of AMD either as a boundary source function, or as a sulphide oxidation-derived internal source. The former is a simpler and less computationally demanding approach but requires the concentration of the oxidation products to be known beforehand. The latter approach is more flexible in that the source is generated as part of the solution. Because MINTOX cannot yet handle certain sulphide oxidation reactions, the boundary source method remains a useful option for some problems.

In this chapter, we will apply both types of source conditions to field scale problems of AMD. The boundary source condition will be used in a simulation of heavy metal transport at the Nordic site near Elliot Lake, while the internal oxidation-derived source will be used to simulate the Nickel Rim impoundment near Sudbury.

Elliot Lake

The Nordic tailings impoundment near Elliot Lake, Ont., is used as an example to illustrate the use of MINTOX in helping to understand the evolution and attenuation of heavy metals including Pb, Cr, and Mn. The approach follows that used by Walter et al. (1994b) in which the source of AMD was specified as a third type (Cauchy) boundary condition at the watertable.

The conceptual model includes a source of AMD above a shallow, unconfined aquifer (Figure 4). The domain measures 100×14 m and is discretized using 200 × 56 elements in the x and z directions, respectively. Background and source concentrations are provided in Table 1. Simulations are completed to 24 years using a uniform time step of 0.025 years. Results are provided in Figure 5 showing plumes of Cl, pH, and the heavy metals Cr, Pb, Mn with their

Table 1. Background and source concentrations of aqueous and solid components for the Elliot Lake model.

Aqueous Species	**Background concentration (moles/L)**	**Concentration in recharge water (moles/L)**	**Solid Species**	**Background concentration (moles/L)**
Ca	6.92×10^{-3}	1.1×10^{-2}	Calcite	0.02
Mg	1.96×10^{-3}	9.7×10^{-4}	Siderite	0.004
Na	1.30×10^{-3}	1.4×10^{-3}	Am. Silica	0.4
K	6.65×10^{-5}	8.1×10^{-4}	Gibbsite	.0025
Cl	1.03×10^{-3}	1.6×10^{-2}	Ferrihydrite	0.002
CO_3^{2-}	3.94×10^{-3}	4.9×10^{-4}	Gypsum	0.0
SO_4^{2-}	7.48×10^{-3}	5.0×10^{-2}	Rhodochrosite	0.0
Fe(II)	5.36×10^{-5}	3.1×10^{-2}	Anglesite	0.0
Fe(III)	2.32×10^{-8}	2.0×10^{-7}	Cerussite	0.0
Al	1.28×10^{-7}	4.3×10^{-3}	Am. Cr. Hydrox.	0.0
Mn	4.73×10^{-5}	7.8×10^{-3}		
Cr	1.0×10^{-8}	1.33×10^{-4}		
Pb	1.0×10^{-8}	1.52×10^{-5}		
pH	6.96	3.99		

mineral precipitates of chromium hydroxide ($Cr(OH)_3$), cerussite ($PbCO_3$), and rhodochrosite ($MnCO_3$). The mineral precipitation/dissolution reactions are controlled by the source pH which after 24 years shows 3 distinct buffer zones controlling the location of mineral precipitation fronts: a background neutral-pH zone buffered by calcite, a zone of $pH \approx 5$ buffered by siderite, and a zone of $pH \approx 4$ buffered by gibbsite. Since they contain significant fractions of the total mass of heavy metals, the formation of metal precipitates are critical in decreasing the aqueous

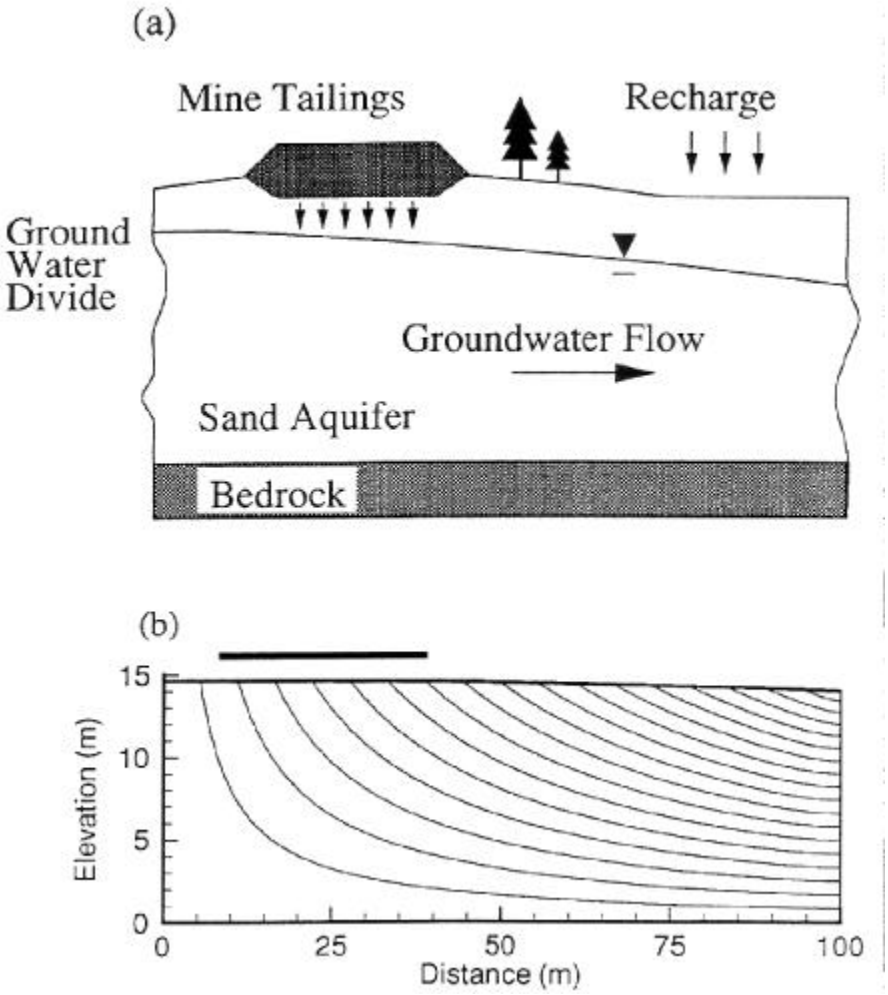

Figure 4. Simplified conceptual model for the Nordic (Elliot Lake) simulation showing (a) boundary conditions, and (b) steady state flow system (after Walter et al., 1994b).

phase metal concentrations. Further details can be found in Walter et al. (1994b).

Calcite, the primary buffer mineral assumed in the Elliot Lake model, is assumed to be present at a concentration of 0.02 mol/L. Because this concentration is not well-defined in the field data, simulations were repeated with variable concentrations to determine its role in the buffering process. Figure 6 compares the arrival curves of the base case model with two additional simulations in which the calcite concentration was first increased, then decreased by a factor of 5

relative to the base case. The differences are quite dramatic, with the high-calcite scenario for example, showing higher pH and lower concentrations of all major metal species. Because of the fixed source conditions, however, the responses are merely delayed in time; once the added calcite has dissolved, the pH eventually reaches the same low levels characteristic of the base case.

The fixed source condition of MINTOX is therefore somewhat limited for predicting the evolution of AMD. Ongoing development of MINTRAN and MINTOX is focussing on extending their capability to enable the oxidation of various metal sulphide minerals including galena and sphalerite. In the next section, we will apply MINTOX to the Nickel Rim site using the process of pyrite oxidation to generate the internal source of AMD.

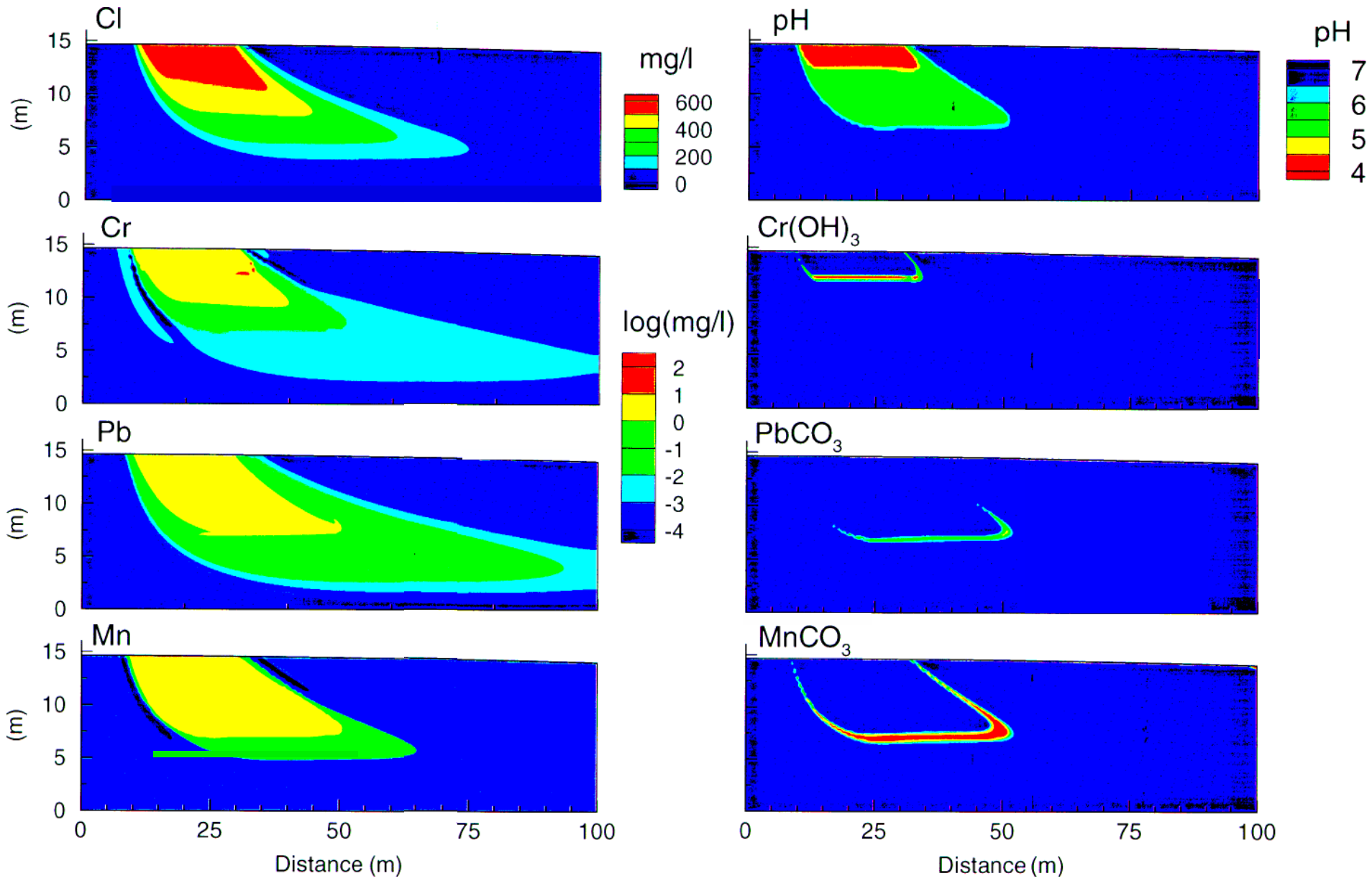

Figure 5. MINTRAN base case simulation: Selected aqueous and solid species at 24 years.

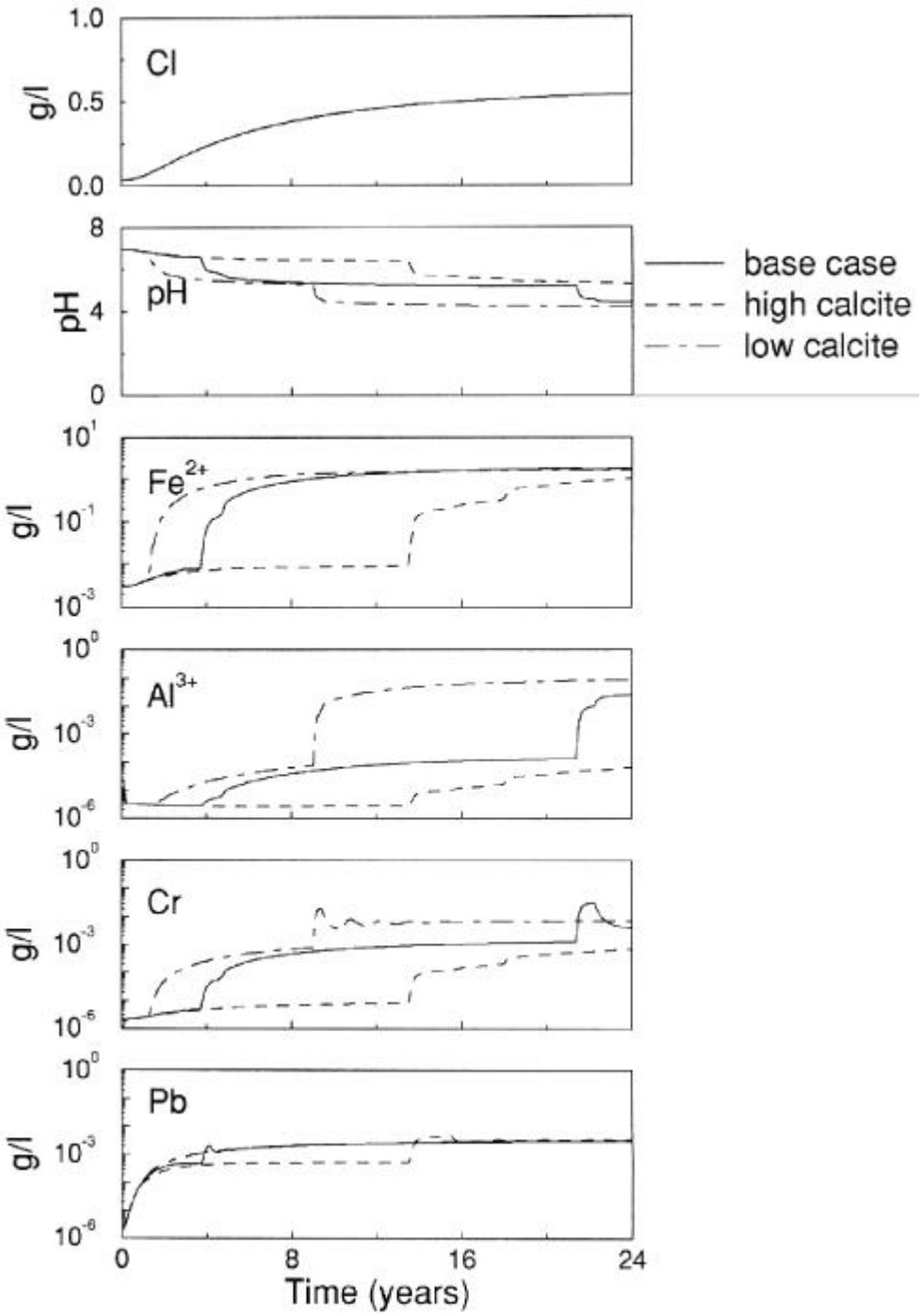

Figure 6. Arrival curves of selected components from the Elliot Lake model showing the effect of calcite on tailings buffer capacity.

Nickel Rim

In this section, we will calibrate MINTOX to the observed geochemistry at the Nickel Rim tailings impoundment. Nickel Rim provides an excellent site for model calibration because it is typical of many sites throughout Ontario, Québec and New Brunswick, it is buffered by existing carbonate minerals, and has been well characterized and monitored over several years (Bain et al., 1995, Bain, 1996).

Site Description:

The Nickel Rim tailings impoundment, located near Sudbury, Ontario, operated during the 1950's and was decommissioned in 1958 (Thomson, 1961). Oxidation of sulphide minerals within the unsaturated zone of the tailings has created low pH tailings water and downgradient plumes characterized by high iron and sulphate concentrations. Environmental impacts include observed metal loading and low pH conditions in surface waters overlying the aquifer, and within Moose Lake, 100m further downgradient.

The Nickel Rim site contains approximately 3-4 wt % sulphide sulphur, primarily as pyrrhotite (Fe_{1-x} S). The tailings deposit is approximately 10m thick and is retained by a porous rock-fill dam, downstream from which lies a 3-8m thick unconfined sand aquifer. Recharge occurs over the tailings with flow velocities ranging from approximately 10-30 m/yr (Bain, 1996, Johnson, 1993).

In the conceptual model, sulphide mineral grains are oxidized within the unsaturated zone of the tailings, releasing H^+, Fe(II) and SO_4^{2-}. The low-pH zones are buffered sequentially by dolomite ($Ca,Mg(CO_3)_2$), siderite ($FeCO_3$), gibbsite ($Al(OH)_3$), ferrihydrite ($Fe(OH)_3$) and jarosite ($KFe_3(SO_4)_2(OH)_6$). Reactions are assumed governed by equilibrium speciation, and the dissolved species are transported downgradient with the ambient steady-state flow system.

Thermal effects and porosity changes are not considered.

The equilibrium approach to precipitation/dissolution reactions is justified for reactions which are fast relative to the groundwater flow. Dolomite is an exception however, since there are kinetic limitations on dolomite precipitation rates. Nevertheless, our assumption of equilibrium speciation is still valid for the simulations considered here in which dolomite is already present as a background mineral and only dissolves during the AMD simulations. Additional minerals such as aluminosilicates, which may also contribute to pH buffering and metal attenuation, generally show kinetic constraints on precipitation/dissolution and are not considered here.

Flow System Simulation

The flow system for the Nickel Rim site was simulated using a modified version of the FLONET model (Guiguer et al., 1994). Modifications allowed larger grid sizes, and an irregular base geometry. The flow modelling approach assumes saturated, steady state conditions and a non-deforming, isothermal porous medium. A finite element grid of 259×51 nodes in the x and z directions respectively, was used to resolve the domain.

The conceptual model and flow boundary conditions are provided in Figure 7. The domain is approximately 350m in length and is bounded below by the bedrock surface which is assumed to be impermeable. The right boundary coincides with an inferred flow divide near the centre of the tailings, while the left (downgradient) discharge boundary coincides with Moose Lake. A variable recharge function is applied over the top watertable boundary and varies from a normal background level of 20 cm/yr, to 1 cm/yr through the dam. Discharge conditions are applied at the toe of the dam to correspond with observed groundwater seeps.

Calibrated hydraulic conductivities varied throughout the site, ranging from 10^{-5} m/s within the

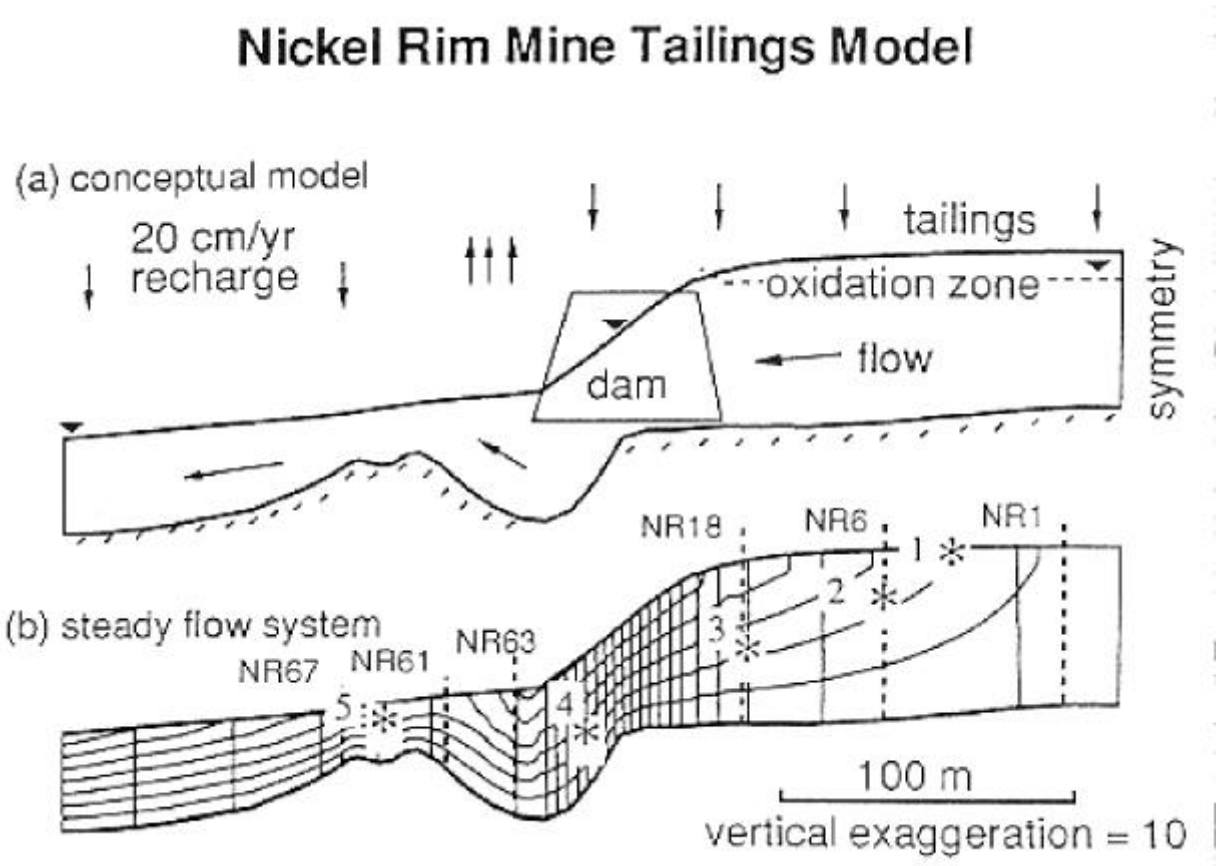

Figure 7. The Nickel Rim site layout: (a) conceptual model and (b) simulated steady state flow system showing streamlines and locations of breakthrough points and multilevel monitors.

aquifer, to 10^{-6} m/s within the dam. The 1m-thick unsaturated oxidation zone is represented in FLONET using a local anisotropy of Kx/Kz = 0.025. Flow therefore becomes essentially vertical through the oxidation layer. A uniform porosity of 0.4 was assumed throughout the domain.

The simulated streamfunction solution, showing groundwater flow directions, reflects a dominantly horizontal flow system below the surface oxidation layer, with local discharge downstream of the dam (Figure 7b). Converging streamlines downgradient from the dam signify

increasing flow velocities which range from approximately 1 m/yr within the tailings to 10-20 m/yr downstream of the dam. These values are consistent with inferred field conditions although 3D effects, not accounted for in the present model, may induce somewhat lower velocities than those simulated near the left discharge boundary. The equilibrium watertable position agreed well with the mean of the observed positions at all piezometer locations (Bain, 1996). Differences are attributable to transient effects which act on time scales much shorter than the transport simulations and can therefore be neglected.

Transport Simulation and Calibration

The transport calibration process involves varying selected model parameters until the simulated plumes of the major chemical species agree with the observed plumes. Specific variables which were adjusted for the Nickel Rim site included background concentrations of calcite, dolomite, siderite and gibbsite, the oxygen diffusion coefficient within the oxidized mineral shell (D_2), and the wt % sulphur in the tailings. During model calibration, significant insight is also gained into the sensitivity of the model to those parameters which have been changed.

The initial (background) source chemistry used in the calibration is provided in Table 2 (see also the MINTOX data file *nickel3.dat* in Appendix B). The oxidation process was controlled in the calibration using a D_2 value of 1.5×10^{-14} m^2/s, a grain radius of 7.8×10^{-5} m, a wt % sulphur = 4.5% and an oxidation zone depth of 1.0m.

Table 2. Summary of component concentrations in the background pore water and in boundary recharge for the Nickel Rim calibration (base case) simulation. Initial solid species' concentrations are also provided.

Aqueous Species	**Background concentration (moles/L)**	**Concentration in recharge water (moles/L)**	**Solid Species**	**Concentration (moles/L pore space)**
Ca	1.36×10^{-2}	1.1×10^{-2}	Dolomite	0.04
Mg	2.49×10^{-2}	6.8×10^{-3}	Gibbsite	0.08
Na	1.09×10^{-2}	1.3×10^{-3}	Siderite	0.0
K	5.14×10^{-3}	6.7×10^{-3}	Ferrihydrite	0.0
Cl	4.25×10^{-4}	3.0×10^{-3}	Gypsum	0.0
CO_3^{2-}	1.07×10^{-2}	1.4×10^{-2}	K Jarosite	0.0
SO_4^{2-}	3.39×10^{-2}	7.4×10^{-3}	FeS	0.0
Fe(II)	2.47×10^{-5}	1.9×10^{-5}		
Fe(III)	1.25×10^{-8}	1.2×10^{-8}		
Al	5.71×10^{-9}	5.1×10^{-9}		

Physical transport parameters were also adjusted during calibration, with the final simulation using 5.0 m and 0.05 m for the longitudinal (α_L) and transverse(α_T) dispersivities, respectively. An aqueous diffusion coefficient of 1.6×10^{-10} m^2/s was used for all components. A finite element grid identical to that used in the flow simulation was used for the transport simulations (259×51 nodes), with a uniform time step of 0.05 years (18.25 days) used throughout the full 75-year simulation. A third-type (Cauchy) boundary condition was applied across the watertable for the aqueous phase chemical components recharging from precipitation.

A total of 14 aqueous components and 9 solid reactions were involved in the calibration process. Although the model was calibrated primarily using observed concentrations of pH, Fe(II) and

sulphate, the simulated behaviour of all relevant components was verified to be consistent with the conceptual model. A complete time sequence showing plume evolution at 10, 25, 50 and 75 years is included in Appendix A.

Since the last of the tailings were deposited in the late 1950's, a simulation time of 36 years will correspond to a period from approximately 1990-1995. The conceptual model and numerical model calibration was based on field data obtained over this period (Bain, 1996).

The MINTOX simulation of the Nickel Rim site is shown in Figures 8 and 9 showing the distribution of selected aqueous components and solid phase minerals in the vertical cross-section after 36 years.

Looking at the correlation between the primary buffering minerals of dolomite, siderite and gibbsite with pH, Fe(II), and sulphate (Figures 8 and 9), we observe dolomite dissolving in the low-pH region near the source, while siderite precipitates at the leading edge where dolomite has already been dissolved. Similarly, gibbsite becomes the third buffering mineral where siderite has already been depleted. These trends, which agree with many similar tailings sites in Ontario, Quebec and New Brunswick, continue to 75 years (Appendix A).

In order to provide a basis for comparison with the reactive species, the simulated non-reactive chloride plume is also provided in the model calibration of Figure 8. The chloride plume is generated from a fixed source concentration of 0.003 mol/l (100 mg/l) which recharges through the tailings. The plume therefore grows steadily in time, with concentrations of 50 mg/L reaching the downstream boundary after 36 years. Discharge of the Cl plume is also evident at the toe of the dam where groundwater discharge is also observed in the field. The low vertical dispersivity constrains the plume vertically in the aquifer and prevents excessive smearing. This behaviour is consistent with existing non-reactive plumes in similar unconfined flow systems.

Figure 10 shows a good comparison between the observed and simulated concentrations of Fe(II) and sulphate at the vertical profiles corresponding to sample locations of NR18 and NR6 (see Figure 7b for locations). In particular, the simulated peak concentrations of Fe(II) and SO_4^{2-} (3800 and 10000 mg/L respectively) agree well with the corresponding observed concentrations (3600 and 11000 mg/L respectively). The elevations at which these peaks occur (314 masl) also correlate well. Although the simulated profiles are somewhat more dispersed, this characteristic is less significant to the overall interpretation of the conceptual model.

Vertical profiles of all major components at 36 years, at the location corresponding to monitor point NR6, are provided in Figure 11 and the arrival curves of selected aqueous components and solid minerals, at all arrival points, are shown in Figure 12 and 13 respectively.

The sequence of reactions at the Nickel Rim site is controlled primarily by the generation of acidic, or low-pH conditions resulting from oxidation of the sulphide minerals within the tailings. A well-defined sequence of mineral buffering reactions constrains the pH to specific levels or plateaus corresponding with the specific buffering mineral present. The sequence of buffering minerals, from high to low pH, proceeds from dolomite ($(CaMg)(CO_3)_2$) and siderite ($FeCO_3$) to gibbsite ($Al(OH)_3$), ferrihydrite ($Fe(OH)_3$) and jarosite ($KFe_3(SO_4)_2(OH)_6$). Between the plateaus, the pH changes relatively abruptly producing sharp fronts at various stages in the plume development (Figure 11).

In the vertical depth profiles of Figure 11, dolomite appears as the primary buffering mineral at neutral pH. Below a pH of 6, dolomite declines rapidly, and is totally absent for pH<5.2 where siderite becomes the primary buffering mineral. Siderite precipitates at the leading edge of the Fe(II) plume generated from pyrite oxidation.

Gibbsite acts as the third buffering mineral, maintaining pH levels at approximately 4.2. The gibbsite depth profile shows a slight rise from background levels of 0.08 mol/l to approximately

0.13 mol/l. The excess gibbsite originates from high concentrations of Al transported from the overlying low-pH zone where gibbsite is dissolved. Similarly, the Al released from gibbsite dissolution accumulates to form a peak concentration of 800 mg/l at an elevation of 317.5 m.

Gypsum precipitates throughout most of the tailings where sulphate concentrations are high. Peak concentrations are found at the leading edge of the oxidizing zone.

The Fe(II) profile decreases upward from a maximum of almost 4000 mg/l at an elevation of 314m to a low of approximately 1500 mg/l within the oxidizing zone. The peak Fe(II) levels are remnants from early time (<10 years) when oxidation rates were highest. Fe(II) concentrations decrease toward surface due to depletion of the oxidizable pyrite grain coatings and corresponding decrease in Fe(II) generation. The sulphate profile shows similar trends, although concentrations are much higher, approaching 10,000 mg/L. Although density effects may begin to occur at these concentrations causing the plumes to sink further in the aquifer, we have neglected them here.

Calcium concentrations remain at relatively uniform levels of 400-500 mg/l due to dissolution of dolomite and equilibration with gypsum. Carbonate concentrations are depleted in the low-pH zone and show a high plateau where CO_3^{2-} equilibrates with siderite.

Finally, the profile of non-reactive chloride shows a dispersion front near the base of the tailings, with concentrations increasing smoothly upwards to the source level of 0.003 mol/l.

The development of the low-pH plume follows the rate of sulphide oxidation. Once the bulk of the grains have been oxidized, the generation of acid will begin to decrease. In this case, the minimum pH level at arrival point 1 (pH≈1.2) was reached after approximately 10 years, and after 76 years the source pH has recovered to approximately 2 (Figure 12).

Pyrite oxidation releases Fe(II) and SO_4^{2-} according to (Walter et al., 1994a):

$$FeS_2 + 14Fe^{3+} + 8H_2O \Rightarrow 15Fe^{2+} + 2SO_4^{2-} + 16H^+ \quad (33)$$

The Fe(II) can be further oxidized to Fe(III) which can then hydrolyse, releasing additional H^+. The concentrations of Fe(II) are also affected by the precipitation or dissolution of siderite, while SO_4 can be modified by the precipitation or dissolution of gypsum. Since the rate of sulphide oxidation is highest during the first 10 years, both plumes show highest source concentrations at early time (within 5-10 years), and progressively decreasing levels thereafter. In addition to the decreasing source strength, the peak concentration of the plumes decrease over time due to mineral precipitation reactions and hydrodynamic dispersion.

Influence of Dolomite

Because pH plays such a dominant role in governing the geochemistry of mine tailings, variations in the amount of pH-buffering minerals can have significant effects on plume behaviour.

The influence of the background dolomite concentration, for example, can be profound (Figure 14). Increasing the dolomite concentration from the calibration value of 0.04 mol/L to 0.08 mol/L results in a significant decrease in both Fe(II) and sulphate concentrations (Figure 14a). A high dolomite concentration produces generally higher pH levels over time through a complex interrelationship among species concentrations, activities and accumulation of additional buffering minerals.

Although dolomite is perhaps the most significant buffering mineral, the remaining buffers, siderite, gibbsite, ferrihydrite and jarosite, also play significant, and generally not easily predicted roles. The MINTOX model now allows such complex behaviour to be quantified and predicted with reasonable accuracy.

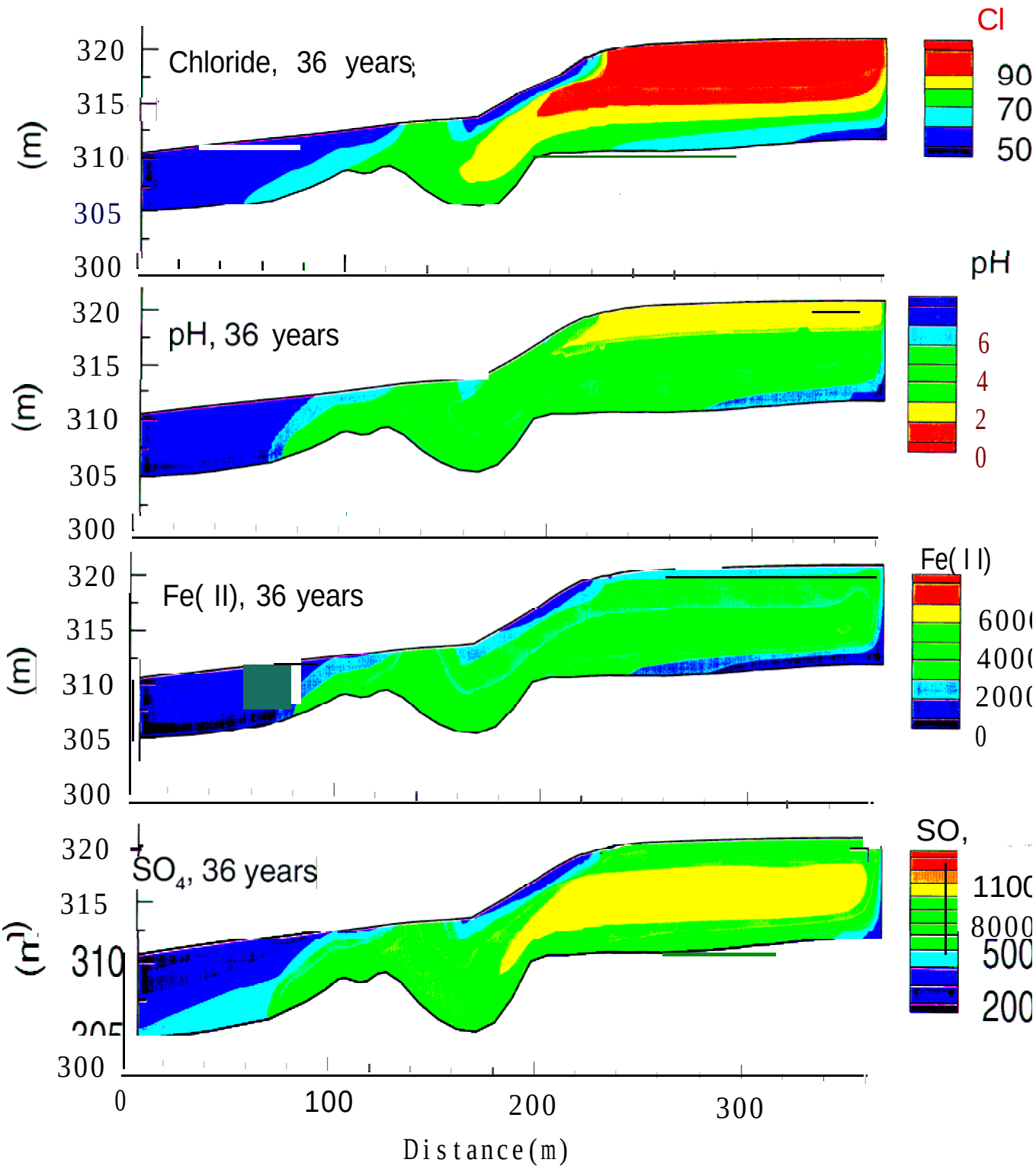

Figure 8. Nickel Rim base case simulation: Selected aqueous plumes at 36 years.

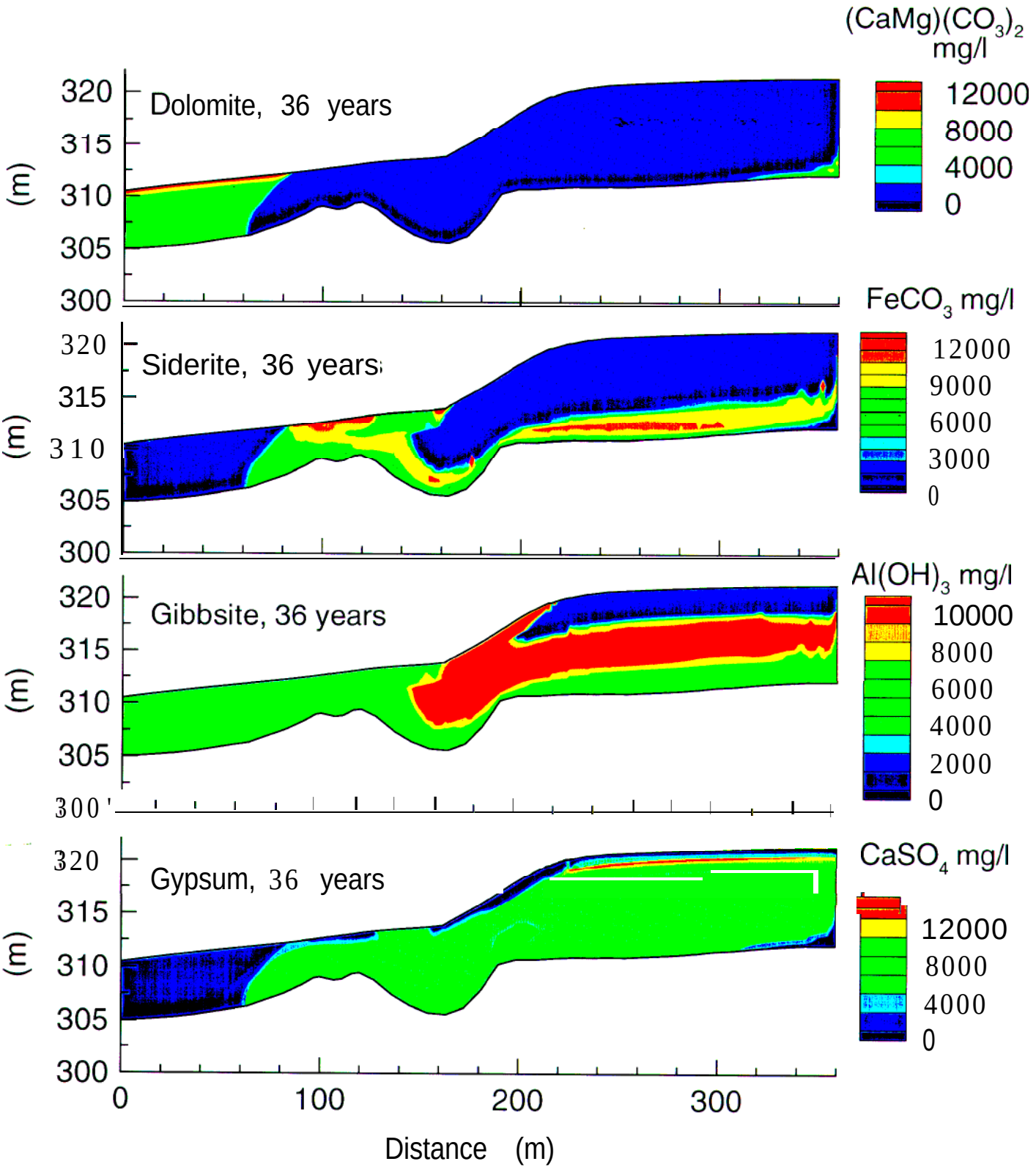

Figure 9. Nickel Rim base case simulation:
Distribution of selected solid minerals at 36 years.

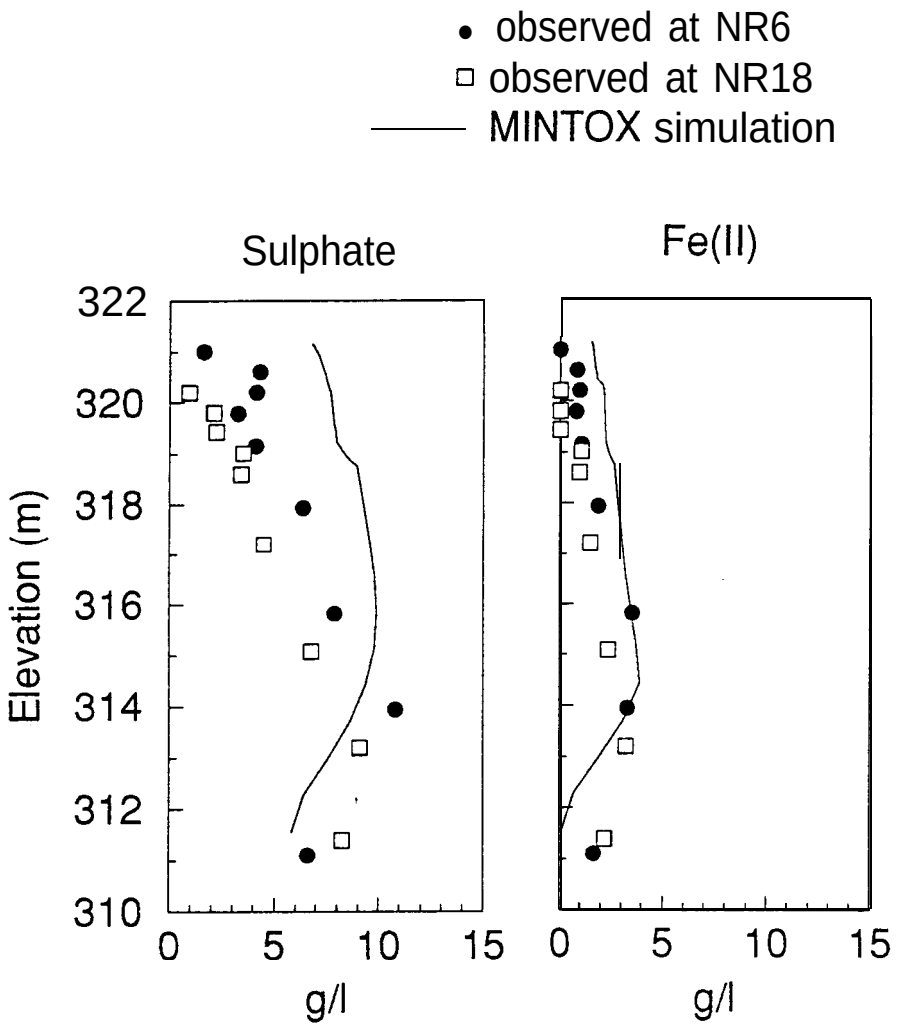

Figure 10. Observed and simulated vertical profiles of SO_4^{2-} and Fe(II) at 36 years for the Nickel Rim calibration.

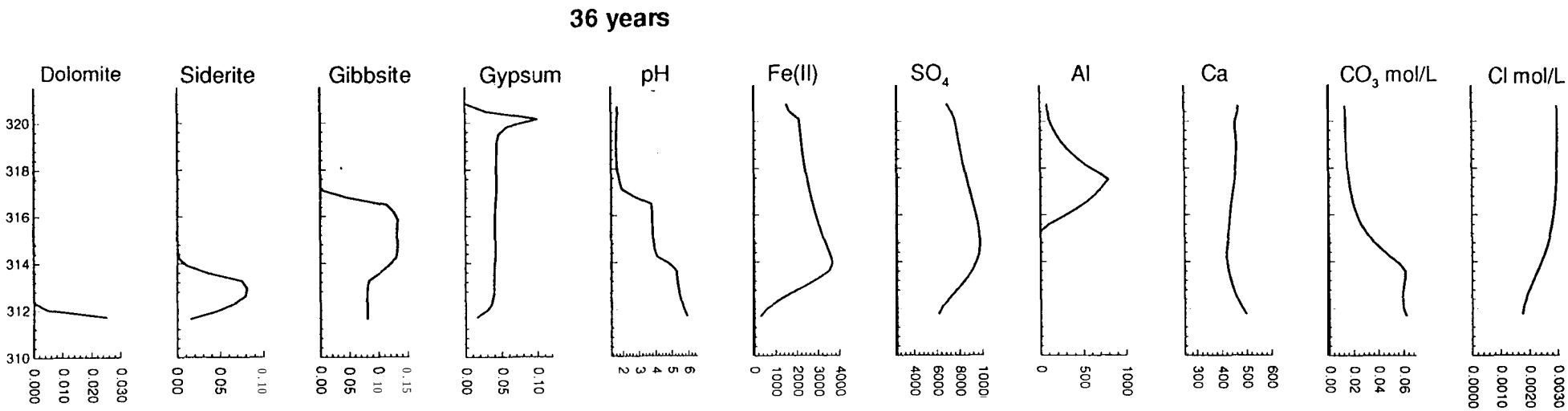

Figure 11. Vertical depth profiles of selected components through the tailings impoundment at 36 years (solid concentrations in mol/L, aqueous concentrations in mg/L unless otherwise indicated.

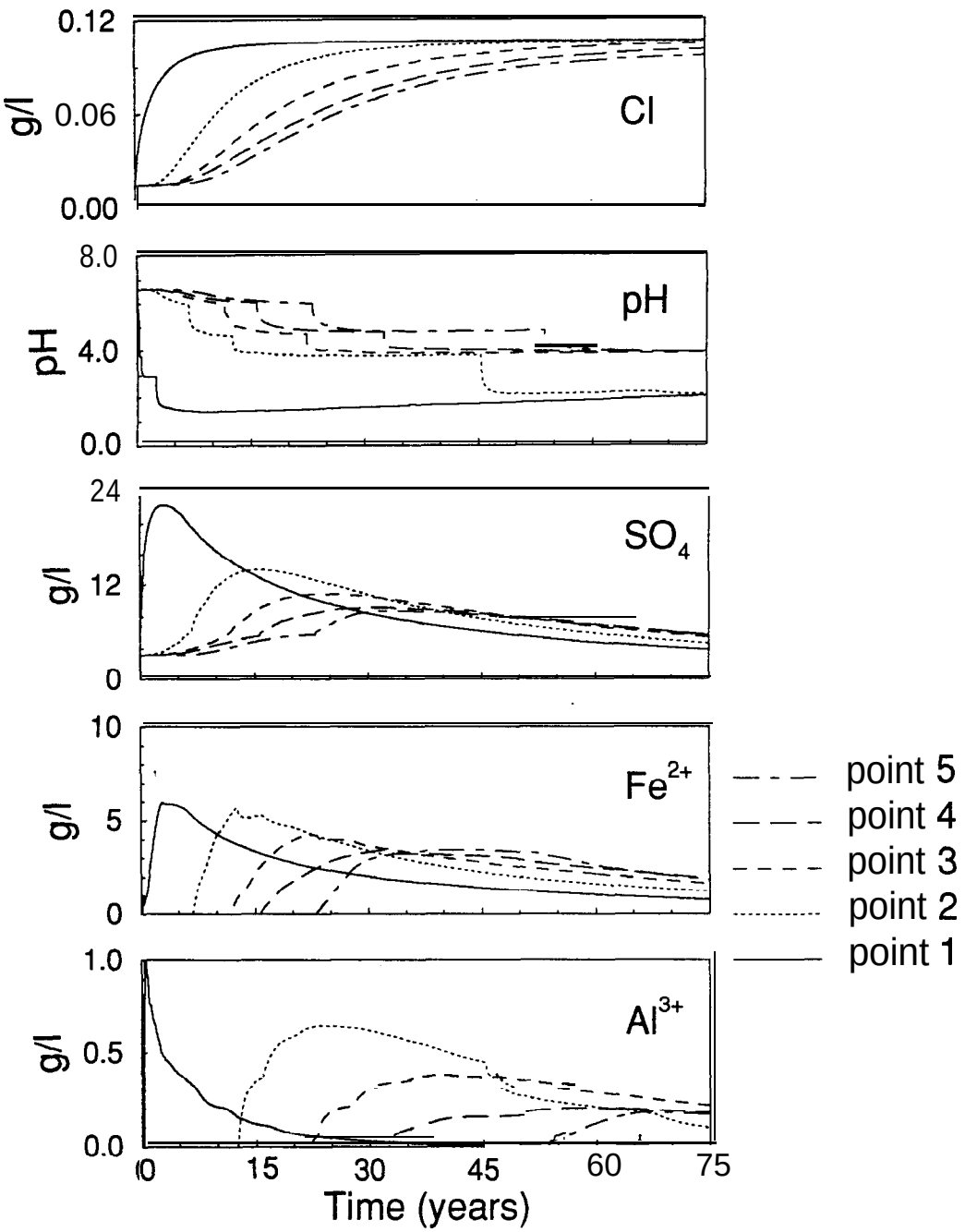

Figure 12. Arrival curves of selected species, at all points, for the Nickel Rim base case simulation.

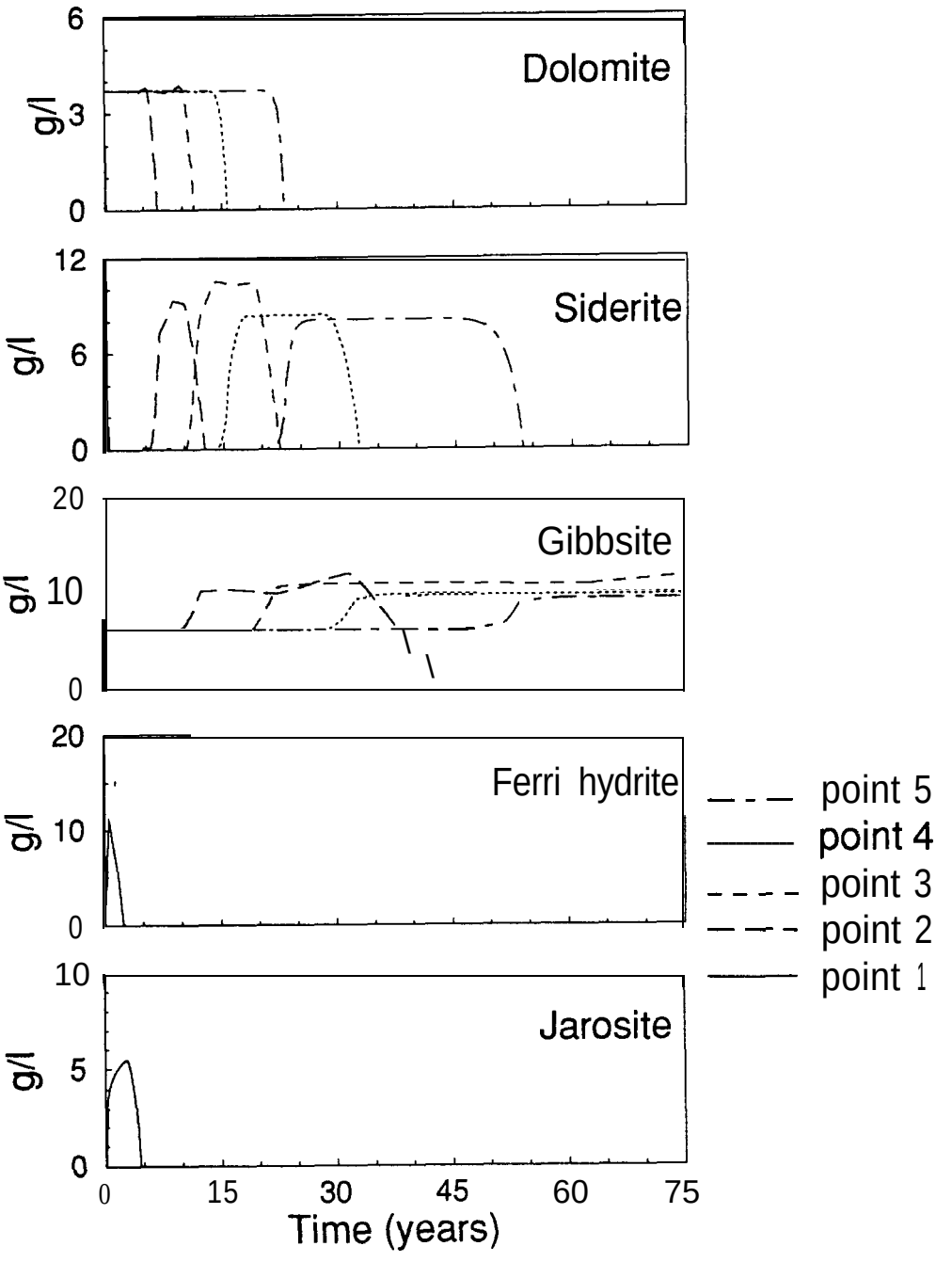

Figure 13. Arrival curves of solid mineral species, at all arrival points, for the Nickel Rim base case simulation.

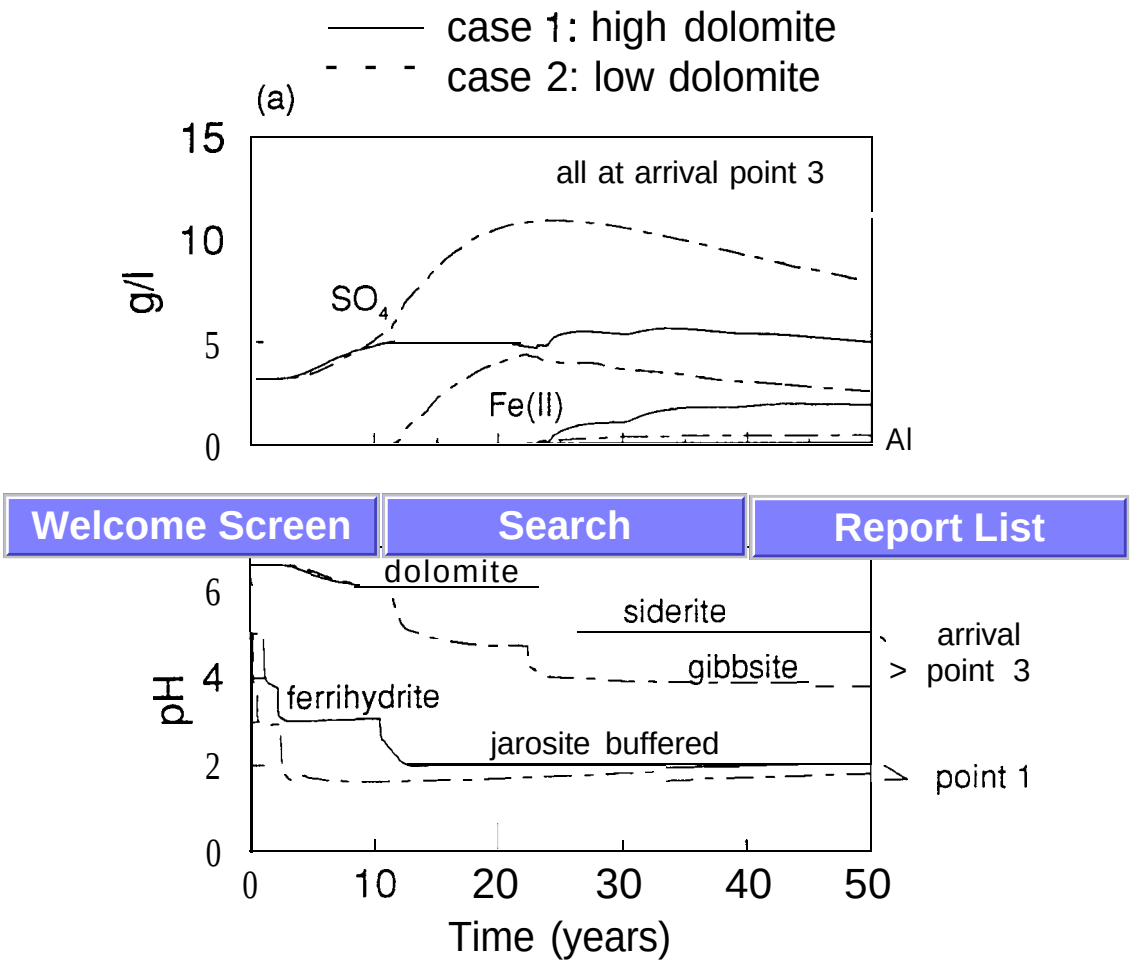

Figure 14. Arrival curves of selected species at Nickel Rim showing the effect of changing background concentrations of dolomite: (a) arrival of SO_4^{2-}, Fe(II) and Al, and (b) arrival of pH showing pH plateaus due to sequences of buffering minerals. See Figure 7b for location of arrival points.

Reducing the Impact of AMD

The MINTOX model application to the Nickel Rim site has provided significant insight into the reactive processes of sulphide mineral oxidation and transport. In this section, we use the Nickel Rim site to evaluate the effectiveness of two commonly proposed remediation measures: oxidation reduction through tailings flooding, and source attenuation through limestone addition. Although these measures are not proposed for Nickel Rim because of its age, the site is nevertheless useful for comparison purposes. Additional methods of AMD control are reviewed by Blowes et al. (1994).

Tailings Flood

The acid-generating sulphide mineral oxidation reactions can potentially be controlled by flooding the tailings surface, thereby reducing the diffusion rate of oxygen by several orders of magnitude. By specifying the water content within the tailings oxidation zone at near-saturation levels, MINTOX can simulate the flooding process quite effectively. The higher water content reduces the oxidation rate by reducing the computed diffusion coefficient of oxygen through the tailings (eq. 17), reducing its availability at the grain surfaces.

To illustrate the effect of a tailings flood, the Nickel Rim base case (calibration) simulation was repeated, with the only change occurring after 5 years when the water content within the 1m oxidation zone was instantaneously increased to saturation levels. Profound differences between the two simulations are evident in the concentration contour plots after 10 years (Figures 15), which can be compared to the 10-year base case results shown in Appendix A.

The most significant effect of the tailings flood is evident by the absence of the low-pH conditions typical of the base case simulation. Concentrations of Fe(II) and SO_4^{2-} have also been considerably reduced, with the peak concentrations of the sulphate plume also much reduced in

areal extent. The longer term remedial effect of the tailings flood is shown in the arrival curves at point 2 (see Figure 7b for locations), provided in Figure 16. Within 50 years, for example, the pH and concentrations of Fe(II) and SO_4^{2-} have returned to near-background levels. Of particular interest in the flood scenario are the very low Al concentrations, due to a reduction of gibbsite dissolution in the higher pH environment.

Enhanced Buffer Capacity

A second approach to reduce the impact of AMD is through enhancing the buffer capacity through the addition of lime or limestone to the tailings slurry. The buffer capacity can be increased in MINTOX by altering the initial background chemistry within the tailings area of the model domain.

In order to quantify and compare the geochemical evolution of AMD under conditions of enhanced buffer capacity, the Nickel Rim base (calibration) simulation was repeated with calcite added to the surface tailings at a concentration of 0.8 mol/L. The plume concentrations are again shown at 10 years (Figure 17) for comparison to the base case simulation of Appendix A.

Under the imposed conditions, the impact of enhanced buffering capacity is not as effective as the tailings flood scenario. The pH, for example, while at most times clearly higher than in the base case, eventually reaches base case levels with the effect only being a delay in arrival time. Concentrations of SO_4^{2-} and Fe(II) are not significantly reduced with arrival times of peak concentrations delayed by 10-15 years. Levels of buffering material required to prevent unacceptable levels of contaminants can be assessed using MINTOX on a site by site basis.

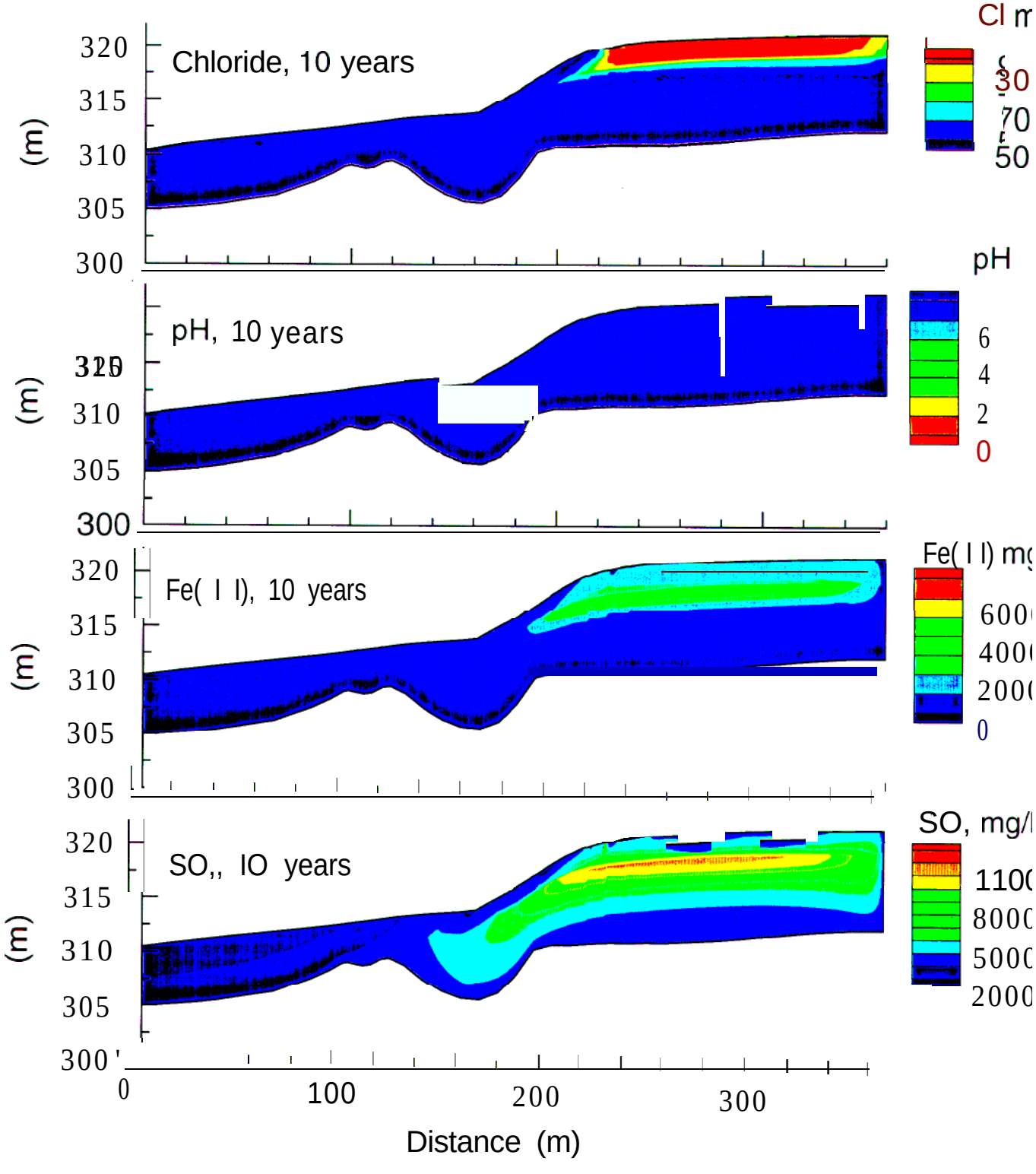

Figure 15. Nickel Rim simulation with flooded tailings after 5 years: Selected aqueous plumes at IO years.

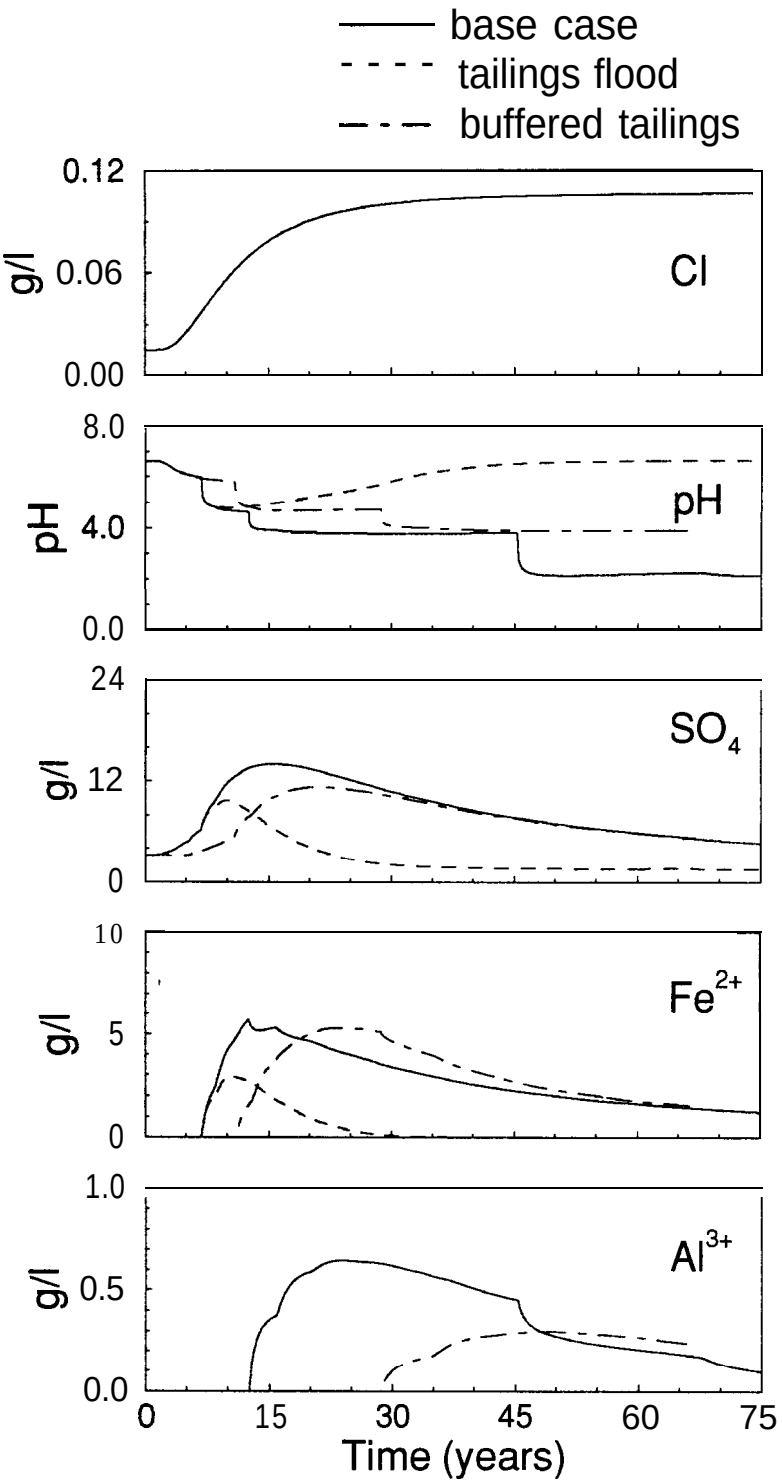

Figure 16. Nickel Rim arrival curves for selected species at arrival point 2, showing comparison between base case, tailings flood and buffered tailings simulations.

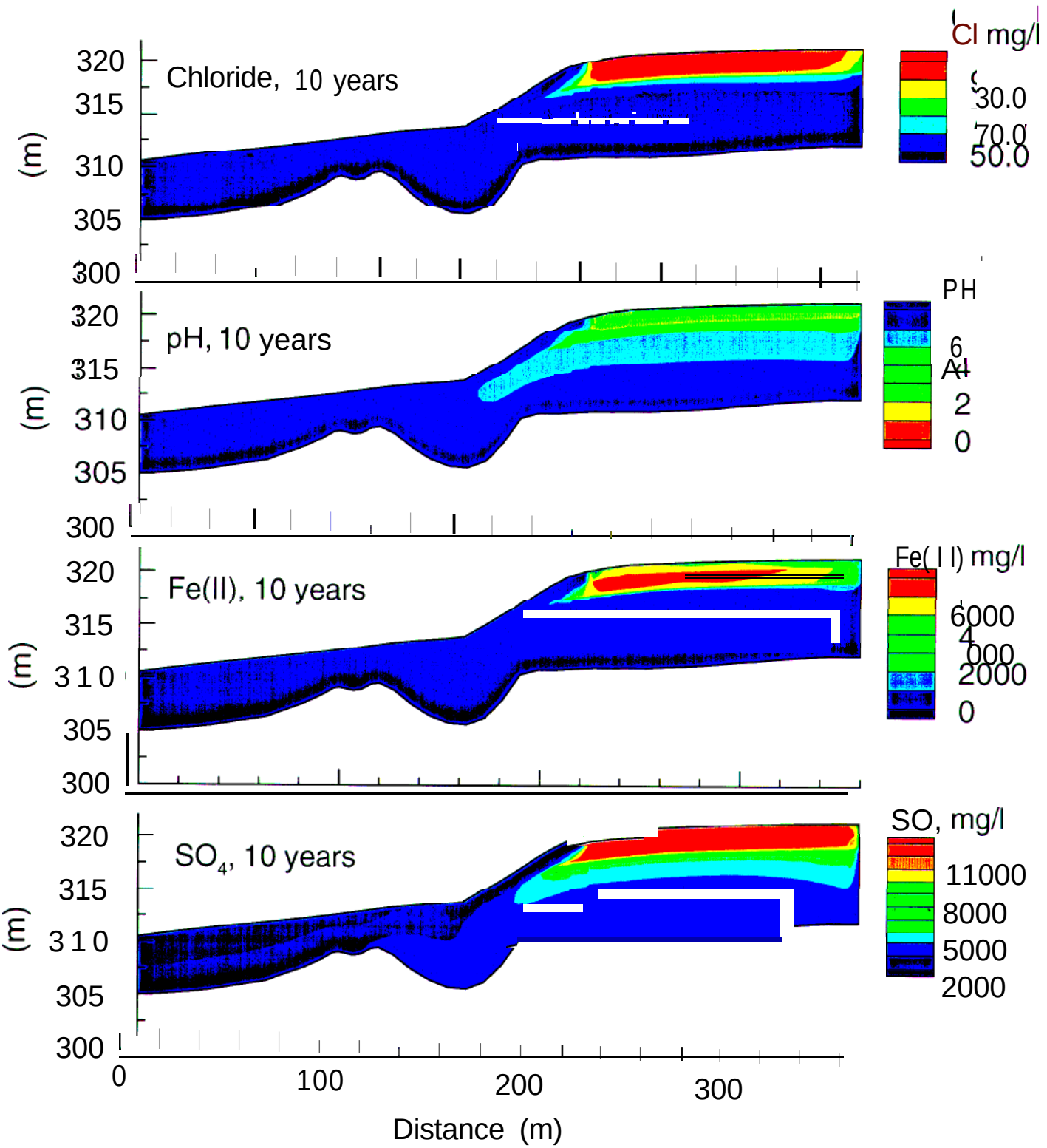

Figure 17. Nickel Rim simulation with calcite-enhanced tailings: Selected aqueous plumes at 10 years.

Sensitivity Analysis:

During calibration of the MINTOX model to the Nickel Rim site, several parameters were adjusted within reasonable ranges to acquire a solution consistent with the observed trends. To quantify model sensitivity to these parameters, a sensitivity analysis was completed on a 1D vertical section through the tailings. This analysis also serves to test the model with respect to stability and robustness under different conditions, and helps provide insight into the controlling processes affecting the evolution of AMD.

The conceptual model for the sensitivity simulations is based on a 1D simplified analogue of the calibrated Nickel Rim model. The vertical column is 10m long with a surface oxidation layer 1m deep. Groundwater flow velocity is assumed uniform at 0.6 m/yr which is consistent with the vertical velocity component within the shallow tailings area. A grid spacing of 0.1 m was used with a time step of 0.01 years.

A base case, or reference simulation was first defined using identical background and source aqueous chemistry from the calibration simulation (see Table 2). Solid mineral phase concentrations were also identical, with the exception that calcite was used in place of dolomite as the initial buffer mineral. A summary of the parameters for the 1D base case sensitivity run is provided in Table 3.

Table 3. Parameters used in the sensitivity simulations: base case values and parameter ranges.

	D_2 (m^2/s)	fs (%)	R (µm)	Calcite %	Dolomite %	Siderite %
Base Case	10^{-14}	5	76	100	0	0
Range	10^{-13}, 10^{-14},10^{-15}	1 ,5, 10	50, 76, 100	0, 50, 100	0, 50, 100	0, 50, 100

Note: solid phase fractions represent initial conditions only.

Base Case

The base case simulation was completed to 6 years with results shown as vertical profiles at 1, 3 and 6 year simulation times (Figure 18). The 6-year profile, shown as a solid line, is repeated in each of the sensitivity runs to provide a direct comparison. For clarity, only selected aqueous species are shown (pH, Fe(II), SO_4^{2-}, Al) together with the solid mineral phases of calcite, dolomite and/or siderite.

In the base case profiles, we observe trends consistent with those observed in the vertical profiles from the Nickel Rim calibration simulation (see Figure 11). For example, four distinct pH plateaus are observed at 6 years corresponding to, in order of decreasing pH, calcite (buffering at pH≈6.8), siderite (pH≈5), gibbsite (pH≈3.8), ferrihydrite (pH≈3.) and jarosite (pH≈2).

In the base case simulation, Fe(II) and SO_4^{2-} concentrations peak by about 3 years, then increase in extent as the plumes evolve to 6 years. Calcite dissolution zones and gypsum precipitation zones are consistent with the simulated pH plateaus.

Oxygen Grain Diffusion Rate (D_2)

Changes to the oxygen diffusion rate within the solid mineral grains (D_2) directly affects oxidation rates and the evolution of AMD. Increasing D_2 to 10^{-13} m^2/s for example, causes a significant drop in pH throughout the profile at 6 years (Figure 19), with corresponding increases in Fe(II), SO_4^{2-} and Al concentrations. In contrast, a decrease in D_2 to 10^{-15} m^2/s, virtually inhibits the oxidation process leaving Fe(II) SO_4^{2-} and Al concentrations near background levels. Solid mineral profiles change in response to the pH changes.

Fraction of Sulphur (fs)

MINTOX uses the mass fraction of sulphur within the tailings (fs) to specify the initial amount of oxidizable sulphur within the unsaturated zone. Variations in tailings mineralogy, even within a single tailings site, can lead to relatively large changes in fs which can in turn influence the generation of AMD. Murray (1977) for example, found sulphur fractions for several sites ranging from about 0.01 to 40 %, with an average of 4%. Jambor (1994) provides an excellent review of tailings mineralogy with examples from several sites throughout Canada.

The behaviour of the 1D system using sulphur fractions of 1% and 10% are compared to the base case simulation with fs=5% (Figure 20). Using fs=10%, peak Fe(II) concentrations have almost doubled to reach approximately 15 g/l while SO_4^{2-} concentrations have also increased. The calcite and gypsum solids show only minor changes since the pH profile has remained close to that of the base case. The high pH jump near the surface may be a boundary effect occurring at these relatively extreme conditions; this behaviour is currently being investigated.

Grain Radius (R)

The sulphide mineral grain radius (r) can vary among different tailings sites due to variations in processing methods and rock type, or within the same site due to sorting during tailings deposition. Robertson (1994) for example, provides grain size distribution curves for several locations within tailings sites at Copper Cliff and Kidd Creek, showing typical tailings grain diameters ranging from 1 to 200 µm.

Figure 21 Shows the effects of changing grain radius on the oxidation process in the 1D column. Decreasing the grain radius from the base case value of r=76 µm to 50 µm decreases the pH throughout the profile, and within the oxidation layer in particular. This behaviour is consistent

with higher oxidation rates occurring due to relatively larger surface areas exposed to oxidation per volume of porous media. The higher oxidation rates produce higher concentrations of Fe(II), SO_4^{2-} and Al, and push the calcite dissolution zone deeper within the section. In contrast, a larger grain diameter of 100 µm results in higher pH, and lower concentrations of the dissolved aqueous species.

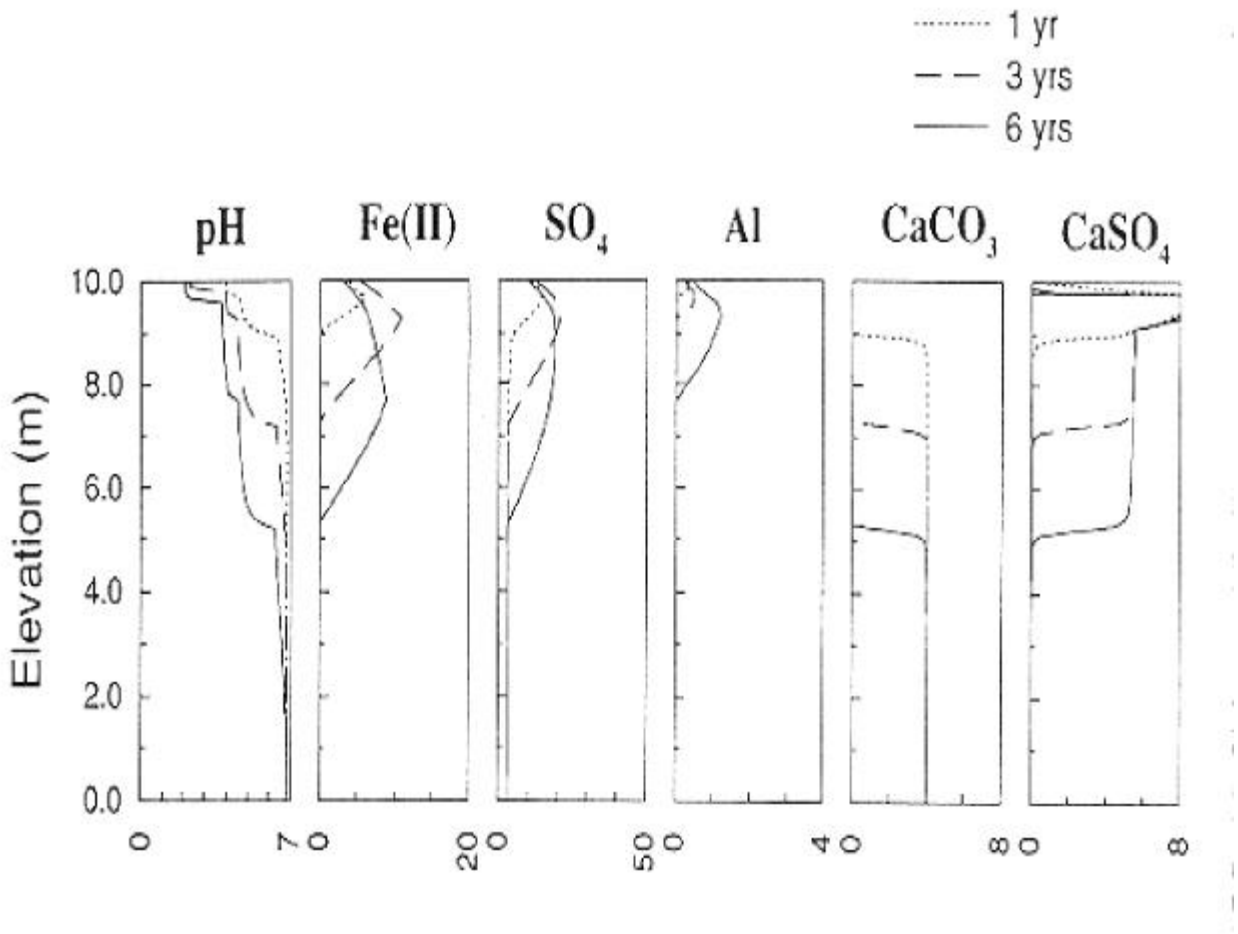

Figure 18. MINTOX 1D sensitivity simulation: Base case oxidation showing profiles of selected species at 1, 3 and 6 years. Axes units are pH and g/L.

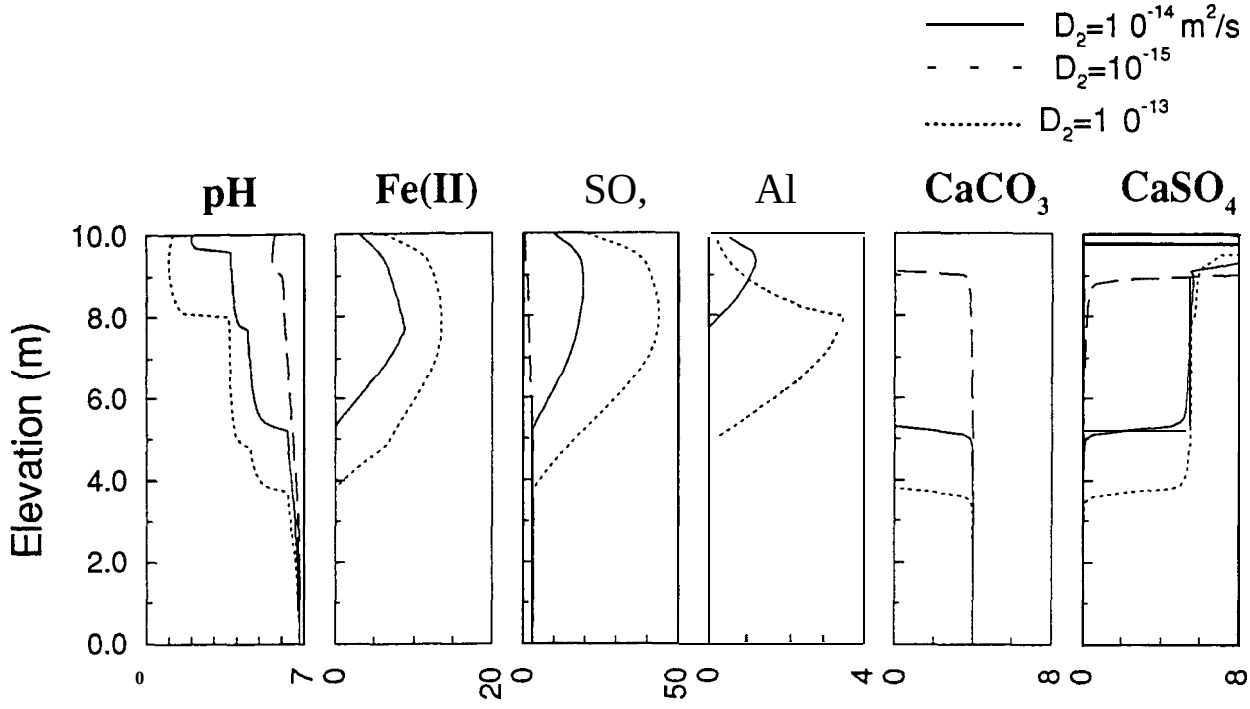

Figure 19. MINTOX 1D sensitivity simulation: Effect of oxygen diffusion rate through oxidation coating (D2). Axes units are pH and g/L, results shown at t=6 years.

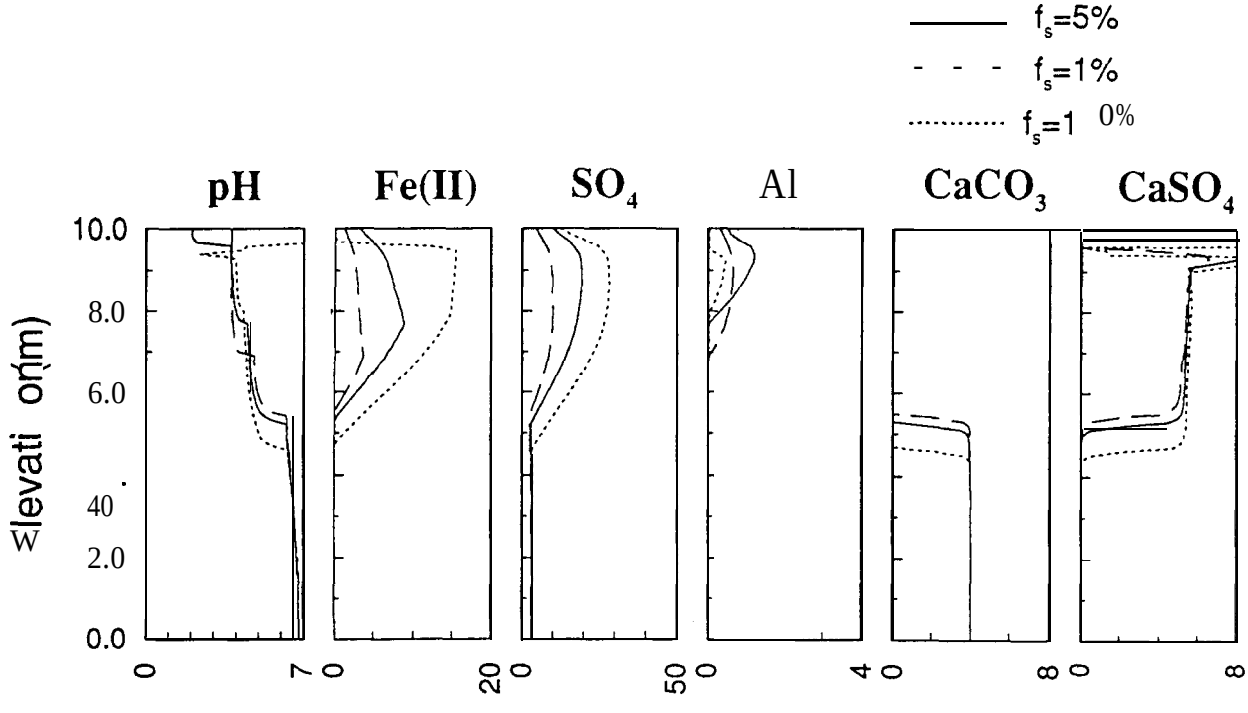

Figure 20. MINTOX 1D sensitivity simulation: Effect of initial fraction of sulphur (fs) in tailings. Axes units are pH and g/L, results shown at t=6 years.

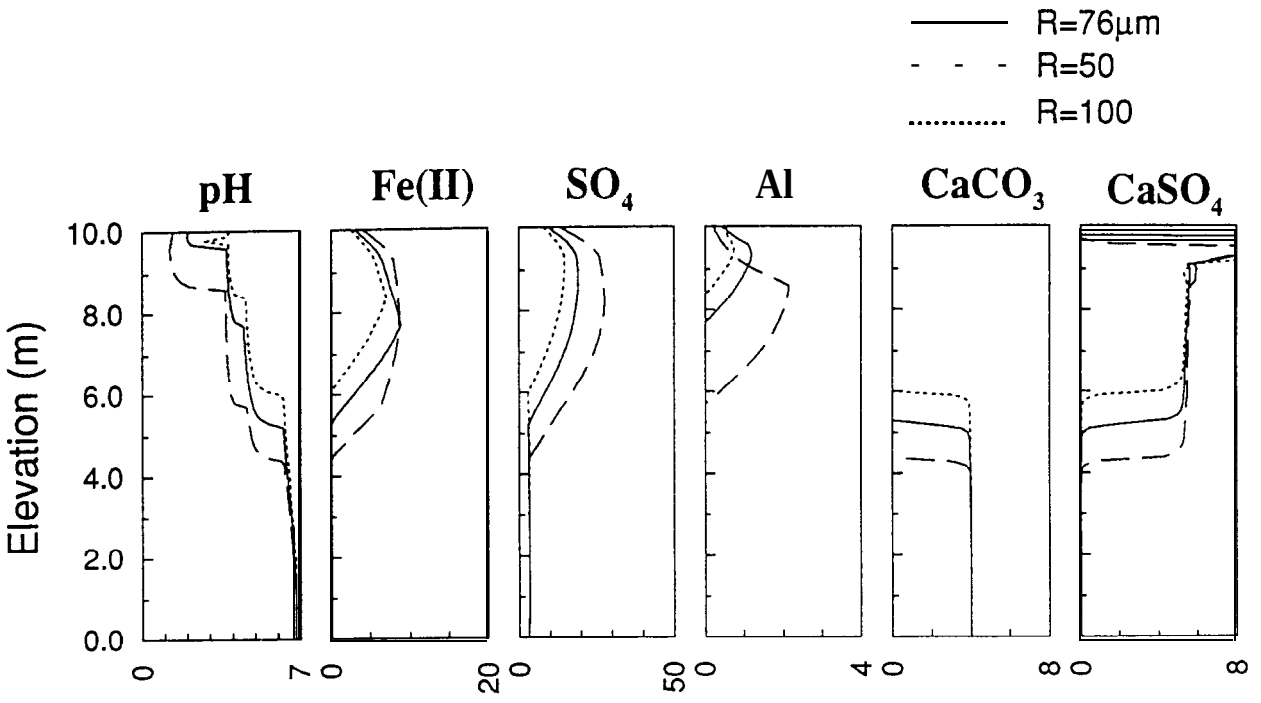

Figure 21. MINTOX 1D sensitivity simulation: Effect of grain radius. Axes units are pH and g/L, results shown at t=6 **years.**

Carbonate Buffer Minerals

Background carbonate buffer minerals within tailings and downgradient aquifers typically include either calcite ($CaCO_3$), dolomite $(CaMg)(CO_3)_2$) or siderite ($FeCO_3$), or some combination of each. To assess the importance of carbonate mineralogy on AMD generation, several additional simulations were made by varying the type, and concentrations of these common minerals.

Calcite/Dolomite

In the first case, the base case simulation is repeated assuming 100% dolomite (0.04 mol/l) and a 50/50 molar mixture of dolomite/calcite (0.02 mol/l each). These are compared to the base case profiles which assumed a natural buffer composition of 100% calcite (Figure 22).

The behaviour of all components for the three cases are similar due to similar mineralogies between calcite and dolomite, although subtle differences are apparent. Comparing the 100% calcite with 100% dolomite 6-year pH profiles, for example, shows that below a depth of about 5m, the solution equilibrates to a lower pH with dolomite. The equivalent dolomite equilibration zone is, however, more extensive than that of calcite which therefore maintains the buffering at pH≈6 up to an elevation of 6m. Because dolomite dissolution releases twice the amount of carbonate per mole of mineral, the equivalent siderite concentrations within the dolomite dissolution zone have doubled relative to the calcite case, although the siderite-buffered zone has become somewhat narrower. The high siderite concentrations in the 100% dolomite case also correlate well with lower Fe(II) concentrations. Above the siderite precipitation zone (>7.8m), and within the gibbsite buffer zone (pH≈3.9), lower pH levels of the dolomite case dissolves more gibbsite which in turn releases additional Al. Since sulphate is only indirectly affected by the background carbonate mineralogy, primarily through precipitation and dissolution of gypsum, it is not significantly affected by the carbonate mineralogy in this case.

Profiles from the mixture of calcite and dolomite show higher pH, and generally lower Fe(II) and Al concentrations relative to the base case. At depths below 6m (within the dolomite buffer zone), the pH profile follows that of the dolomite case since the calcite fraction becomes completely dissolved. The siderite buffer zone extends from 6-8.4 m, and is higher in concentration relative to the base case because of higher CO_3^{2-} concentrations from dolomite dissolution.

Calcite/Siderite

With a background buffer mineral composed entirely of siderite, the 1D simulations show consistently lower pH and higher levels of Fe(II), SO_4^{2-} and Al (Figure 23). There is no pH buffer at pH≈6-7 as there is with calcite; instead, the pH drop extends almost completely through the entire profile. The lower pH again produces high Al concentrations from gibbsite dissolution. Gypsum concentrations are low due to the absence of a Ca source which is present in the calcite dissolution case, and since gypsum is not precipitating, sulphate concentrations remain high from sulphide oxidation.

Buffer Concentrations

Increasing the background calcite concentration from the base case value of 0.04 mol/L to 0.4 mol/L maintains higher pH levels, with lower concentrations of Fe(II), SO_4^{2-} and Al (Figure 24). The calcite dissolution zone also extends only about 2m down from the surface, compared to over 4m in the base case. Decreasing the calcite concentration by a factor of 10 has the opposite effect of extending the low-pH profile, and causing generally higher concentrations of Fe(II), SO_4^{2-} and Al. Changes in dolomite concentrations (Figure 25) produce very similar responses.

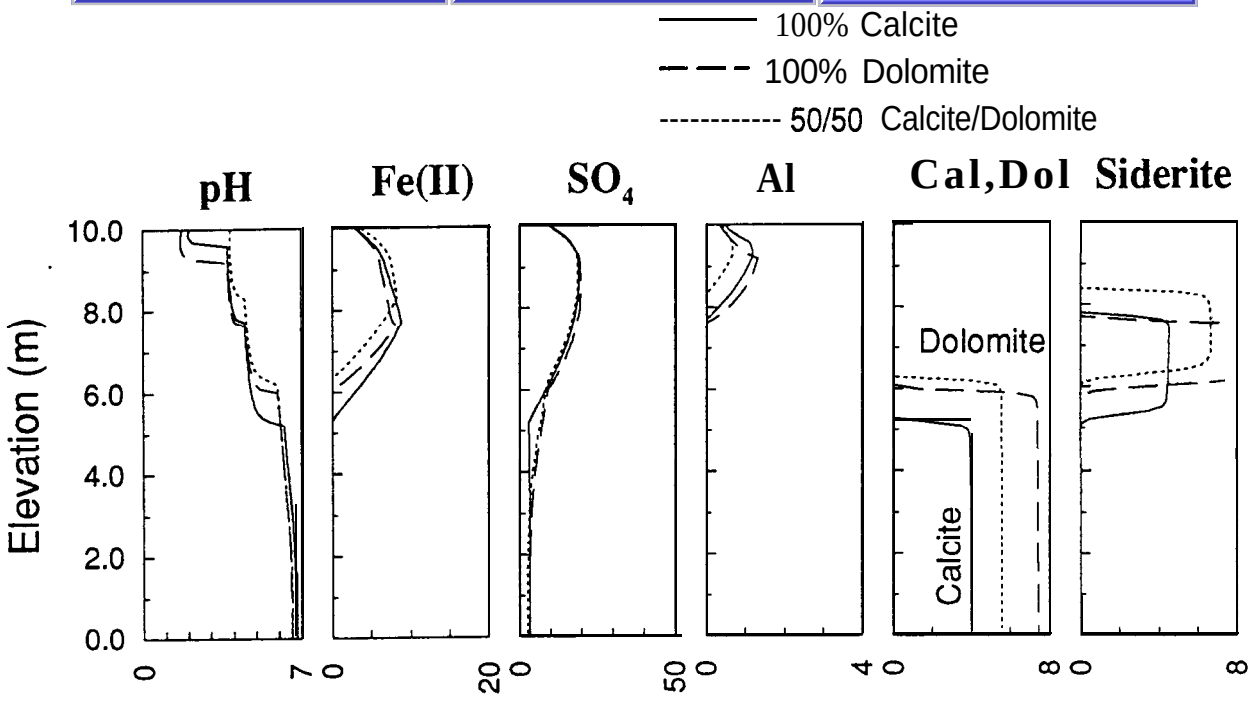

Figure 22. MINTOX 1D sensitivity simulation: Effect of carbonate mineralogy: calcite/dolomite. Axes units are pH and g/L, results shown at t=6 years.

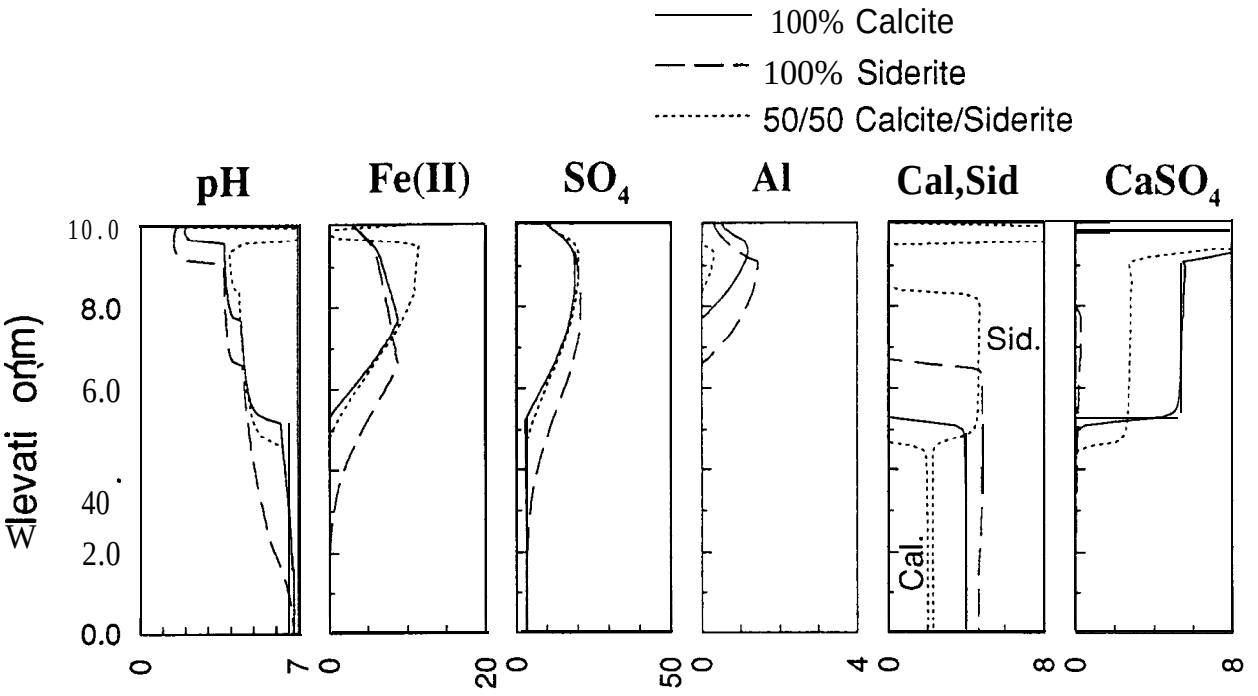

Figure 23. MINTOX 1D sensitivity simulation: Effect of carbonate mineralogy: calcite/siderite. Axes units are pH and g/L, results shown at t=6 years.

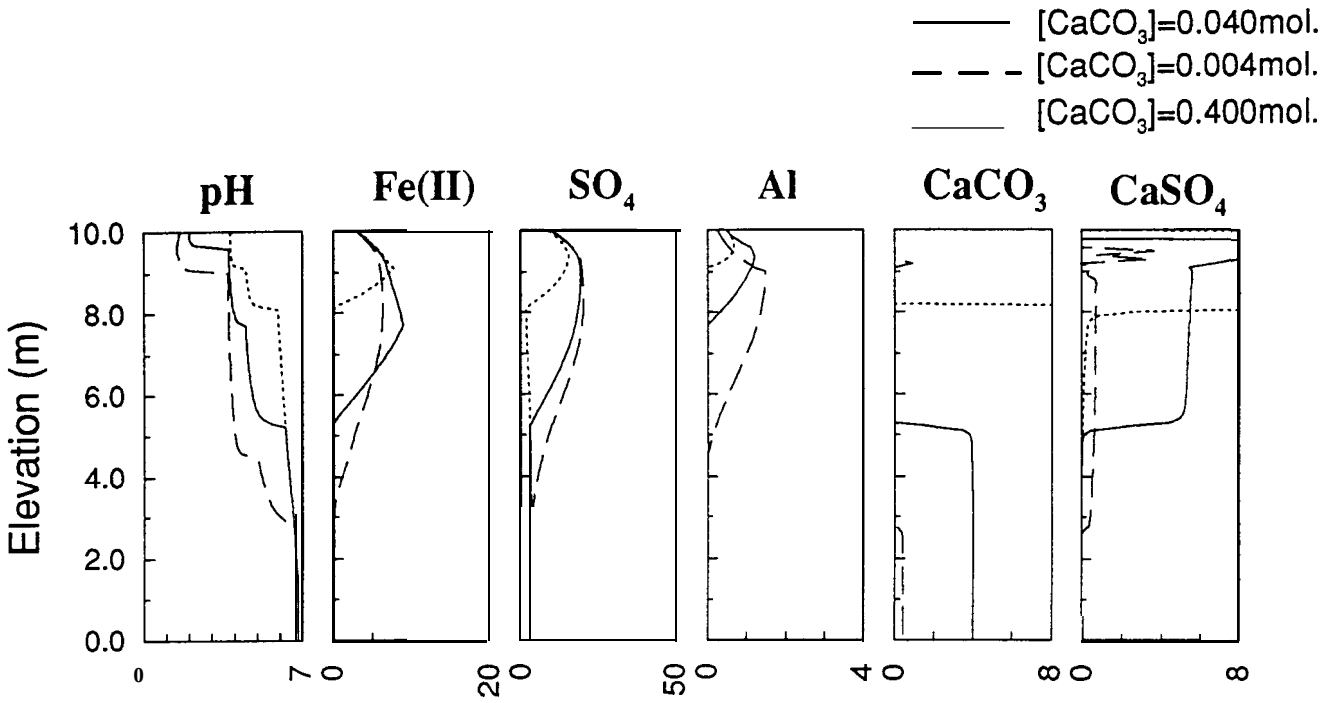

Figure 24. MINTOX1D sensitivity simulation: Effect of calcite buffer concentration. Axes units are pH and g/L, results shown at t=6 years.

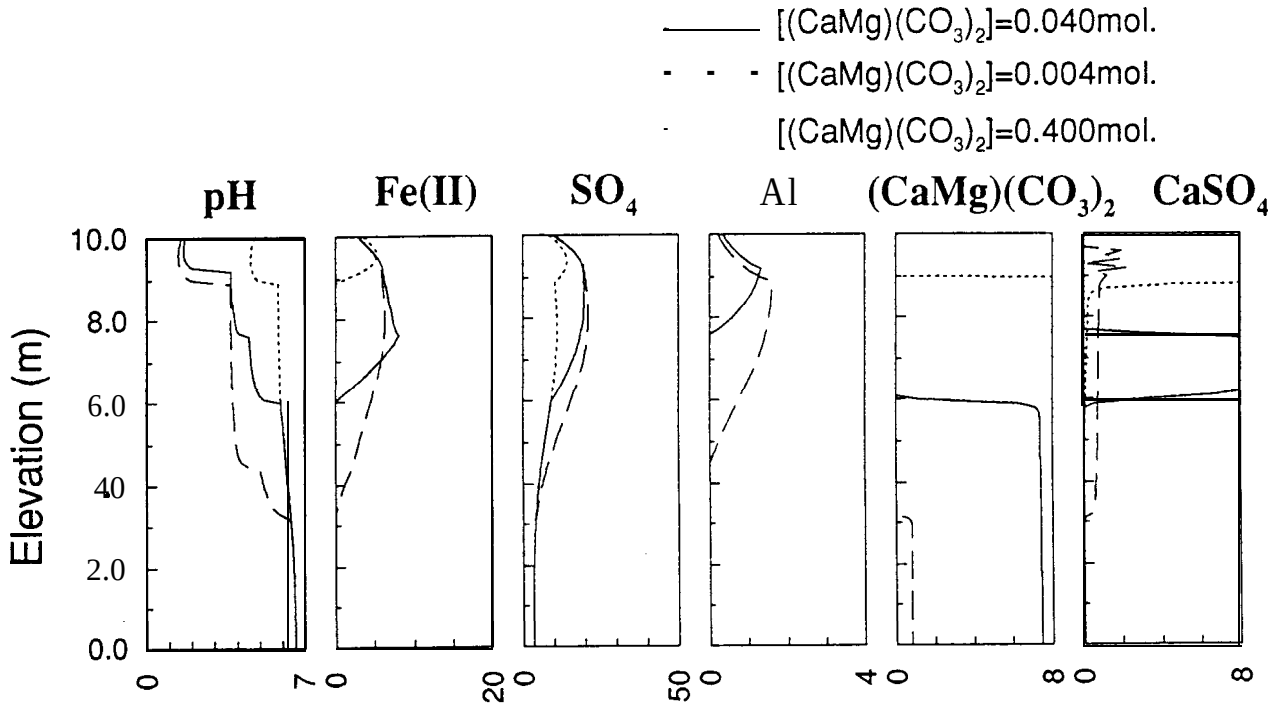

Figure 25. MINTOX1D sensitivity simulation: Effect of dolomite buffer concentration. Axes units are pH and g/L, results shown at t=6 years.

Summary and Conclusions

A new numerical model, MINTOX, has been shown to be an effective tool for gaining insight into the coupled processes of oxygen diffusion, sulphide oxidation, mineral speciation and advective-dispersive transport within mine tailings environments. Model evaluation, which has included applications to the Nordic (Elliot Lake) and Nickel Rim tailings impoundments, has shown results consistent with the conceptual models developed for each site although some differences persist due to the assumption of local geochemical equilibrium.

The Elliot Lake simulations showed that under favourable conditions, heavy metals can be effectively immobilized within carbonate-bearing tailings. By buffering pH changes, the background concentration of the carbonate minerals was shown to be important to the immobilization process.

The MINTOX application to the Nickel Rim tailings site successfully simulated the evolution of AMD, including 14 aqueous components, and 9 mineral solids, for a period 75 years. Model results at 36 years correlated well with the observed high Fe(II) and SO_4^{2-} concentrations. Although peak oxidation rates were reached within 10 years, long-term trends showed low-pH and high concentrations of oxidation products persisting for over 50 years.

The effectiveness of two remedial measures for controlling AMD was evaluated by applying MINTOX to simulate a tailings flood scenario, and a scenario in which the tailings buffer capacity was increased. The flood scenario showed the most favourable result with pH rapidly recovering, and lower Fe(II) and SO_4^{2-} concentrations following the flood.

A 1D sensitivity analysis based on the Nickel Rim site showed a significant influence of all major parameters including the oxygen diffusion coefficient within the grains (D_2), the fraction of sulphide mineral (fs), grain radius (R) and buffer mineralogy. Results suggest that spatial

variation in tailings properties may have a significant effect on the generation of AMD. Inherent uncertainty in the model predictions must be acknowledged, and the model should be used primarily for testing conceptual models and for comparing the effectiveness of alternative remediation strategies.

References

Allison, J.D., D.S. Brown, and K.J. Nova-Gradac, MINTEQA2/PRODEFA2, A geochemical assessment model for environmental systems: Version 3 User's Manual, US/EPA/3-87/012, Environmental Protection Agency, Athens, Georgia, 1990.

Appelo, C.A.J. and A. Willemsen, Geochemical calculations and observations on saltwater intrusion, I, A combined geochemical/mixing cell model, J. Hydrol., 94, 313-330, 1987.

Bain, J.G., Hydrogeochemical investigation and reactive transport modelling of an aquifer impacted by mine drainage, MSc. Thesis, University of Waterloo, 1996.

Bain, J.G., D.W. Blowes, W.D. Robertson, The hydrogeochemistry of a sand aquifer affected by discharge from the Nickel Rim Tailings, Sudbury, Ontario, Proceedings, Sudbury '95, Conference on Mining and the Environment, Sudbury, Ontario, May 1995.

Bear, J., *Dynamics of Fluids in Porous Media*, American Elsevier, New York, 1972.

Blowes, D.W., C.J. Ptacek and J.L. Jambor, Remediation and prevention of low-quality drainage from tailings impoundments, *Short Course Handbook on Environmental Geochemistry of Sulphide Mine-Wastes*, J.L. Jambor & D.W. Blowes (Ed.), Chapter 13, Mineralogical Association of Canada (1994).

Daus, A.D., E.O. Frind, and E.A. Sudicky, Comparative error analysis in finite element formulations of the advection-dispersion equation, Adv. Water Resour., 8, 86-95, 1985.

Davis, G.B., and A.I.M. Ritchie, A model of oxidation in pyritic mine wastes: Part 1: equations and approximate solution, Applied mathematical modelling, 10, 314-322, 1986.

Davis, G.B., G. Doherty, and A.I.M. Ritchie, A model of oxidation in pyritic mine wastes: Part 2: comparison of numerical and approximate solution, Applied mathematical modelling, 10, 323-329, 1986.

Davis, G.B., and A.I.M. Ritchie, A model of oxidation in pyritic mine wastes: Part 3: import of particle size distribution, Applied mathematical modelling, 10, 314-322, 1987.

Feasby, G. And R.K. Jones, Report of Results of a Workshop on Mine Reclamation, Canada Centre for Mineral and Energy Technology, Toronto, Ontario, March 10-11, 1994.

Felmy, A.R., D.C. Girvin, and E.A. Jenne, MINTEQ: A computer program for calculating aqueous geochemical equilibria, Report, U.S. Environmental Protection Agency, Washington D.C., 1983.

Frind, E.O., W.H.M. Duynisveld, O. Strebel, and J. Boettcher, Modelling of multicomponent transport with microbial transformation in groundwater: The Fuhrberg case, Water Resour. Res., 26(8), 1707-1719, 1990.

Gerke, H.H., E.O. Frind, and J.W. Molson, Modelling the effect of chemical heterogeneity on acidification and solute leaching in overburden mine spoils, in submission, Journal of Hydrology, 1997.

Guiguer, N., T. Franz, J.W. Molson, and E.O. Frind, *FLONET User Guide*, Waterloo Hydrogeologic and WCGR, 1994.

Huyakorn, P.S., and G.F. Pinder, *Computational Methods in Subsurface Flow*, Academic Press, 1983.

Jambor, J.L., Mineralogy of sulphide-rich tailings and their oxidation products, *Short Course Handbook on Environmental Geochemistry of Sulphide Mine-Wastes*, J.L. Jambor & D.W. Blowes (Ed.), Chapter 3, Mineralogical Association of Canada, 1994.

Johnson, H.R., The physical and chemical hydrogeology of the Nickel Rim mine tailings, Sudbury, Ontario, Msc. Thesis, University of Waterloo, 1993.

Leismann, H.M., and E.O. Frind, A symmetric matrix time integration scheme for the efficient solution of the advection-dispersion problem, Water Resour. Res., 25(6), 1133-1139, 1989.

Levenspiel, O., Chemical Reaction Engineering, 2nd edition, J. Wiley & Sons, New York, 1972.

Liu, C.W. and T.N. Narasimhan, Redox-controlled multiple-species reactive chemical transport 1. Model development, Water Resour. Res., 25(5), 862-882, 1989.

Mangold, C.D., and C.F. Tsang, A summary of subsurface hydrological and hydrochemical models, Rev. Geophys., 29(1), 51-71, 1991.

Mayer, K.U., Modelling of reactive transport in variably saturated porous, Paper presented at the Geological Society of America, Denver, Colorado, fall, 1996.

Molson, J.W., E.O. Frind, D.W. Blowes, and C.J. Ptacek, Predicting the behaviour of thermal energy and temperature-dependent reactive mass transport in shallow aquifers, Proceedings, CALORSTOCK '94, 6th International Conference on Thermal Energy Storage, Espoo, Finland, August 1994.

Morin, K.A., J.A. Cherry, N.K. Davé, T.P.Lim, and A.J. Vivyurka, Migration of acidic groundwater seepage from uranium-tailings impoundments 1. Field study and conceptual hydrogeochemical model, Jour. of Cont. Hydrology, 2, 271-303.

Murray, J.W., Iron Oxides, *Reviews in Mineralogy 6*, 47-98 (1979).

Robertson, W.D., The physical hydrogeology of mill-tailings impoundments, *Short Course Handbook on Environmental Geochemistry of Sulphide Mine-Wastes*, J.L. Jambor & D.W. Blowes (Ed.), Chapter 1, Mineralogical Association of Canada, 1994.

Schmid, G., and D. Braess, Comparison of fast equation solvers for groundwater flow problems, in *Groundwater Flow and Quality Modelling*, NATO ASI Ser., Ser. C, 224, 173-188, 1988.

Schulz, H.D. and E.J. Reardon, A combined mixing cell/analytical model to describe two-dimensional reacting solute transport for unidirectional groundwater flow, Water Resour. Res., 19(2), 493-502, 1983.

Steefel, C.I., and K.T.B. MacQuarrie, Approaches to modelling of reactive transport in porous media, In: *Reactive Transport in Porous Media*, Reviews in Mineralogy Vol. 34, Chapter 2, P.H. Ribbe (Ed.), Mineralogical Society of America, 1996.

Stumm, W., and J.J. Morgan, *Aquatic Chemistry*, Wiley-Interscience, New York, 1981.
Thomson, Jas. E., *MacLennan and Scadding Townships*, Geological Report No. 2, Ontario Dept. Of Mines: 25-27, 1961.

Walter, A.L., E.O. Frind, D.W. Blowes, C.J. Ptacek, and J.W. Molson, Modelling of multicomponent reactive transport in groundwater 1. Model development and evaluation, Water Resour. Res., 30(11), 3137-3148, 1994a.

Walter, A.L., E.O. Frind, D.W. Blowes, C.J. Ptacek, and J.W. Molson, Modelling of multicomponent reactive transport in groundwater 2. Metal mobility in aquifers impacted by acidic mine tailings discharge, Water Resour. Res., 30(11), 3149-3158, 1994b.

Wunderly, M.D., D.W. Blowes, E.O. Frind, and C.J. Ptacek, Sulphide mineral oxidation and subsequent reactive transport of oxidation products in mine tailings impoundments: A numerical model, Water Resources Research, 32(10):3173-3187, 1996.

Wunderly, M.D., D.W. Blowes, E.O. Frind, C.J. Ptacek, T.A. Al, A multi-component reactive transport model incorporating kinetically controlled pyrite oxidation, Proceedings, Sudbury '95, Conference on Mining and the Environment, Sudbury, Ontario, May 1995.

Appendix A
The Nickel Rim Transport Model: Time Evolution of AMD

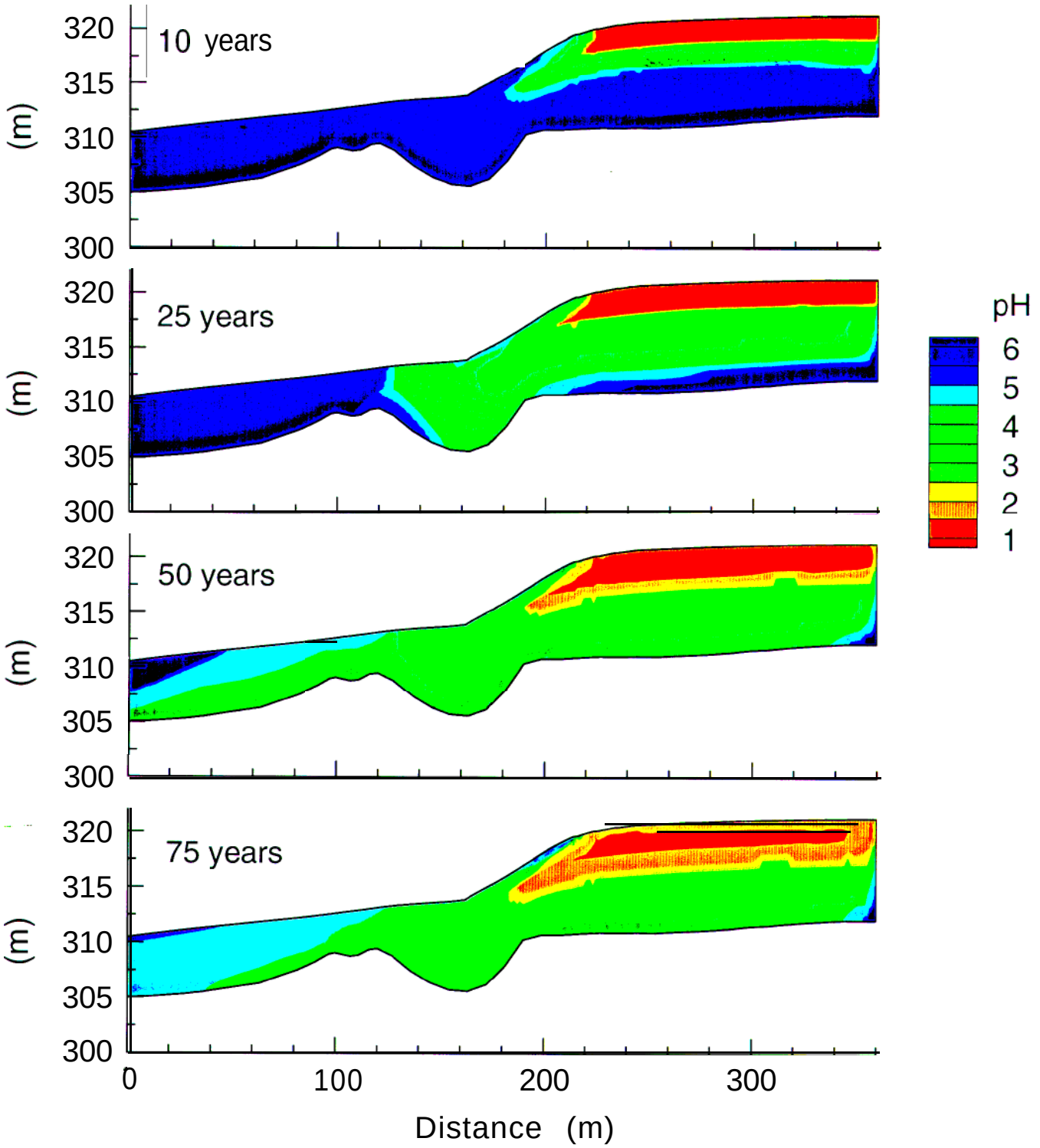

Figure Al. Nickel Rim base case simulation: pH plume at IO, 25, 50 and 75 years.

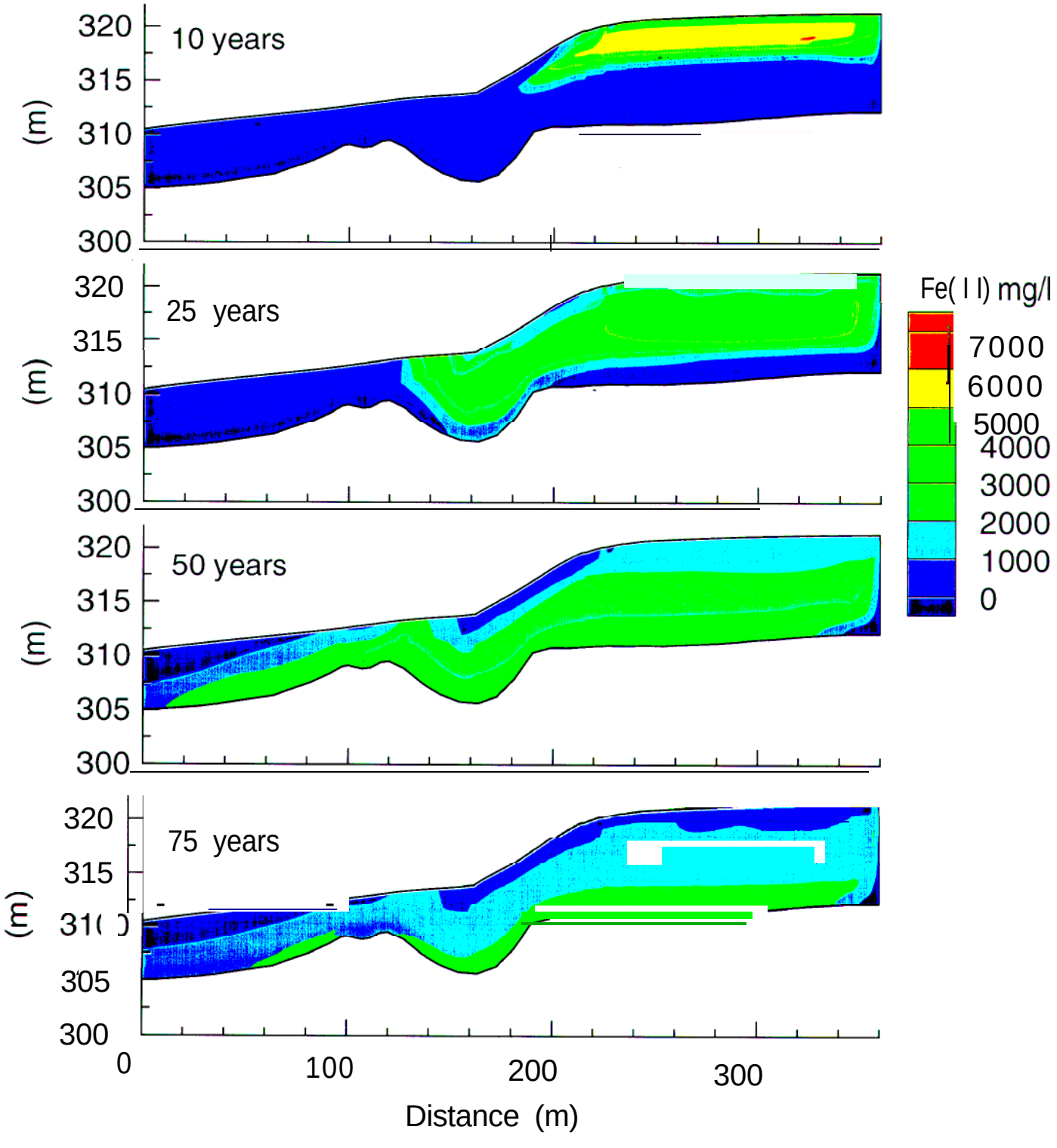

Figure A2. Nickel Rim base case simulation: Fe(II) plume at IO, 25, 50 and 75 years.

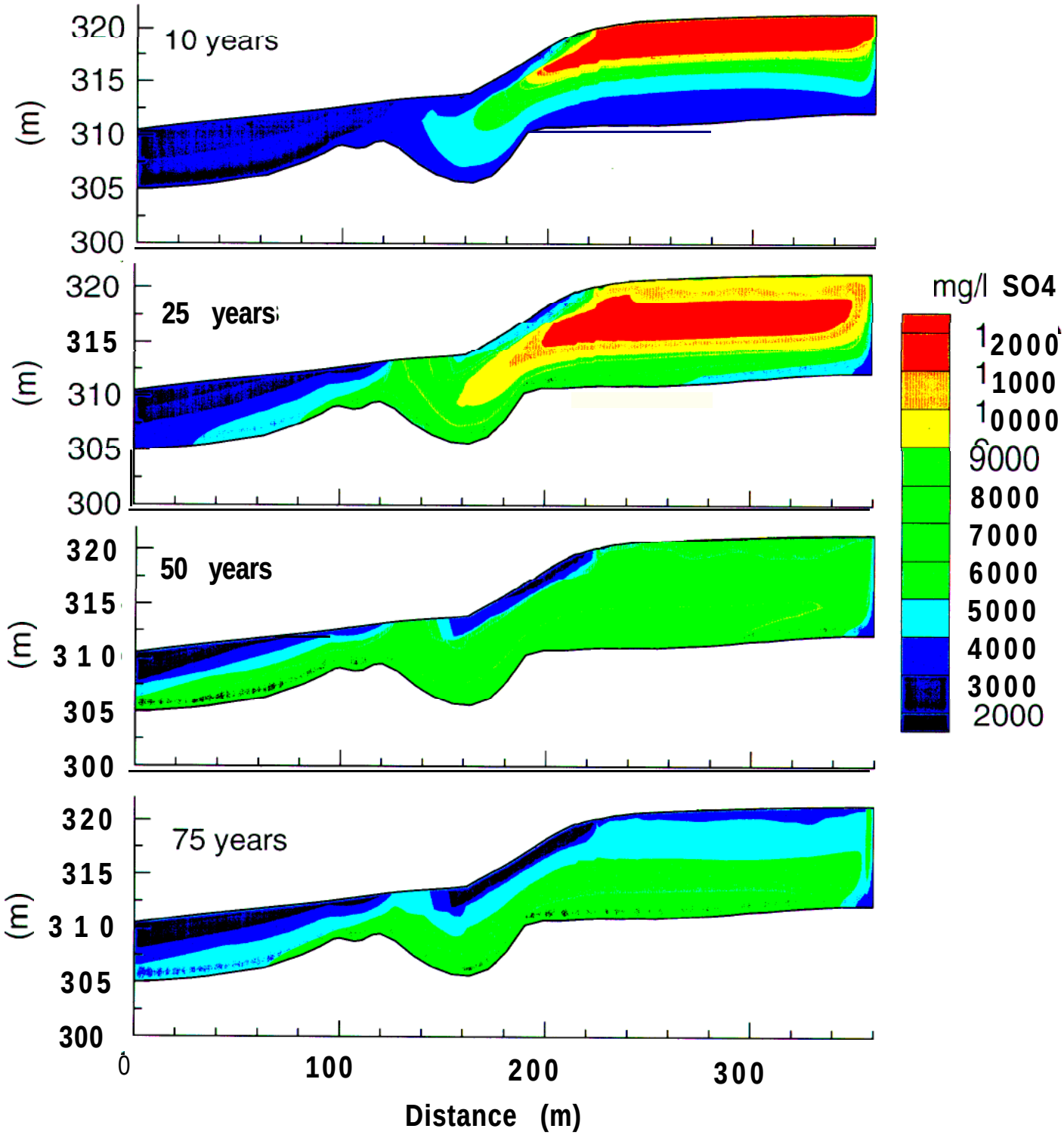

Figure A3. Simulated Nickel Rim sulphate plume at IO, 25, 50 and 75 years.

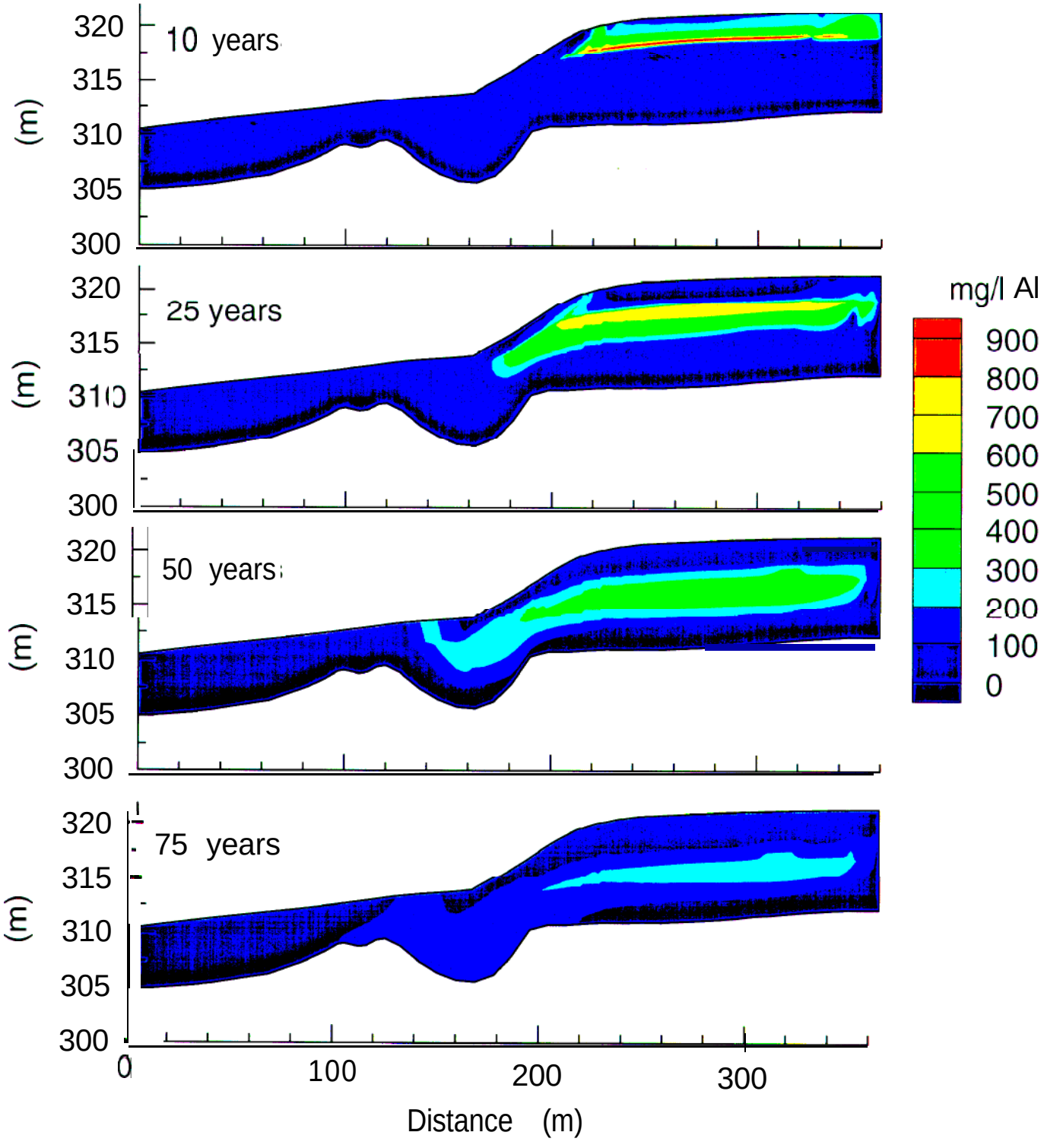

Figure A4. Nickel Rim base case simulation: Aluminum plume at 10, 25, 50 and 75 years.

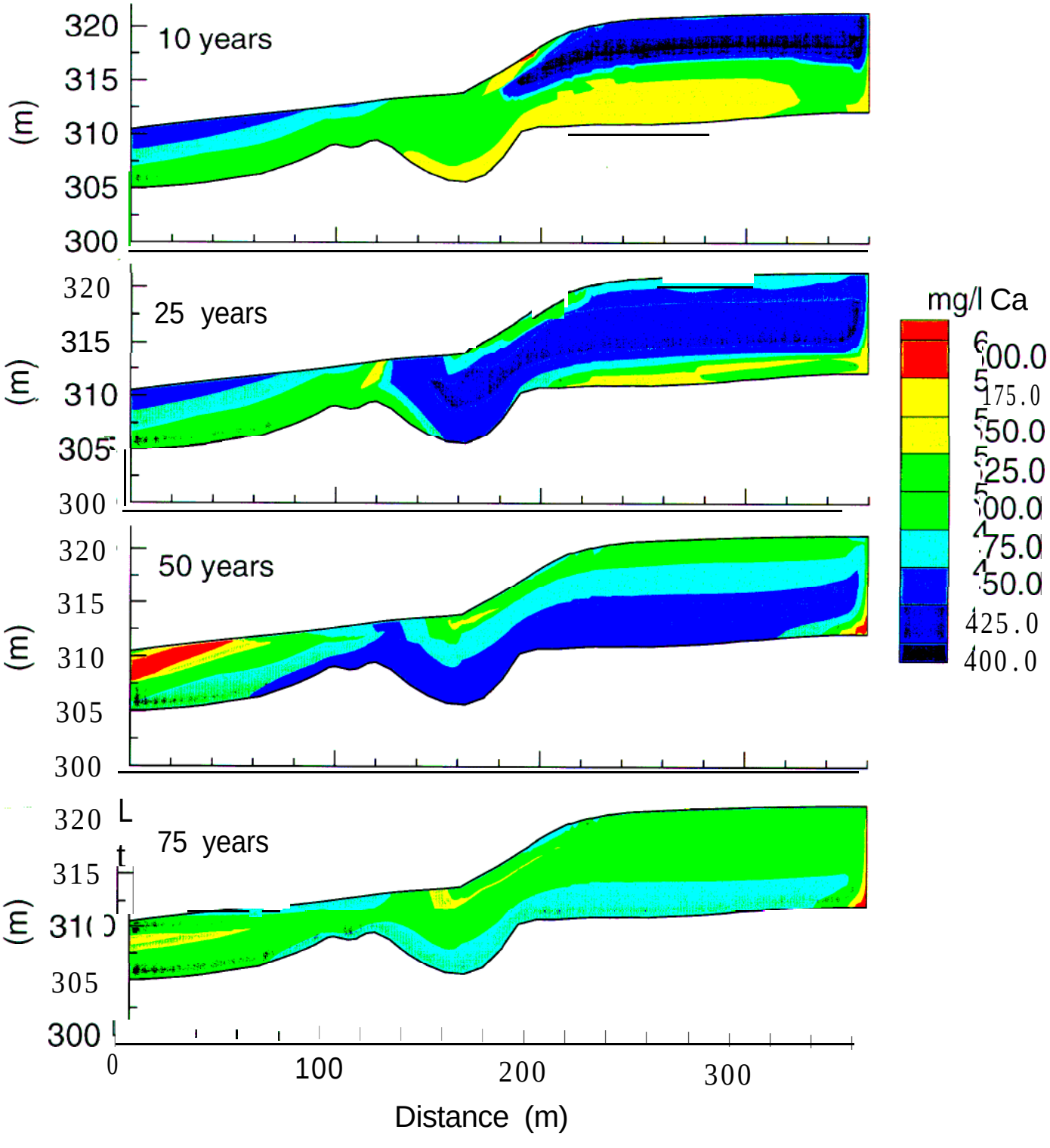

Figure A5. Nickel Rim base case simulation: Calcium plume at 10, 25, 50 and 75 years.

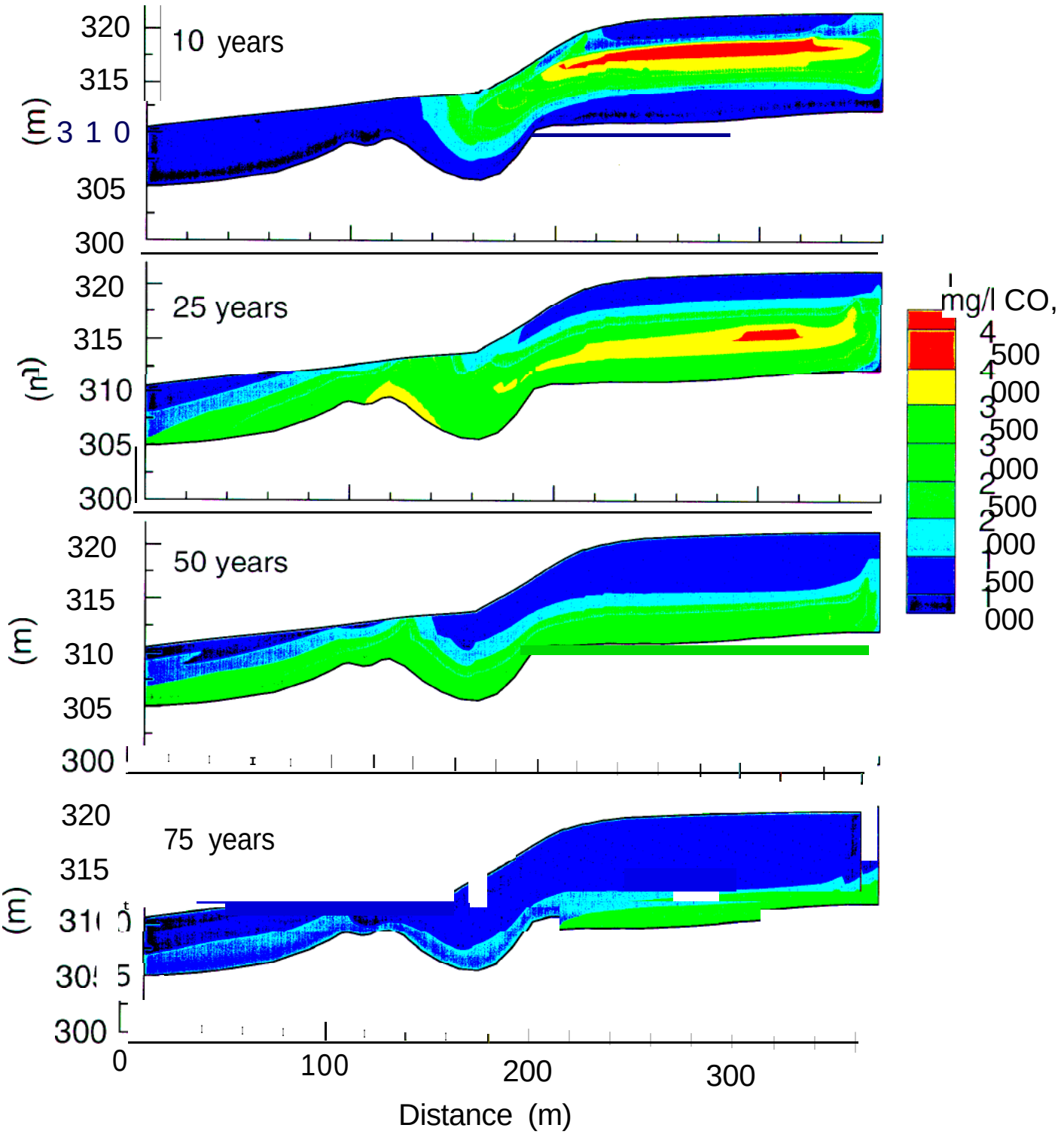

Figure A6. Nickel Rim base case simulation: Carbonate plume at 10, 25, 50 and 75 years.

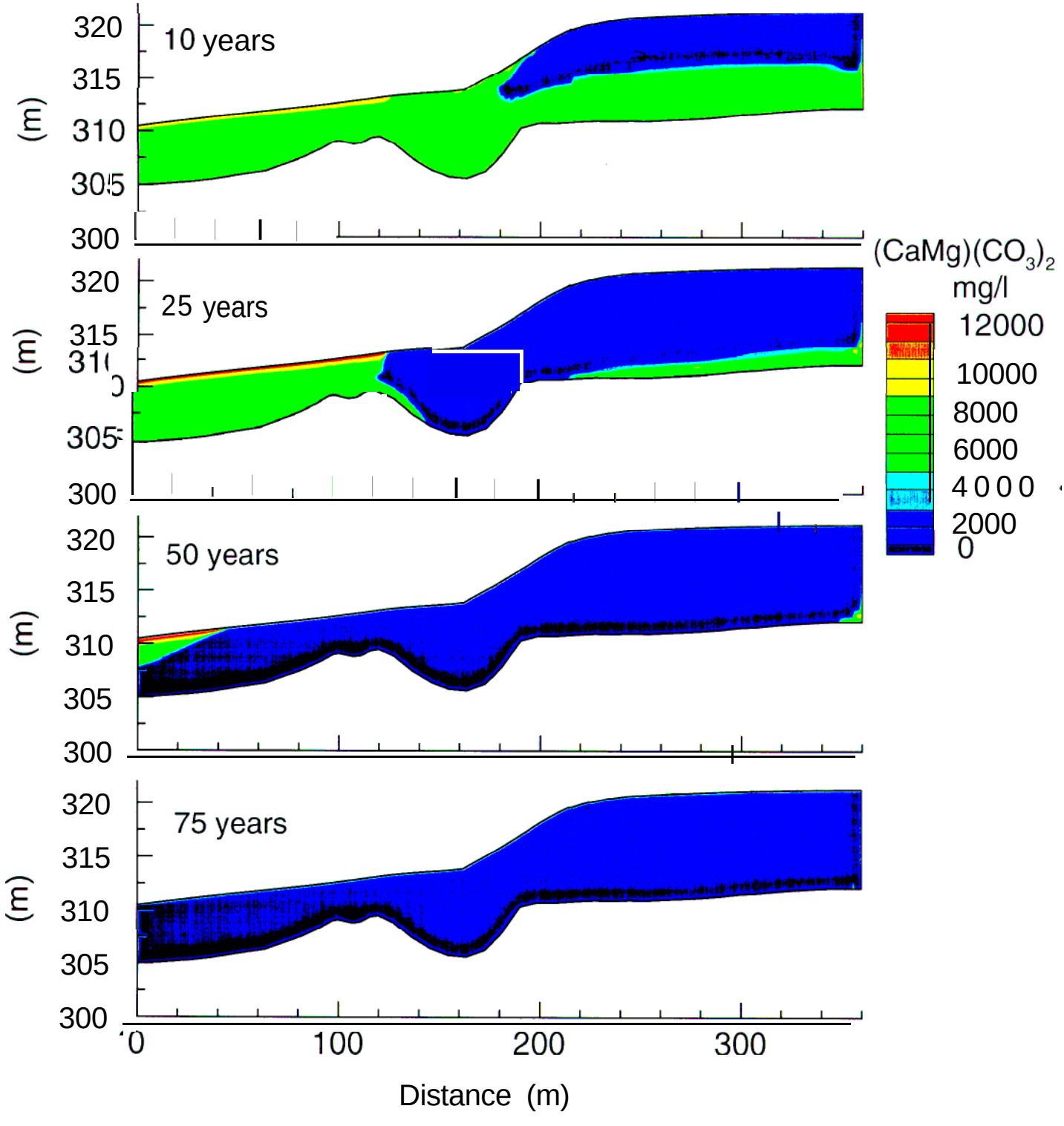

Figure A7. Nickel Rim base case simulation:
Dolomite dissolution plume at IO, 25, 50 and 75 years.

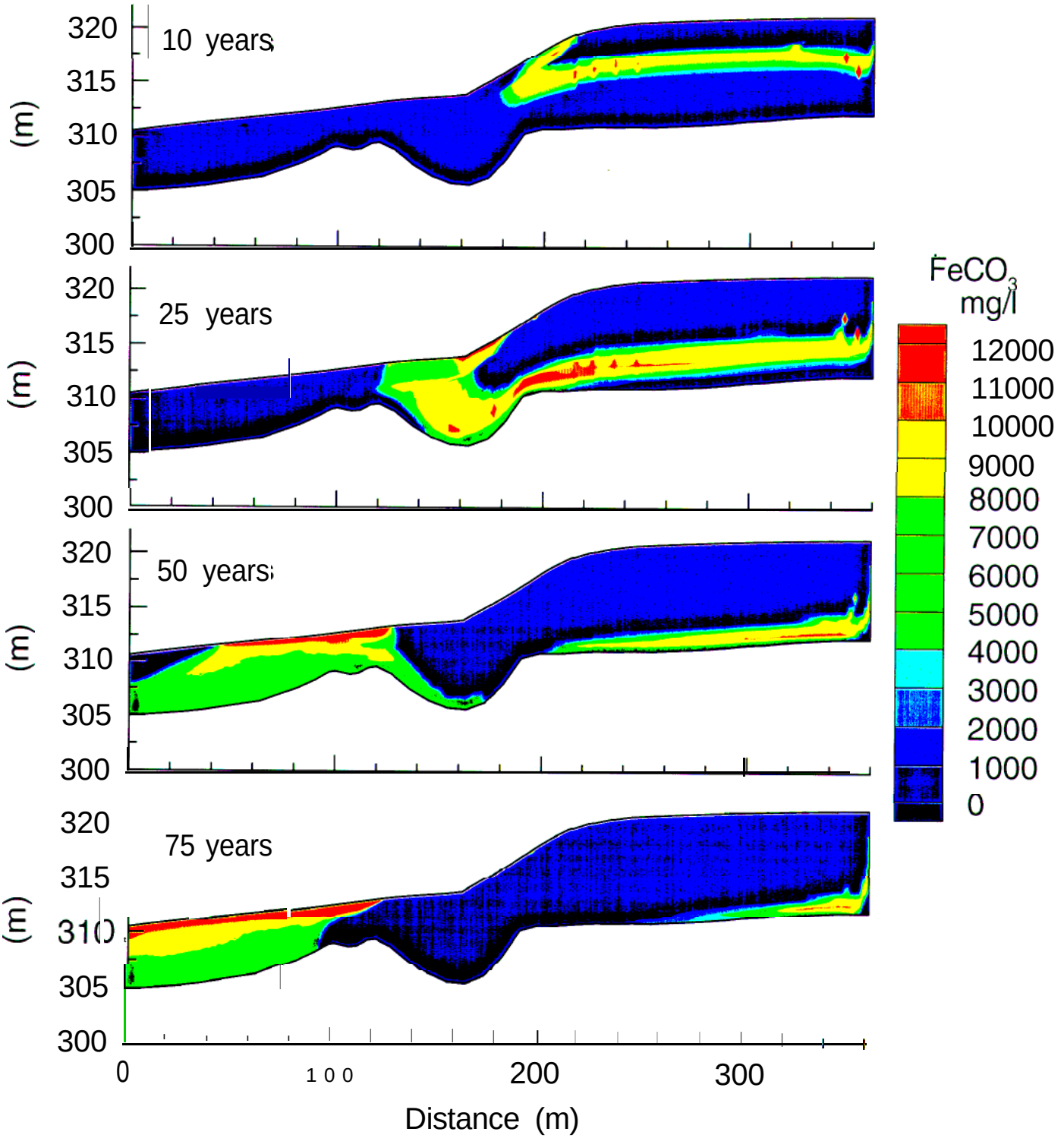

Figure A8. Nickel Rim base case simulation: Siderite distribution at 10, 25, 50 and 75 years.

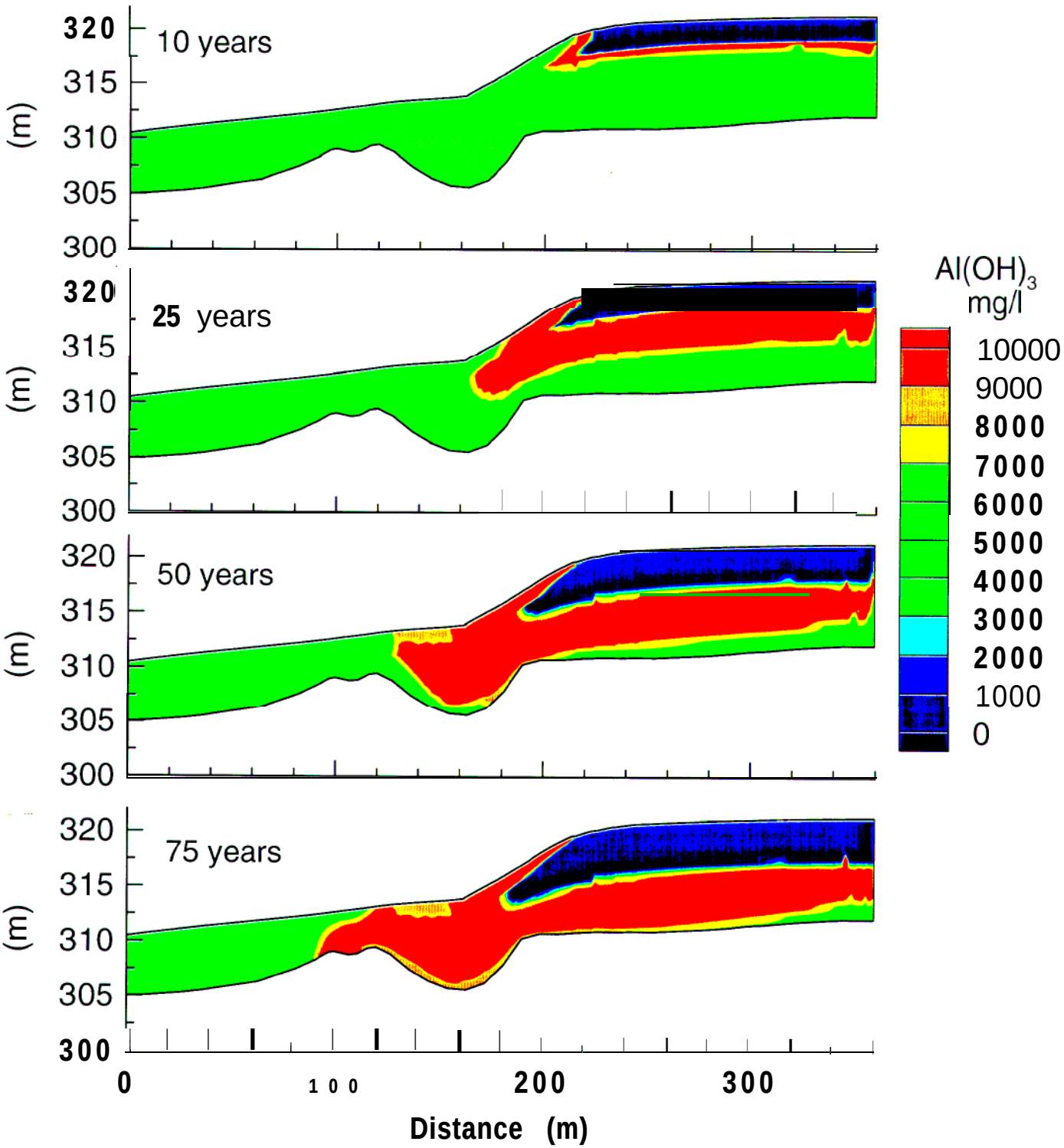

Figure A9. Nickel Rim base case simulation: Gibbsite distribution at 10, 25, 50 and 75 years.

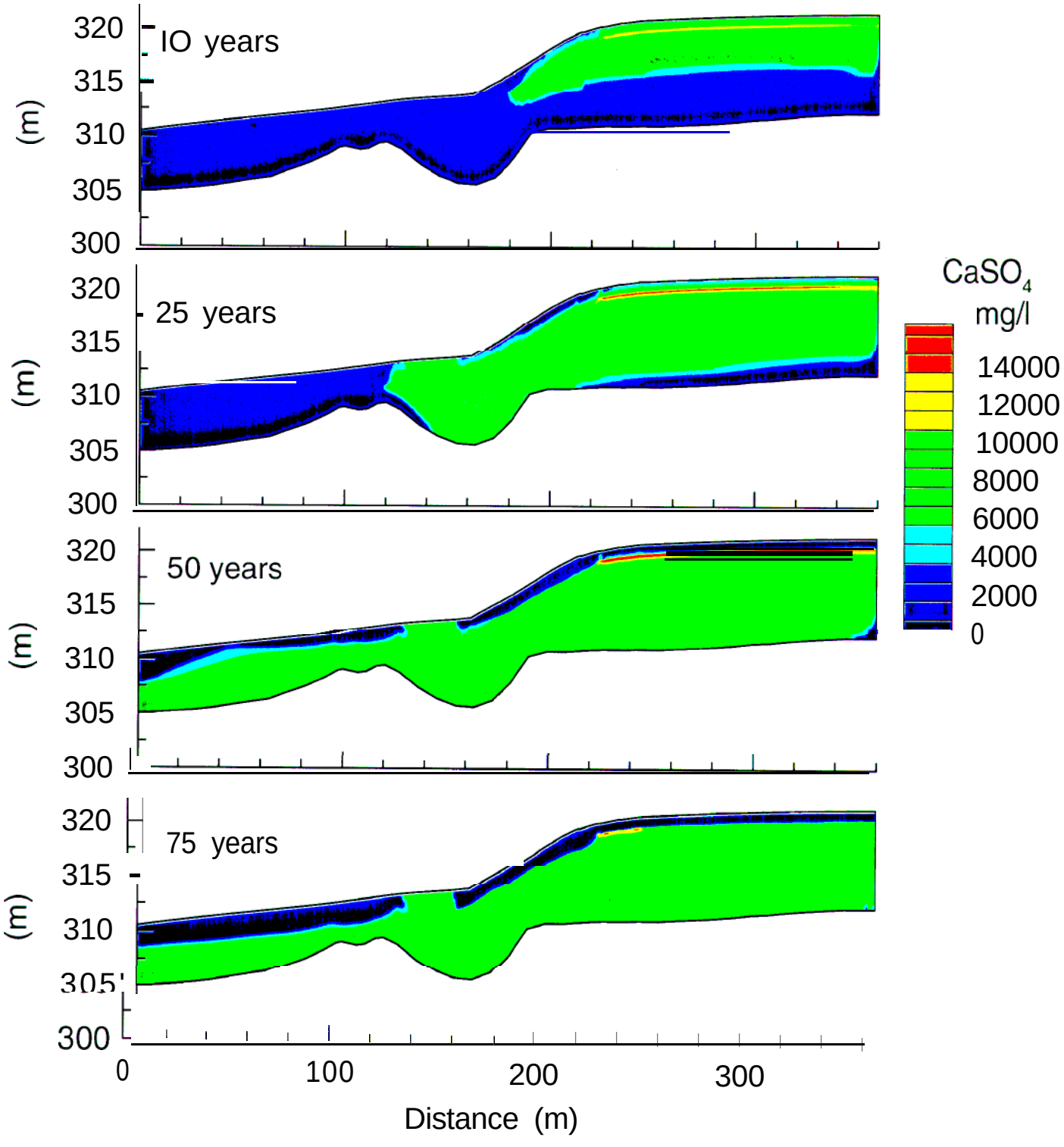

Figure Al 0. Nickel Rim base case simulation: Gypsum distribution at IO, 25, 50 and 75 years.

Appendix B
FLONET and MINTOX Data Files

```
flow_nickel_nov9.data          Thu Dec 14 19:54:05 1995

FLONET: HEAD / STREAM FUNCTION MODEL: CENTRB FOR GROUNDWATER RESEARCH
FLOW.DATA  - SAMPLE DATA FILE -  Nickel Rim
Nov. 22, 1995
    0     0    -999.                                          ;SSINK
    0          11     0     1                                ;kp,kv,kg,kread,ksol
v
  259    31     360.      320.       1     1                 ;NX,NY,XL,YL,NGX,NGY
   15    15  0.01    300.                                    ;maxit,nwtl,tol,datum
    0                                                         ;WATERTABLE CODE(KW
)
   20.          0.0         .25      0.0                     ;WATERTABLE shape
    1    1    31     1    10.47                              ;BOUNDARY CONDITION
S
    a     1  102     0  6.00e-9                              ;BOUNDARY CONDITIONS
    2  103  110     0  -0.19-0
    2  110  115     0  -0.5e-8
    2  115  120     0  -l.Oe-8
    2  120  122     0  -3.9-S
    2  123  145     0  a.ooe-9                              ;BOUNDARY CONDITIONS
    2  146  999     0  6.00e-9                              ;BOUNDARY CONDITIONS
    3    1  999     0     0.                                ;BOUNDARY CONDITION
S
    4    1  999     0     O.                                ;BOUNDARY CONDITION
S
   -1                                                      ;END BOUNDARY CONDITIO
NS
   -1                                                      ;END INTERNAL DIR NODE
S
    1 15480 l.lOOB-05  l.lOOB-05   0.0      0.40  ..l        ;hydraulic K
   95.5  161.    311.5    320.    4.50e-6   4.50e-6   O.   .40  +1  ;
  143.    151.    310.5    312.    4.500-6   4.50e-6   0.   .40  +1  ; ds. from dam
  151.    164.    310.     311.5   4.50e-6   4.50e-6   0.   .40  +1  ;
  161.    170.    308.0    320.5   2.50e-6   2.50e-6   0.   .40  +1  ;
  161.    215.    305.0    321.    1.20e-6   1.20e-6   0.   .40  +1  ; DAM
  215.    225.    308.     322.    1.70e-6   1.70e-6   0.   .40  +1  ; med K tail
  225.    235.    308.     322.    2.30e-6   2.30e-6   0.   .40  +1  ; med K tail
  235.    245.    308.     322.    3.30e-6   3.30e-6   0.   .40  +1  ; med K tail
  245.    361.    308.     322.    7.50e-6   6.50e-6   0.   .40  -1  ; main tail
  294     516     24     30        1.70e-7   6.50e-6   0.   .40  -1  ; unsat zone



c   1   40    1    25    1.0E-09   1.00-09   0.0        0.3
C THE LAST LINES SPBCIFY INTERNAL CONDUCTIVITY CHANGES BY REGION
```

```
 2D NR Oct. 27 4.5%S pyrite, with FeSjeff (numerical. integ.)
 1.0 0.5 0.0                          ;WP,WA,WB,Leissman terms
 0 50.0 0 0 1 1                       ;KMAS,PTIME,KTS,kiter,kbypass,kint
 0 6 2 0 0                            ;KPRT,NPRT,LPRT,N1,N2
 10. 25. 36. 50. 75. 100.               ;PPRTT(I)
  258     30    2    3                 ;NEX,NEZ,NVTYP,NGTYP
 2.150e+02 1.000E+01 1.000e+03        ;XL,ZL,CONF
    0    0    0                       ;IS1,IS2,NCHS
    0    0    0    3                                ;KB(4),BOUNDARY CODES

    0.    0.                                        ;vx,vz
 5.0000e+00 5.00-02 5.046e-03 4.000e-01 0.050        ;Al,At,DD,POR,DT
10.0  0.0  14    9  00                 ;TEMP,FIONS,NNN,NR,NAS
 0 0 3 0 4 0 0 0 0 0 0                ;IFL(11)
0   0   0                             ;IADS,NUMADS,IABG
  1259   1   24   1                  ;ix1,ix2,iy1,iy2 define background
    150 1.3563-02 -1.86 0.0             ;CA b/g main tailings IDX,T,GX,STAD
    460 2.490E-02 -1.68 0.0             ;MG              "
    500 1.093E-02 -1.96 0.0             ;NA              "
    410 5.140E-03 -2.29 0.0             ;K               "
    180  4.252%04  -3.37  0.0           ;CL              "
    140 1.0663-02 -1.93 0.0             ;CO3             "
    732 3.390E-02 -1.53 0.0             ;SO4             "
    280 2.468E-05 -3.61 0.0             ;FE2             "
    281 1.249e-08 -7.90 0.0             ;FE3             "
    030 5.711E-09 -0.24 0.0             ;AL              "
    330 1.309E-02 0.0 0.0             ;H               "
    730 1.000E-06 0.0 0.0             rhs               "
    731 1.000E-06 0.0 0.0             ;s               "
    001 0.000E+00 0.0 0.0             ;E               "
  3   3                               ;LTY,LRX     SOLID & REACTION VALUES
2812800 0.0 0.0 0.0                   ;FE2/FE3 IDYS,GKS,DHS,CONS
  0                                   ;NC,(IDD,STOC)*NC
  4   2                               ;LTY,LRX
5015002 0.000E+00 000.00 0.04          ;Dolomite IDYS,GKS,DHS,CONS
  3    150 001.00 460 1.00 140 2.00     ;NC,(IDD,STOC)*NC
  4   2                               ;LTY,LRX
2003003 0.000E+00 000.00 0.08         ;GIBSITE
  3       30    1.00      330   -3.00    2  3.00  ;
  5   2                               ;
5028000 0.0 0.0            0.000      ;SIDERITE
  2      280    1.00      140    1.00     ;
  5   2                               ;
2028100 0.0 0.0            0.000e-00  ;FERRIHYDRITE
  2      281    1.00      330   -3.00     ;
  5   2                               ;
6015001 0.0 0.0            0.000      ;GYPSUM
  2      150    1.00      732    1.00     ;
  5   2                               ;
6041002 0.0 0.0            0.000e-00  ;k jarosite
  5      281  3.00  330  -6.00  410  1.0  732  2.0  002  6.0  ;
  4   2                               ,
1028002   0.0   0.0       1.3         ;FES jeff
  5 330 8.0 280 9.0 732 1.0 002 -4.0 281 -8.0 ;
  6   4                               ;
    001 0.0 0.0 0.0                   ;e-
 0                                    ;
 0                                   ;idnrx
 1259  25   31   -1                  ;ix1,ix2,iy1,iy2 define background
   150 1.356E-02 -1.86 0.0             ;CA b/g aquifer IDX,T,GX,STAD
   460 2.490E-02 -1.60 0.0             ;MG              "
   500 1.093E-02 -1.96 0.0             ;NA              "
   410 5.1403-03  -2.29  0.0           ;K               "
   180  4.252E-04  -3.37  0.0          ;CL              "
   140 1.066E-02 -1.93 0.0             ;CO3             "
   732 3.390E-02 -1.53 0.0             ;SO4             "
   280 2.468%05  -3.61  0.0            ;FE2             "
   281 1.249e-08 -7.90 0.0             ;FE3             "
   030 5.7113-09  -8.24  0.0           ;AL              "
   330 1.309%02  0.0  0.0            ;H               "
   730 1.000E-06 0.0 0.0             ;hs               "
   731 1.000E-06 0.0 0.0             is                "
   001 0.000E+00 0.0 0.0             ;E                "
  3   3                               ;LTY,LRX     SOLID & REACTION VALUES
2812800 0.0 0.0 0.0                   ;FE2/FE3 IDYS,GKS,DHS,CONS
  0                                   ;NC,(IDD,STOC)*NC
  4   2                               ;LTY,LRX
5015002 0.000E+00 000.00 0.04          ;Dolomite IDYS,GKS,DHS,CONS
  3    150 001.00 460 1.00 140 2.00     ;NC,(IDD,STOC)*NC
  4   2                               ;LTY,LRX
2003003 0.000E+00 000.00 0.08         ;GIBSITE
  3       30    1.00      330   -3.00    2  3.00  ;
  5   2                               ,
5028000 0.0 0.0            0.000      ;SIDERITE
  2      280    1.00      140    1.00     ;
  5   2                               ;
2028100 0.0 0.0            0.000e-00  ;FERRIHYDRITE
  2      281    1.00      330   -3.00     ;
  5   2                               ;
6015001 0.0 0.0            0.000      ;GYPSUM
  2      150    1.00      732    1.00     ;
  4   2                               ;
6041002 0.0 0.0            0.001    ;k jaroaite
  5      281  3.00  330  -6.00  410  1.0  732  2.0  002  6.0  ;
  5   2                               ;
1028002   0.0   0.0       0.00        ;FES jeff
  5 330 8.0 280 9.0 732 1.0 002 -4.0 281 -8.0 ;
  6   4                               ;
    001 0.0 0.0 0.0                   ;e-
 0                                    ,
 0                                   ;idnrx
 0                                   ;ntsn
 1 1 2 2 7 7 3 4 5 6 0 0 0 0 0 0      ;KPLT(I),I=1,NNN
 0 1 2 3 4 5 6 7 0 0 0 0              ;KPLTS(I),I=1,NR
 1 0 0 0 1 1 1 0 0 1 1 1 1 1 0 0      ;KPNT(I),I=1,NNN
 0 1 1 0 1 1 1 1 1 1 1 0              ;KPNTS(I),I=1,NR
2.000E-03 1.3753-02                   ;CA    TOLERANCE  AND  RELATIVE  VALUES
2.000%03  2.490E-02                   ;MG              "
2.000E-03 1.093E-02                   ;NA              "
2.000E-03 5.1403-03                   ;K               "
2.0001-03 4.2521-04                   ;CL              "
2.000E-03 1.380E-02                   ;CO3             "
2.000E-03 3.390E-02                   ;SO4             "
2.000E-03 2.468E-05                   ;FE2             "
2.0003-03 1.249e-08                   ;FE3             "
2.000E-03 5.711E-09                   ;AL              "
```

```
2.000E-03 1.309E-02                ;H              "
2.000E-03 1.000E-06                ;Hs              "
2.000E-03 1.000E-06                ;s              "
2.000E-03 1.000E+00                ;E              "
    1                              ;NTSC #OF CONSTANT TIME STEPS
    5                              ;NTB,CAUCHY BDRY FLUX,#BDY SBG
 0.189   101                       ;Flux, NBS(# elements ON BDRY SEGMENT)
    150 1.100E-02                  ;CA influx to aquifer IDX,UIN
    460 6.7643-03                  ;MG         "
    500 1.300E-03                  ;NA         "
    410 6.651E-05                  ;K          "
    180 1.000E-03                  ;CL         "
    140 1.380e-02                  ;C03        "
    732 7.479e-03                  ;SO4        "
    280 1.698E-05                  ;FE2        "
    281 1.199E-08                  ;FE3        "
    030 5.080E-09                  ;AL         "
    330 1.697E-02                  ;H          "
    730 1.000X-06                  ;hs             "
    731 1.000E-06                  ;s             "
    001 0.000e-00                  ;E          "
 0.000   20                        ;Flux, NBS(# elements ON BDRY SEGMENT)
    150 0.000E-02                  ;CA INFLUX AT TOE DAM IDX,UIN
    460 0.000B-03                  ;MG         "
    500 0.000B-03                  ;NA         "
    410 0.000E-05                  ;K          "
    180 0.000E-03                  ;CL         "
    140 0.000e-03                  ;C03        "
    732 0.000e-03                  ;SO4        "
    280 0.000E-05                  ;FE2        "
    281 0.000E-08                  ;FE3        "
    030 0.000E-09                  ;AL         "
    330 0.000E-02                  ;H          "
    730 0.000E-04                  ;hs             "
    731 0.000E-04                  is             "
    001 0.000e-00                  ;E          "
 0.063   22                        ;Flux, NBS(# elements ON BDRY SEGMENT)
    150 1.100E-02                  ;CA influx to aquifer IDX,UIN
    460 6.764E-03                  ;MG         "
    500 1.300E-03                  ;NA         "
    410 6.651E-05                  ;K          "
    180 1.000E-03                  ;CL         "
    140 1.380e-02                  ;C03        "
    732 7.479e-03                  ;SO4        "
    280 1.698E-05                  ;FE2        "
    281 1.199E-08                  ;FE3        "
    030 5.080E-09                  ;AL         "
    330 1.697E-02                  ;H          "
    730 1.000%06                   ;hs             "
    731 l.000E-06                  is             "
    001 0.0008-00                  ;E          "
 0.189    23                       ;Flux, NBS(# elements ON BDRY SEGMENT)
    150 1.100E-02                  ;CA influx to aquifer IDX,UIN
    460 6.764E-03                  ;MG         "
    500 1.300E-03                  ;NA         "
    410 6.6513-05                  ;K          "
    180 1.000E-03                  ;CL         "
    140 1.380e-02                  ;C03        "
    732 7.479e-03                  ;SO4        "
    280 1.698E-05                  ;FE2        "
    281 1.199E-08                  ;FE3        "
    030 5.080E-09                  ;AL         "
    330 1.697E-02                  ;H          "
    730 1.000E-06                  ;hs             "
    731  l.000E-06                 is             "
    001 0.000e-00                  ;E          "
0.24    93                         ;NBS
    150 1.100E-02                  ;CA influx to tailings IDX,UIN
    460 6.764E-03                  ;MG         "
    500 1.300E-03                  ;NA         "
    410  6.6513-05                 ;K          "
    180 3.000E-03                  ;CL         "
    140 1.380e-02                  ;C03        "
    732 7.400e-03                  ;SO4        "
    280 1.893E-05                  ;FE2        "
    281 1.199E-08                  ;FE3        "
    030 5.080E-09                  ;AL         "
    330  1.690%02                 ;H          "
    730 1.000E-06                  ;hs             "
    731 1.000E-06                  ;s             "
    001 0.000e-00                  ;E          "
 3263  4066  5370  6427  6754     ;breakthrough node numbers
0.000E+00  100.0  0.050  25      ;DT,MAXIT
1                                    ;oxflag 1=include oxidation
167  1  5                         ;npadl,npadr,nec
25                                 ;maxskip
```

```
 oxidat.dat         Sat Nov 16 18:31:27 1996        1

.5       1        0        0             ;fracyear,mineral,niwt%,znwt%              0.045   0.415    0.35       5    1550
0.000078     0.99                         ;grain radius,starting radius(0-1)         0.045   0.415    0.35       5    1550
1.50d-14                             ;d2 for oxidized coating
1.0d-3         0.2      75               ;dt,ptime,end time
      1.0      51                       ;depth of unsat, number of nodes in uns
at
    0.045    0.415     0.02       15     1550    ;fracsulf,por,moist. cont.,temp,rh
ob
    0.045    0.415     0.06       15     1550
    0.045    0.415    0.085       15     1550
    0.045    0.415     0.11       15     1550
    0.045    0.415    0.135       15     1550
    0.045    0.415     0.16       13     1550
    0.045    0.415     0.19       13     1550
    0.045    0.415     0.21       13     1550
    0.045    0.415     0.22       13     1550
    0.045    0.415     0.22       13     1550
    0.045    0.415   0.2175       11     1550
    0.045    0.415    0.215       11     1550
    0.045    0.415   0.2125       11     1550
    0.045    0.415     0.21       11     1550
    0.045    0.415    0.215       10     1550
    0.045    0.415    0.236       10     1550
    0.045    0.415    0.245       10     1550
    0.045    0.415     0.26       10     1550
    0.045    0.415     0.29       10     1550
    0.045    0.415     0.32       10     1550
    0.045    0.415    0.323       10     1550
    0.045    0.415    0.328       10     1550
    0.045    0.415    0.329       10     1550
    0.045    0.415   0.3295       10     1550
    0.045    0.415     0.33       10     1550
    0.045    0.415     0.32       10     1550
    0.045    0.415     0.29       10     1550
    0.045    0.415     0.27       10     1550
    0.045    0.415   0.2625       10     1550
    0.045    0.415     0.26       10     1550
    0.045    0.415   0.2625       10     1550
    0.045    0.415     0.27       10     1550
    0.045    0.415     0.29       10     1550
    0.045    0.415     0.31       10     1550
    0.045    0.415     0.32       10     1550
    0.045    0.415    0.335       10     1550
    0.045    0.415    0.345       10     1550
    0.045    0.415    0.355       10     1550
    0.045    0.415    0.355       10     1550
    0.045    0.415    0.355       10     1550
    0.045    0.415   0.3555       10     1550
    0.045    0.415    0.355       10     1550
    0.045    0.415    0.353       10     1550
    0.045    0.415    0.351       10     1550
    0.045    0.415     0.35       10     1550
    0.045    0.415    0.353       10     1550
    0.045    0.415    0.355       10     1550
    0.045    0.415    0.355       10     1550
    0.045    0.415    0.355        5     1550
    0.045    0.415   0.3555        5     1550
    0.045    0.415     0.35        5     1550
```

test.dat Sun Nov 17 00:23:24 1996 1

```
 1D NR 5.0%S as pyrite, FeSjeff and Fe(OH)3 10 meter column
 1.0 0.5 0.0                          ;WP,WA,WB,Leissman terms
 0 50.0 0 0 10                         ;KMAS,PTIME,KTS,kiter,kbypass,kint
 0 4 5 0 0                            ;KPRT,NPRT,LPRT,N1,N2
 1.0 3.00 6.0 8.0                     ;PPRTT(I)
  1   100   1   1                     ;NEX,NEZ,NVTYP,NGTYP
 0.1  10.0   1000.                    ;XL,ZL,CONF
    0    0    0                      ;IS1,IS2,NCHS
    0  0  0       3                  ;KB(4),BOUNDARY CODES
    0.   -0.6                        ;vx,vz
 0.500e+00 0.01 5.046e-03 4.000e-01 0.01     ;Al,At,DD,POR,DT
10.0  0.0  14  10  00                ;TEMP,FIONS,NNN,NR,NAS
 0 0 3 0 4 0 0 0 0 0 0               ;IFL(11)
0   0   0                            ;IADS,NUMADS,IABG
  1 2    1  101  -1                  ;ix1,ix2,iy1,iy2 define background
    150 1.356E-02 -1.86 0.0            ;CA b/g main tailings IDX,T,GX,STAD
    460 2.490E-02 -1.68 0.0            ;MG              "
    500 1.093E-02 -1.96 0.0            ;NA              "
    410 5.140x-03 -2.29 0.0            ;K               "
    180 4.252E-04 -3.37 0.0            ;CL              "
    140 1.066E-02 -1.93 0.0            ico3             "
    732 3.390E-02 -1.53 0.0            ;SO4             "
    280 2.468E-05 -3.61 0.0            ;FE2             "
    281 1.249e-08 -7.90 0.0            ;FE3             "
    030 5.7113-09 -0.24 0.0            ;AL              "
    330 1.3093-02 0.0 0.0            ;H               "
    730 1.000E-06 0.0 0.0            ;hs               "
    731 1.000E-06 0.0 0.0            ;s               "
    001 0.000E+00 0.0 0.0            ;E               "
  3   3                              ;LTY,LRX b/g SOLID & REACTION  VALUES
2812800 0.0 0.0 0.0                  ;FE2/FE3 IDYS,GKS,DHS,CONS
  0                                  ;NC,(IDD,STOC)*NC
  5   2                              ;LTY,LRX
5015002 0.000E+00 000.00 0.0000       ;Dolomite IDYS,GKS,DHS,CONS
  3   150 001.00 460 1.00 140 2.00     ;NC,(IDD,STOC)*NC
  4   2                              ;LTY,LRX
5015001 0.000E+00 000.00 0.04        ;CALCITE IDYS,GKS,DHS,CONS
  2 0000150 001.00 0000140 001.00    ;NC,(IDD,STOC)*NC
  4   2                              ;LTY,LRX
2003003 0.000E+00 000.00 0.1         ;GIBSITE
  3    30     1.00     330  -3.00  2  3.00  ;
  5   2                              ;
5028000 0.0 0.0          0.0000   ;SIDERITE
  2    280    1.00     140    1.00    ;
  5   2                              ;
2028100 0.0 0.0          0 . 0 0 0   ;FERRIHYDRITE
  2    281    1.00     330    -3.00    ;
  5   2                              i
6015001 0.0 0.0          0.000       ;GYPSUM
  2    150    1.00     732    1.00    ;
  5   2                              i
6041002 0.0 0.0          0.000e-00  ;k  jarosite
  5   281   3.00   330 -6.00 410 1.0 732 2.0 002 6.0  ;
  4   2                              ;
1028002   0.0   0.0      1.3        ;FES  jeff
  5 330 8.0 280 9.0 732 1.0 002 -4.0 281 -8.0 i
  6   4                              ;
    001 0.0 0.0 0.0                  ;e-
 0                                   ;
 0                                   ;idnrx
 0                                   ; ntsn
 1 1 2 2 7 7 3 4 5 6 0 0 0 0 0 0     ;KPLT(I),I=1,NNN
 0 1 2 3 4 5 6 7 0 0 0 0             ;KPLTS(I),I=1,NR
 1 0 0 0 1 1 1 0 0 1 1 1 1 1 0 0     ;KPNT(I),I=1,NNN
 0 1 1 0 1 1 1 1 1 1 1 0             ;KPNTS(I),I=1,NR
2.000E-03 1.375E-02                  ;CA    TOLERANCE AND RELATIVE VALUES
2.000E-03 2.490E-02                  ;MG              "
2.000E-03 1.093E-02                  ;NA              "
2.000E-03 5.140E-03                  ;K               "
2.000E-03 4.252E-04                  ;CL              "
2.000E-03 1.3803-02                  ;CO3             "
2.000E-03 3.390E-02                  ;SO4             "
2.000E-03 2.468E-05                  ;FE2             "
2.000E-03 1.249e-08                  ;FE3             "
2.000E-03 5.711E-09                  ;AL              "
2.000E-03 1.309E-02                  ;H               "
2.000E-03 1.000E-06                  ;Hs               "
2.000E-03 l.OOO%-06                  ;s               "
2.000E-03 1.000E+00                  ;E               "
    1                                ;NTSC #OF CONSTANT TIM% STEPS
    1                                ;NTB,CAUCHY BDRY FLUX,#BDY SEG
 0.24   1                            ;NBS
    150 1.100E-02                    ;CA influx to tailings IDX,UIN
    460 6.800E-03                    ;MG              "
    500 1.300E-03                    ;NA              "
    410  6.6003-05                  ;K               "
    180 3.000E-03                    ;CL              "
    140 1.300e-02                    ;C03             "
    732 7.400e-03                    is04             "
    280 1.900E-05                    ; FE2            "
    281 1.200E-08                    ;FE3             "
    030 5.100E-09                    ;AL              "
    330 1.700E-02                    ;H               "
    730 1.000E-06                    ;hs                 "
    731 1.000E-06                    ;s                "
    001 0.000e-00                    ;E               "
  100  80  60  40  10                ;breakthrough node numbers
0.000E+00 6.0 0.01 25                ;t0,t1,DT,MAXIT
0                                     ;oxflag 1=include oxidation
00   5                             ;npadl,npadr,nec
10                                   ;maxskip
```

```
.5       1        0        0            ;fracyear,mineral,niwt%,znwt%              0.050  0.415     0.35        5     1550
0.000076     0.99                       ;grain radius,starting radius(0-1)         0.050  0.415     0.35        5     1550
1.00d-14                             ;d2 for oxidized coating
l.Od-3        1.5      100.05              ;dt,ptime,end time
      1.0'      51                        ;depth of unsat,  number of nodes in uns
at
   0.050    0.415     0.02       15     1550    ;fracsulf,por,moist. cont.,temp,rh
ob
   0.050   0.415     0.06       15     1550
   0.050   0.415    0.085       15     1550
   0.050   0.415     0.11       15     1550
   0.050   0.415    0.135       15     1550
   0.050   0.415     0.16       13     1550
   0.050   0.415     0.19       13     1550
   0.050   0.415     0.21       13     1550
   0.050   0.415     0.22       13     1550
   0.050   0.415     0.22       13     1550
   0.050   0.415   0.2175       11     1550
   0.050   0.415    0.215       11     1550
   0.050   0.415   0.2125       11     1550
   0.050   0.415     0.21       11     1550
   0.050   0.415    0.215       10     1550
   0.050   0.415    0.236       10     1550
   0.050   0.415    0.245       10     1550
   0.050   0.415     0.26       10     1550
   0.050   0.415     0.29       10     1550
   0.050   0.415     0.32       10     1550
   0.050   0.415    0.323       10     1550
   0.050   0.415    0.328       10     1550
   0.050   0.415    0.329       10     1550
   0.050   0.415   0.3295       10     1550
   0.050   0.415     0.33       10     1550
   0.050   0.415     0.32       10     1550
   0.050   0.415     0.29       10     1550
   0.050   0.415     0.27       10     1550
   0.050   0.415   0.2625       10     1550
   0.050   0.415     0.26       10     1550
   0.050   0.415   0.2625       10     1550
   0.050   0.415     0.27       10     1550
   0.050   0.415     0.29       10     1550
   0.050   0.415     0.31       10     1550
   0.050   0.415     0.32       10     1550
   0.050   0.415    0.335       10     1550
   0.050   0.415    0.345       10     1550
   0.050   0.415    0.355       10     1550
   0.050   0.415    0.355       10     1550
   0.050   0.415    0.355       10     1550
   0.050   0.415   0.3555       10     1550
   0.050   0.415    0.355       10     1550
   0.050   0.415    0.353       10     1550
   0.050   0.415    0.351       10     1550
   0.050   0.415     0.35       10     1550
   0.050   0.415    0.353       10     1550
   0.050   0.415    0.355       10     1550
   0.050   0.415    0.355       10     1550
   0.050   0.415    0.355        5     1550
   0.050   0.415   0.3555        5     1550
   0.050   0.415     0.35        5     1550
```

Appendix C
MINTOX User Guide

MINTOX

User's Manual

by

Murray Wunderly

based on the work of:
Murray Wunderly
Andrea Walter
Emil Frind
Dave Blowes
John Molson

Waterloo Centre for Groundwater Research
University of Waterloo Waterloo, Ontario
N2L 3Gl

Disclaimer

Although great care has been taken in preparing the MINTOX program and documentation, the authors cannot be held responsible for any errors or omissions. As such, this code is offered as *is*. **The* user is expected to be familiar with finite element mass-transport and chemical equilibrium (especially MINTEQA2) models, and FORTRAN programming. The authors make no warranty of any kind, express or implied. The authors shall not be liable for any damages arising from a failure of the program or any of the contained subroutines to operate in the manner desired by the user. The authors shall not be liable for any damage to data or property which may be caused directly or indirectly by the use of the model. In no event will the authors be liable for any damages, including, but not limited to, lost profits, lost savings or other incidental or consequential damages arising out of the use, or inability to use, the MINTOX program and subroutines. Use, attempted use, and/or installation of this program shall constitute implied acceptance of the above conditions.

Authorized users encountering problems with the code, or requiring implementations not supported in this version , are encouraged to contact the authors for possible assistance.

TABLE OF CONTENTS

1. INTRODUCTION .

MINTOX is a computer model comprised of three modules, each performing a separate function. Two of the three modules were previously coupled (Walter et al. 1994a) into the program MINTRAN, which is capable of simulating multicomponent reactive transport over a wide range of geochemical equilibrium conditions. The third module was written specifically for this application and then coupled to MINTRAN. The result is a versatile multicomponent reactive transport model capable of simulating a wide range of equilibrium geochemical conditions, as well as kinetically-controlled sulfide-mineral oxidation.

The three main modules are: a finite element transport model (PLUME2D), an equilibrium geochemistry model (MINTEQA2), and an oxygen diffusion and sulfide-mineral oxidation model (PYROX). The function of each of these modules will be discussed separately in the following sections.

2. MATHEMATICAL MODELS

2.1 *Mass Transport (PLUME2D)*

2.1.1 *Aqueous Chemistry*

Transport of aqueous chemical components is based on the advective- dispersive equation:

$$\frac{\partial C_k}{\partial t} - \frac{\partial}{\partial x_i}\left(D_{ij}\frac{\partial C_k}{\partial x_j}\right) + \frac{\partial}{\partial x_i}(v_i C_k) - R_k = 0 \qquad k = 1,\ldots,N_c \tag{1}$$

where,

C_k - aqueous concentration of the component k [mol/kg]
D_{ij} - hydrodynamic dispersion tensor (see Bear, 1972) [m²/s]
v_i - vector component of the average fluid velocity [m/s]
R_k - chemical source/sink term [mol/kg s]

The boundary conditions for the aqueous components are either first type (Dirichlet) where the concentration is specified and constant along the boundary, or third type (Cauchy), where the mass flux is specified along the boundary.

Equation 1 is discretized in space and time using the standard Galerkin finite element technique, along with a time weighting scheme developed by Leismann and Frind (1989). The time weighting scheme results in a coefficient matrix which is symmetric and second order accurate in time. Matrix equations are then solved using a preconditioned conjugate gradient solver.

2.1.2 *Solid Chemistry*

The solid components are treated somewhat differently because they are stationary and therefore not transported in the groundwater. However, if the groundwater becomes undersaturated with respect to a particular solid, it may then dissolve and thus its constituents become mobile.

For the solid components the mass continuity equation is (Walter et al., 1994a):

$$\frac{\partial S_k}{\partial t} - R_k^s = 0 \qquad k = 1,\ldots,N_c \qquad (2)$$

where,

S_k - solid phase concentration [mol/kg]
R_k^s - source/sink term for precipitation/dissolution and sorption/desorption reactions [mol/kg]

The mass of solid phase that is lost or gained due to precipitation/dissolution or sorption/desorption reactions is determined by the geochemical equilibrium model which is described later. The total mass of a component, T_k, remains constant throughout and can be expressed as the sum of aqueous and solid phases (Walter et al., 1994a):

$$T_k = C_k + S_k \qquad k = 1, \ldots, N_c \qquad (3)$$

If the application of the model is limited to dilute systems, the units of concentrations for both aqueous and solid phases will be in mol/l.

The solid and aqueous phase component concentrations can further be broken down into the sum of the components (*k* components) in all species (I species) multiplied by the components stoichiometric coefficient in those species (Walter et al., 1994a).

$$C_k = \sum_{l=1}^{n_a} a_{lk}\, c_l \qquad k = 1,\ldots, N_c \qquad (4)$$

$$S_k = \sum_{l=1}^{n_s} b_{lk}\, s_l \qquad k = 1,\ldots, N_c \qquad (5)$$

where

c_l , s_l -concentration of species *l* in the aqueous and solid phases respectively
n_a , n_s -number of aqueous and solid species respectively
a_{lk} -stoichiometric coefficient of aqueous component *k* in species *l*
b_{lk} -stoichiometric coefficient of solid component *k* in species *l*

2.2 *Geochemical Equilibrium (MINTEQA2)*

The United States Environmental Protection Agency program MINTEQA2 (Allison et al., 1990), is the basis of the geochemical equilibrium module. MINTEQA2 has an extensive thermodynamic data base and is capable of modelling a wide variety of equilibrium geochemical reactions. These reactions include: chemical speciation, redox, acid-base, adsorption/desorption and precipitation/dissolution reactions.

2.2.1 *Chemical speciation*

By using the equilibrium constants for all species and stoichiometry for all components of these species, a set of nonlinear mass-action equations can be written for the aqueous form (Walter et al., 1994a):

$$K_{c_l} = \chi_l \prod_{k=1}^{N_c} \chi_k^{-a_{lk}} \qquad l = 1, \ldots, n_a \qquad (6)$$

where K_{c_l} - equilibrium formation constant for species l

χ_l - activity of species l

The activity and concentration of a species are related through the following:

$$\chi_l = \gamma_l c_l \qquad (7)$$

where γ_l - activity coefficient calculated using the extended Debye-Hiickel or similar empirical equation

The resulting equations'relate species concentration, activities and ionic strength. The equations are non-linear and therefore must be solved using an iterative technique. MINTEQA2 uses a Newton-Raphson technique to solve these equations (Felmy et al., 1983).

2.2.2 *Redox reactions and acid-base reactions*

The oxidation-reduction potential within the MINTEQA2 module is either input as a fixed solution pe, or may be calculated using the activities of a redox pair and the Nernst equation. Because concentrations of Fe(II) and Fe(III) are calculated within the PYROX module, the latter approach is used. Within the PYROX module it is assumed that concentrations and activities are equivalent. The resulting Fe(II) and Fe(III) concentrations calculated within PYROX are subsequently input into MINTEQA2 where equilibrium speciation is performed and the redox potential is calculated using the Nernst equation and the activities of Fe^{2+} and Fe^{3+}.

Reactions involving the transfer of protons from acids (proton donors) to bases (proton acceptors) are solved using the proton condition (Felmy et al. 1983). This method establishes a reference level for protons in a solution. Deviations from this reference level constitute either a positive or negative proton condition. The proton condition is the primary variable in the solution, representing the total analytical component concentration of H^+. (Walter et al., 1994)

2.2.3 *Adsorption*

MINTEQA2 is capable of mathematically formulating adsorption reactions as either isotherm, mass action/ion exchange, or surface competition/electrostatic models. Isotherm models may be linear (activity K_d) or non-linear (Langmuir or Freundlich). For surface complexion/electrostatic models MINTEQA2 uses either the constant-capacitance, diffuse layer, or triple layer model. To date the reactive transport model MINTRAN has only been validated using the ion exchange model. The ion exchange model assumes that a surface site is fully occupied by ions which may be exchanged for other ions in solution. It also assumes that there is a fixed number of exchange sites, and that the surface charge is constant. Under the changing pH conditions present in most tailings impoundments a variable surface-charge model, with surface charge dependent on pH, is probably the best suited adsorption model. Although variable surface charge models are present in MINTRAN, their application has yet to be tested.

2.2.4 *Mineral precipitationldissolution reactions*

Mass-action equations, which relate ion activities and a solid specific solubility product, describe mineral precipitation and dissolution reactions. These reactions can be written as follows (Walter et al., 1994a):

$$A_aB_{b(s)} \Leftrightarrow aA_{(aq)} + bB_{(aq)} \qquad (8)$$

The subscripts *(s)* and *(aq)* refer to solid and aqueous phases respectively. The thermodynamic solubility product for a given solid is described by:

$$K_{sp} = \frac{[A]^a[B]^b}{[A_aB_b]} \qquad (9)$$

where K_{sp} is the solubility product for the solid described in equation 2.8.

Solids described within MINTEQA2 may be designated as being one of three types: 1) infinite solids which are always in equilibrium and always present, 2) finite solids, which are initially present but in some finite amount which must be specified as a concentration, 3) undersaturated solids, which are not present in the original solution but may precipitate if conditions change. The designation of solids can also change, for example if a solid completely dissolves it would be redesignated from a (2) finite solid to a (3) undersaturated solid.

MINTEQA2 determines whether a mineral will precipitate, or dissolve, by calculating the minerals saturation index (S-1.). The saturation index is calculated as follows:

$$\log\left(\frac{IAP}{K_{sp}}\right) = S.I. \qquad (10)$$

This expression is derived from equation 2.9, noting that $[A_aB]$ = 1 for a pure solid. When the S.I. = 0, the mineral is in equilibrium. If S.I. > 0, the mineral will tend to precipitate, and for S.I. < 0, the mineral will tend to dissolve. For a multicomponent solution several minerals may be calculated to be supersaturated at one time. If this occurs MINTEQA2 ranks the minerals and determines which mineral is likely to precipitate first. This mineral is allowed to precipitate and the solution re-equilibrated. If more than one supersaturated mineral still remains the minerals are once again ranked and the solution re-equilibrated. This process is repeated until all minerals are at equilibrium.

2.3 *Oxygen diffusion and sulfide mineral oxidation (PYROX)*

The mass-balance equation governing bulk diffusion into the pore space of the tailings can be written mathematically as:

$$apor(x)\frac{\partial U_A^*(x,t)}{\partial t} = D1(x)\frac{\partial^2 U_A^*(x,t)}{\partial x^2} - q(x,t) \qquad (11)$$

where,
- $apor(x)$ - is the air filled porosity of the tailings [ ]
- $D1(x)$ - is the diffusion coefficient for the porous media [m²/s]
- U_A^* - is the oxygen concentration in the pore space [kg/m³] (* means the variable is dimensioned)
- $q(x,t)$ - is the sink term due to oxygen consumption by the particles in the tailings [kg/m³s]

All oxidation reactions are assumed to occur in the aqueous phase, and it is assumed that all particles are surrounded by an immobile water film. Oxygen in the pore space partitions according to Henry's Law from the gas phase to the aqueous phase of the immobile water film and from there it diffuses into the particles. The diffusion of oxygen into the particles is driven by the oxygen concentration gradient between the surface and the core of the particles. As the reaction between oxygen and sulfide minerals within the particles progresses, the radius of the unreacted core will decrease while the thickness of the oxidized shell increases. By rewriting equation 11 in dimensionless form and including the shrinking core model for the sink term $q(x,t)$ the following expression can be derived:

$$apor(x)\frac{\partial U_A(x,t)}{\partial t} = D1(x)\frac{\partial^2 U_A(x,t)}{L^2\partial x^2} - \frac{3(1-por(x))D2}{a^2}\left(\frac{r_c(x,t)}{1-r_c(x,t)}\right)U_A(x,t)\times XHEN \qquad (12)$$

where, a - is the radius of the tailings particles[m]
apor(x) - is the air filled porosity of the tailings [ ]
$por(x)$ - is the porosity of the tailings [ ]
$r_c(x,t)$ - is radius of the unreacted cores in the tailings particles [ ]
$D1(x)$ - is the diffusion coefficient for the porous media [m²/s]
L - is the thickness of the unsaturated zone in the tailings[m]
U_A^* - is the oxygen concentration in the pore space [kg/m³]
(* means the variable is not dimensionless)
$XHEN$ - is the inverse of Henry's constant

Because equation 12 is a function of 2 variables, $U_A(x,t)$ and $r_c(x,t)$, another equation relating these 2 variables is necessary if a unique solution is to be determined. The following equation describing the rate at which the unreacted cores in the tailings impoundment are shrinking and is a function of the same 2 variables as equation 12.

$$\frac{dr_c}{dt} = \frac{D2(1-por)U_0}{\varepsilon\,\rho_s\,a^2}\left(\frac{1}{r_c(x) - r_c(x)^2}\right)U_A(x,t)\times \mathbf{XHEN} \qquad \textbf{(13)}$$

where, $D2$ - is the diffusion coefficient for the oxidized coating forming on the particles [m²/s]
U_0 - is the atmospheric oxygen concentration [kg/m³]
ε - is the mass ratio of O_2 to suifur in the oxidation reaction
ρ_s - is the bulk density of sulfur in the tailings [kg/m³]

Equations 12 and 13 are similar to those developed by Davis and Ritchie (1986). Because the system is non-linear, an iterative approach must be used to solve the equations. Equation 23 is solved using a Galerkin finite element method and equation 13 is solved via the Newton Raphson technique. The program iterates between the two equations until both $U_A(x,t)$ and $r_c(x,t)$, converge simultaneously.

The model presented is a physical non-equilibrium model. Thus, the physical transport of oxygen to the reaction site is considered to be the rate limiting step in the oxidation of the sulfide minerals. Because the actual rate of oxidation occurring at the reaction site is non-limiting, it may be considered to be instantaneous. It is assumed that bacteria are present within the tailings. Their presence will enhance the actual rate of oxidation and thus further confirm the assumption that oxygen which reaches the reaction front is consumed instantaneously. This assumption implies that at the reaction front within the particles the concentration of oxygen will be zero.

3. SOFTWARE FOR MINTOX

The MINTOX program consists of three main file types:

*.for FORTRAN source code files (these files are *.f for UNIX)
*.dbm MINTEQA2 data base files
*.inc include files necessary for

Two MINTOX disks are in circulation, a DOS version and a UNIX version.

3.1 *DOS Version*

The disk containing the DOS version of MINTOX contains the source code and all necessary files needed to run the code. The executable file is included in 'zipped' format.

The size of the simulation that can be run is dependent on the amount of RAM memory on your machine. If not enough memory is available, or the program is requiring too much memory to run, then the maximum dimensions can changed and the program recompiled using a LAHEY FORTRAN compiler. A 'makefile' file is included for easy complation. See the end of this section for necessary modifications.

3.2 UNIX Version

The disk containing the UNIX version of the code has all necessary files to run the program. However, due to size limitations, the executable file is not included and must be compiled from the source code using the 'makefile' file which is included. (simply type 'make'). Sample data files are included, wrr2.dat, and wrr2p.dat and wrr2.vel (the vel file is 'zipped' and in wrr2.zip) The program is executed the same as the DOS version. The user may want to hardwire the input data set names directly in the code to facilitate running the program in batch. The main data file is input in the 'mintfe.f' subroutine and the diffusion data file is input in the 'subpyrox.f' file.

If the program is either too large to run on you machine (either UNIX or DOS) or too small to handle the size of the required simulation, the dimensions of the program can be easily modified. In order to do this one must modify the 'parmt.inc' file. The file looks similar to the following:

```
implicit real*8 (a-h,o-z)
    parameter (maxnn=1000,maxne=1000,maxbe=300,maxn=maxnn,
   +          maxna=5*maxn,laa=maxn*3+maxna,nw=6)
     parameter (nxdim = 22, nydim = 120 , nrdim = 22)
     parameter (maxun=500,maxbt=5,maxtim=1000)
```

The values that can be modified to increase or decrease the memory size required are:

maxnn - maximum number of nodes
maxne - maximum number of elements

maxbe - maximum number of boundary elements
maxun - maximum number of nodes in the unsaturated zone

Once these values have been modified the program can be recompiled by typing ‘make’ (Provided you have a LAHEY compiler on DOS, and XLF on UNIX)

4. RUNNING MINTOX.SIMULATIONS

4.1 Overview

In order to run MINTOX several preliminary steps must be taken. Firstly the oxygen diffusion and sulfide mineral oxidation must be modelled using PYROX. Secondly, some geochemical equilibrium modelling must be done using MINTEQA2 to determine the background aqueous and solid chemistry for the tailings impoundment, and each distinct geochemical zone being modelled. Finally, in the case of 2-D simulations, a steady-state flownet model must be run to determine input velocities, and xy coordinates in the case of an irregularly shaped grid.

4.2 ***Running PYROX***

The PYROX model is relatively easy to use, and runs very quickly. It is however, necessary to have the required input data including: porosity, moisture content, weight percent sulfur as sulfide, bulk density, temperature, particle size, and measurements of O_2 concentrations in the porespace. Example input data files are given in the Appendix, and a full description of input parameters is given in section 5.1.

Once an input file is set up as in section ***5.1,*** the program can be run. The input file must have the extension '.dat,' and the output tile will have the extension '.out'.

From the directory, that PYROX is stored in, type

PY ROX <enter>

The program will then prompt you for the input file name. Enter the filename *without* the '.dat' extension. The program runs, printing out results at the print time interval given in the input file. The program runs until all sulfide minerals have oxidized, or the endtime is reached. For an example run see the Examples Appendix at the end of this manual.

4.3 ***Running MINTOX***

The program can be executed by typing 'MINTOX'. The user will be prompted for the main data file first (i.e. wrrl .dat), and then for the diffusion data file (i.e. wrr1p.dat.). In DOS or in UNIX the the program is run using the same proceedure. If the source code is modified for any reason, the program can be recompiled using the 'makefile' files provided for either the LAHEY compiler, or XLF in UNIX.

In order to run MINTOX, two user created files are necessary. The first is for the oxygen diffusion and sulfide mineral oxidation or PYROX section of the simulation, and the second is for the reactive transport, or MINTRAN section of the simulation. The user should first run the PYROX model until they are satisfied that the diffusion and oxidation is being modelled realistically. The PYROX input file will then be used as input for the MINTOX simulation. (with modifications to the first line of the file). Along with the PYROX input file a MINTRAN type input file is necessary, and possible output files from FLONET or FLOTRANS, for xy coordinates and velocities in the case of 2-D simulations. The input data files are described in detail in the next section.

5. MINTOX INPUT FILE GUIDE

5.1 Diffusion/oxidation files

It is essential to run PYROX before running MINTOX. This is necessary because the results from PYROX must be matched to results seen in the field, or at least checked to see that the rates of oxygen diffusion and sulfide mineral oxidation are realistic. The main reason for this "reality check" is that the oxidation process is extremely sensitive to the moisture content in the unsaturated zone. If the moisture content was measured during an exceptionally dry time, or following a rainfall event, the steady state diffusion results calculated would be completely unrealistic. It is essential that the moisture content profile input is representative of the average moisture content during the months that oxidation occurs.

A summarized PYROX input file is shown below. The filename must have the '.dat' extension. Following the input files, the individual terms in the files are defined. Note that the parameters are free format, so column spacing is not important, as long as there is at least one space between entries.

```
2      0      0                                   ;mineral,fracni,fraczn
0.000075  0.99                                    ;grain radius[m],starting radius(0-1)
1.50d-14                                          ;D2 for oxidized coating[m2/s]
1 .Od-2      2.5     200                          ;dt[yr],ptime,end time
1.     51                                         ;depth of unsat.[m],# nodes in unsat
0.025  0.415  0.020     15     1550               ;fracsulf,por,mois.cont.,temp[C],rhob[kg/m3]
0.025  0.415  0.060     14   1550
0.025  0.415  0.085     13   1550
                  .
                  .
                  .
0.025  0.415  0.350     10   1550
```

Definition of terms:

LINE I.

mineral - defines the sulfide mineral that is oxidizing. 1=pyrite, 2=pyrrhotite.
Note: any other input here will halt program and print message.

fracni - fraction of nickel present in the sulfide mineral as an impurity. The program calculates how much nickel is released as the sulfide mineral oxidizes. Note: this option not yet available in MINTOX

fraczn - Same as above only for zinc.

LINE 2

grain - this is the radius of the sulfide mineral grains in metres.

starting radius- the starting position for the radius of the unreacted cores. The value is normalized such that a value of 1 would mean the particles are completely unreacted and a value of zero would mean completely oxidized. The shrinking core model requires that this value be less that one. Usually 0.99 or greater works fine. In extreme cases the value may have to be reduced to 0.98 or lower.

LINE 3

D2 - diffusion coefficient for the oxidized coating forming on the sulfide mineral grains. Since this value cannot be easily measured, it is essentially a fitting parameter. Units are m^2/s.

LINE 4

dt - time step in years. 1.0d-2 usually works. Should be at least an order of magnitude smaller than the time step used in the reactive transport section.

ptime - print time in years. ie. 5 means output is printed every 5 years.

end time - in years. program will run until end time is reached or all sulfide minerals have oxidized which ever comes first.

LINE 5

depth - depth of unsaturated zone in metres.

 # nodes - this is the number of nodes being modelled in the unsaturated zone.

*LINE 6 to LINE **(6 + # nodes-1)***

fracsulf - fraction of bulk density that consists of sulfide in the form of sulfide minerals.

por - porosity of tailings.

mois. cont. - volumetric moisture content of tailings.

Note: Ideally if this value is equal to the porosity the medium is fully saturated. However due to limitations in the empirical formula used to calculate the bulk diffusion coefficient, this value may never be greater that 0.06 less than the porosity or the program will bomb. example - if the porosity of the medium is 0.40, then the maximum allowable moisture content

is 0.34, even if the medium is fully saturated. This should not cause problems for the majority of cases.

temp - temperature in degrees Celsius. The diffusion coefficient calculated is a function of temperature.

rhob - bulk density of the tailings in kg/m^3.

Once PYROX is producing reasonable results, the first line of the input file can be modified as follows.

0.5 2 ;fracyear, mineral

where the first term is is **fracyear** and is the fraction of a year that oxidation occurs. i.e. if the ground is frozen for six months of the year, then fracyear should be 0.5. The second term is **mineral** which is the same as above.

An example run can be found in Appendix 1.

5.2 *Reactive transport files*

The user should refer to the user's manual for MINTRAN for a complete description of the reactive transport section of the program. MINTOX uses the same format input file as does MINTRAN with the only difference being the addition of 3 lines to the end of the MINTRAN input file. One of the three lines includes a flag for oxidation. If oxidation is flagged as off, the MINTOX program operates exactly as MINTRAN does with no oxidation input file is required.

The MINTOX input filename must have the ".dat" extension. The terms in the input file are explained below, the reader is referred to Appendix 1 for an example file. Note that the parameters are free format, so column spacing is not important, as long as there is at least one space between entries.

The following descriptions are from, or modified from MINTRAN User's Guide, 1992.

5.2.1 Basic input

LINE 1 **title [C] -** alphanumeric title, 32 characters maximum.

LINE 2 **wp [R], wa [R]** and **wb[R]**, the Liesmann weighting terms for the physical dispersion, the augmentation, and the boundary terms respectively. Recommended values are: 1.0,0.5, and 0.0 respectively.

LINE 3 kmas [I], the mass weighting term for transport =0 for lumped, 1 for consistent formulation. ptime **[R]** print time to create a restart file, kts [I] is the restart option = 0 for normal start, = 1 to restart simulations from nodal concentration values read from a file. Note : restart is not usable if sulfide mineral oxidation is included. i.e., kts=0. kiter [I], is the option for iterative of sequential solution. =0 sequential, =1 iterative. (use sequential since run times are much faster, and differences are negligible). kbypass [I], option to bypass equilibrium step for nodes which have not changed chemically since previous time step. =1 for bypass if change less than tolerance value (input further down), = 0 for equilibrate every node during each time step. (use kbypass =1, but make sure tolerances input later on are reasonable).

LINE 4 kprt [I], intermediate print option for the transport solution =0 for no printing, =1 to print, nprt [I], is the number of print times required per simulation, and lprt [I], is the print option for simulation type.

- lprt **[1]** = one-dimensional column simulations to produce concentration verses time plots at the exit boundary.
- lprt **[2]** = two dimensional simulations to produce concentration contour plots at specified times.
- lprt **[3]** = one-dimensional simulations to produce concentration verses distance plots at specified times.
- lprt **[4]** = one dimensional simulations to produce concentration verses time plots at two separate x distances, nl [I], and n2 [I], the two nodes that correspond to the two x distances to be plotted. If lprt ≠ 4 then input 0 for n1, and n2
- lprt **[5]** = same as option lprt [3] except the column is vertical instead of horizontal. This option must be used for 1-D simulations when oxidation is being modelled. i.e. unsaturated zone at the top.

LINE 5 prntt(nprt) **[R],** an array of nprt print times.

5.2.2 Physical domain and transport parameters

LINE 6 **nex** [I], number of elements in the x dimension, **nez [I],** number of elements in the z dimension, **nvtyp** [I], velocity option, =1 for a one dimensional flow field, = 2 for a two-dimensional flow field (vx and vy are not constant and are read in from file 'filename.vel'). **ngtyp [I]** is the grid option, =1 for a rectangular grid with constant element dimensions, = 2 for a rectangular grid with variable element dimension in x and/or z dimension (variable dimensions are read from file 'filename.vel'), and = 3 when the grid coordinates are read from a file (filename.vel'). If ngtyp = 4 then the grid is read in from directly from FLONET, or FLOTRANS output file 'filename'.hds.

NOTE: filenames with a '.vel' extension will be required for two cases; when a rectangular grid is used, but the element dimensions are variable, and when a two-dimensional flow field is used in the simulation. For variable element dimensions (ngtyp = 2 and nvtpy = 1), the x and z values along the rectangular grid are read from the tile 'filename'.vel. The x and z values are read in on separate lines in free format as x1(nx) [R] and z1(nz) [R] respectively. i.e. for a 20 X 15 m grid with x intervals at 0,1,2,4,8,12,20 m, and z intervals at 0, 1, 2, 4, 6, 10, 12, 15 m, the input file is;

0.0 1.0 2.0 4.0 8.0 12.0 20.0
0.0 1.0 2.0 4.0 6.0 8.0 12.0 15.0

When a two-dimensional flow field is required (ngtyp = 3 and nvtyp = 2), then the coordinate and velocity values must be generated by an external steady-state flow model which are then read into the program. In order that the two models are compatible, the steady-state flow model must accommodate rectangular and slightly deformed (at the water table) elements. A model with triangular elements could be used but the two adjacent elemental velocities must be averaged. The file which should be generated from the flow model will be 'filename'.vel and it should contain all of the nodal coordinate and elemental velocity data in the following format: the nodal coordinates are read in first, with a loop over the number of nodes in the z dimension (nz) inside a loop over the number of nodes in the x dimension (nx).

If the simulation is small enough that the flow can be simulated using FLONET or FLOTRANS, then the velocities and coordinates can be read in directly from their output files. (ngtyp = 4 and nvtyp = 2) In this case the '.hds' and '.vst' output files from the flow model must be named 'filename'.hds and 'filename'.vst. These files will be automatically read when MINTOX is executed.

LINE 7 xl **[R]**, total length of the solution domain in the x dimension in the required units (i.e. m, cm). **zl [R]**, total length of the solution domain in the z dimension. **conf [R]**, the unit conversion factor to account for the unit change between the grid dimension and the chemical concentration units

(always = moles/kg ≅ moles/litre for dilute solutions). The value of CONF can be calculated by taking the volume unit (length unit cubed) and determining the number of litres which are contained in this volume unit. For example, if metres are the length unit, then 1000 litres are contained within 1 m^3, and thus CONF = 1000.

LINE 8 **is1** [I] and is2 [I], the first and last nodes with source chemistry input from section source chemistry section, nchs [I], is the nodal increment number between the first and last source nodes. For example, if nodes 1 through 10 are source nodes then is1 = 1 and is2 = 10 and nchs = 1, or if the source nodes are 5, 10, 15 20, then is1 = 5, is2 = 20, and nchs = 5.

LINE 9 kb(4) [I], boundary codes for the 4 boundaries of the two-dimensional domain. The boundary faces are Face 1 along x = 0, Face 2 along x = xl, Face 3 along z = 0, and Face 4 along z = zl. See diagram below. The boundary type for each kb value is =0 for a Neumann boundary with a zero dispersive gradient, = 1 for a Dirichlet boundary, or 3 for a Cauchy boundary.

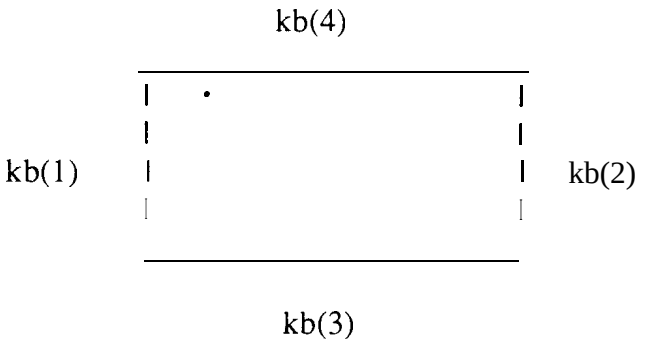

LINE 10 vxl [R] and vzl [R] are the constant x and z component velocities if nvtyp = 1. If the elemental velocities are to be read in from a file (nvtyp = 2) then these values are not applicable, so enter 0.0 and 0.0.

LINE 11 al [R], longitudinal dispersivity (length unit), at [R], transverse dispersivity (length unit), dd [R] diffusion constant (length unit squared/time unit), por [R], porosity, dt [R], time increment.

5.2.3 *Basic chemistry input*

LINE 12 **temp [R]**, temperature in "C, **fions [R]**, **the** ionic strength variation option (see Felmy et al. 1984),**nnn [R]**, number of chemical components not including water or elemental sulphur, nr **[R]**, number of chemical reactions, **nas [R]**, number of adsorbed components (these are also included in the nnn value).

LINE 13 **ifl(11) [I],** an array of 11 values which are equal to the MINTEQA2 input options. A thorough description of these options (except for ifl(11)) is given in Felmy et al. 1984. ifl(11) = IACT, activity correction option, =0 use activity corrections, =1 don't use any activity corrections (i.e. y's =1).

LINE 14 **iads [I],** adsorption model flag, =0 for no adsorption, =1 for ion exchange (the only adsorption model tested in MINTRAN), **numads [I],** number of adsorbing surfaces, **iabq [I]** a number (l-7) indicating the type of adsorption model used in MINTEQA2 (use 4 = ion exchange).

5.2.4 *Background chemistry for simulation*

Background chemistry starts on the 15th line of the input file. For simplicity the line numbers given below will start again at 1 to signify the first line in this section.

LINE 1 **ixl, ix2, iyl, iy2,** these values define nodal range over which the following chemistry applies to. They are: first and last x node, first and last z node respectively. **more** is a flag which indicates if there are more zones of different chemistry to input, = 1 means another chemistry block will be read in, = -1 means that this is the last background chemistry block to read in. For example if the background chemistry for the entire simulation is the same, then enter -1.

Background aqueous chemistry.

LINE 2 - LINE (2+nnn) These lines are for the background component values, one for each component with the same format, the first variable on these lines is **idx(nnn)** [I], the component I.D. number (see comp.dbm data file or Felmy et al. 1984), the second variable is **T(nnn) [R]**, the total analytical component concentration in moles/kg, or for the case of an adsorbed component the concentration of the surface sights in eq/l. The third variable is **gx(nnn) [R]**, the guess for the log of the activity for the component, use zero if a good initial guess is not known and for H^+ and e^- components use the pH and pe values respectively. The final variable of these lines is **stad(nnn) [R],** the reaction stoichiometry for the adsorbed phase components (i.e. Na-S), for dissolved component enter zero. The total component concentrations (T(nnn)) are determined from the chemical analysis of the solutions of interest. Often the chemistry will have to be

modified to be used in MINTRAN or MINTOX by MINTEQA2. This would have to be done for one of the following reasons: for a solution of known pH, the initial proton condition must be determined by fixing the pH to give the initial value for the total analytical concentration of H^+ component, for the simulation of redox reactions, the distribution of the multi-valence elements must be predetermined from the solution pe (same procedure as fixing the pH) and e- (idx=l) must be included as a component (T=O.O), and a type 6 reaction, and for ion-exchange reactions the dissolved and adsorbed phases must both be included as components with the initial surface site concentration of the adsorbed phase determined from the cation exchange capacity (CEC) and the individual selectivity coefficients of the ion-exchange reactions (K,). For ion-exchange reactions, the thermodynamic data base (file thermo.dbm) must be modified. Finally, chemical analyses are generally not perfectly charge balanced and it is advised that the initial background chemistry be charge balanced with a non reactive anion or cation. In summary, run the chemical data through MINTEQA2 and use the equilibrated results as input into MINTRAN or MINTOX.

Background solid chemistry.

LINE (2+NNN+1)- LINE (2+NNN+1+(3*NR)) The following lines are for the background reaction values, three lines for each reaction.

SUBLINE 1 **lty(nr) [I],** MINTEQA2 designated reaction type 2-6 (see Felmy, 1984). **lrx(nr) [I],** is the MINTEQA2 reaction type, = 1 for gas, = 2 for solid, =3 for redox reaction.

SUBLINE 2 **idys(nr) [I],** reaction identification number (see type6.dbm file), **gks(nr) [R]**, the new log K of the reaction, **dhs(nr) [R]**, the new enthalpy of the reaction (use 0.0 for the last two values and they will default to the value in the thermodynamic data base), **cons(nr) [R]**, the initial total mass of a type 4 solid (use 0.0 for all other reaction types in moles of solid per litre of pore water.

SUBLINE 3 **nc [I],** number of components in the reaction ,**(idd(nc) [I], stoc(nc)** [R])xnc. where **idd** is the identification number (as in idx) and **stoc** is the stoichiometry of the component in the reaction (+ or -)

2nd LAST LINE **idnrx [I],** is the reaction identification number for a reaction which will be taken out of the 'reaction sequence once the background chemistry has been equilibrated. This option has been used to initially set the CO_2 for an open system then remove this reaction to represent a closed system. This option has not been well used and it is recommended to leave this value as 0.

LAST LINE **ntsn [I],** is the number of source nodes which have a chemical composition different then the background nodes. If this value is zero then the subroutine SRCHEM is not called and the following Source Chemistry Section inputs are not required.

5.2.5 *Source chemistry section*

This section is only required if a separate (differing background) chemical area occurs within the solution domain. This occurs when a first type boundary condition is used or internal source nodes occur. The input sequence and values are exactly the same as for the background chemistry (except the last two lines described above for idnrx and ntsn are not included) and it should be followed if this option is used. If no source nodes occur (ntsn = 0) then skip this input section and continue the input sequence after the previous section.

5.2.6 *Chemical component and solid phase print and plot options*

LINE 1 **kplt(nnn) [I],** plot options for each chemical component. This array of nnn is used to indicate whether a chemical component should be plotted. If kplt is greater than 0 then the chemical solution for that component can be printed to a separate file. For convenience each component can be printed to a separate file by numbering the kplt values successively, i.e. for a four component simulation if kplt(1) = 1, kplt(2) = 0, kplt(3) = 2, and kplt(4) = 2, then component 1 will be printed to a file 'filename'o.aq1, and components 3 and 4 to 'filename'o.aq2. Up to eight component files are presently available.

LINE. 2 **kplts(nr) [I],** is the plot option for solid phases. This array works exactly the same as the kplt options but is used to print the solid phase values to appropriate plotting files 'filename'o.sol - 'filename'o.so8.

LINE 3 **kpnt(nnn) [I],** print option for each chemical component. This array specifies if the component solution is to be printed to the general output file 'filename'o.gen (all values of kprt > 0 are printed to the one file). This option is overridden for two-dimensional simulations when the number of nodes in the x dimension is greater than 9 or for one-dimensional simulations where lprt = 1, 4, or 5 due to space restrictions.

LINE 4 **kpnts(nr) [I],** print option for the solid phases. This array works the same as the kprt option but is for the solid phases. The results are also printed to the file 'filename'o.gen.

5.2.7 *Component tolerances and relative values*

These two values must be input in the same order as the initial background chemistry.

LINE 1-nnn These lines, one for each component, contain as the first value **tol(nnn) [R]**, the component tolerance as a relative value (i.e. fraction of a representative value for that component). Typically, a value of 10" to 10^{-6} is used. The second value on these lines is **same(nnn) [R]**, the relative value that the tolerance value is calculated from (moles/kg). This value is usually taken to be the larger of the component background (equilibrated) or the Cauchy influx value.

5.2.8 *Cauchy boundary condition specification*

The Cauchy boundary terms are read in with this section. The C_0 concentrations are the same at each time step provided that the program remains within the constant time step loop (which begins after the Cauchy boundary terms are read into the program and the FB boundary matrix is calculated for each component). If the time step interval changes, or the Cauchy boundary component concentrations change (new input source) then the FB matrix must be recalculated. The occurrence of multiple time step intervals or boundary concentrations are afforded in this input section.

LINE 1 **ntsc [I],** number of constant time step increments. If the time step increment does not change then this value should be 1. If there is a change in the Cauchy source concentrations during the simulation (even if dt remains the same), then the input data from here to the end of the input file needs to be read in ntsc times including section 9.

LINE 2 **ntb [I],** number of separate boundary flux segments. This is the number of segments along the boundary which either have differing influx chemistry or influx rates. If ntb > 1, indicating multiple boundary segments, then these segments are read in starting at the left segment for a water table boundary and moving towards the right. If the upstream (left) boundary is the influx boundary, then the segments are input bottom to top.

The next sections are the individual component concentrations that must be read in for each constant time step increment (ntsc). The Cauchy boundary type can be applied to two of the four boundaries: the left hand boundary where X=0 (kb(1)=3) used for the upstream (left) influx concentrations, or the top boundary (kb(4) = 3) at the water table for simulations with two dimensional flow with infiltration.

5.2.8.1 If kb(4) = 3 then use the following

LINE 1 **fbf [R]**, fluid influx over the Cauchy boundary (length unit/time unit) which is generally equal to the infiltration rate or the external flux rate ($v \times \theta$). **nbs [I],** is the number of elements along this boundary segment. = 1 for l=D simulations.

LINE **2-LINE (2+nnn)** The values on these lines are read in as one line per component in the same order as components were previously input. There will be two values per line. **idx(nnn) [I],** the component identification number and **uin(nnn) [R]**, the component concentrations (moles/kg) that enter the boundary. These values are considered to be from outside the porous media domain and the original chemistry (i.e. dilute rain water chemistry) should be used.

5.2.8.2 **If kb(1) = 3 then use the following**

LINE **1** **fbf [R]**, fluid influx over the Cauchy boundary (length unit/time unit) generally equal to the external flux rate $v \times \theta$). **nbs [I],** is the number of elements along this boundary segment. = 1 for l=D simulations.

LINE 2-LINE (2+nnn) The values on these lines are read in as one line per component in the same order as components were previously input. There will be two values per line. **idx(nnn) [I],** the component identification number and **uin(nnn) [R]**, the component concentrations (moles/kg) that enter the boundary. These values are considered to be from inside the porous media, in which case the component chemistry should be equilibrated with the appropriate chemical reactions and solid phases using MINTEQA2.

5.2.9 ***Time increment values***

LINE 1 breakthrough node numbers. Five nodes numbers must be input which breakthrough curves at the end of the simulation will be output into 'filename'o.brk. Enter 0.0 for the five numbers if breakthrough curves are not desired.

LINE 2 **to [R]**, initial time value. Should be 0.0. **tl [R]**, final time value or the time that the simulation will stop. is value should be at least one time step greater that the final print time to ensure that the last print time is printed before the program stops. **dt [R]**, is the time increment for the simulation. **maxit [I],** is the maximum number of iterations between the chemical and

transport solutions (30 should be enough). Generally the program will be run in sequential mode and thus this parameter is not used but must still be read in.

LINE 3 **oxflag** [I], this flag turns the oxidation modelling on. = means include oxidation. = 0 means program runs the same as MINTRAN and no oxidation file is read in.

LINE 4 **npadl** [I], and **npadr** [I], are number of nodes on the left and right had side of the domain to pad as no oxidation zones. This is used to include zones along the surface which are outside the tailings impoundment. i.e. if your domain were 100 nodes wide with the left half of the domain being aquifer, and the right half consisting of tailings, then values of 50 and 0 would be input for npadl and npadr respectively. **nec** [I] is the number of element compression that occurs between the oxidation model and the reactive transport model. Because the oxidation model requires finer discretization than the reactive transport model, this term is necessary. If a value of 5 is used, then the oxidation code must be set up such that 5 times the number of elements are used in the oxidation code as in the reactive transport code for the same thickness of unsaturated zone. i.e. if the unsaturated zone is 1 m thick and the discretization is 10 cm for the reactive transport section, then if nec = 5, then the oxidation input should be set up with a discretization of 2 cm. The program automatically linearly interpolates data transferred between the two sections of code, either transposing five elements into one, or vice-versa.

LINE 5 **maxskip [I],** value is the maximum number of nodes which will be ignored within one time step if MINTEQA2 is unable to equilibrate the chemistry at those nodes. Generally, if MINTEQA2 has gone through 1000 iterations at a particular node and the chemistry has not converged, then the input chemistry for that node will be truncated and another attempt to equilibrated the chemistry will be made. This procedure is repeated three times. if at that point convergence still has not occurred, then equilibration at that node will'be skipped for the present time step. This option is useful in simulations where sharp reaction fronts cause extreme chemical variations from one element to the next. By skipping a node, the sharpness of the front is somewhat smeared for that time step. The effect of a couple skipped nodes is minor, however, a large number of skipped nodes may represent a serious problem such as too large a time step, or unrealistic input chemistry.

6. REFERENCES

Allison, J.D., D.S. Brown, and K.J.Nova-Gradac. 1990. MINTEQA2/PRODEFA2, A Geochemical Assessment Model For Environmental Systems: Version 3.0 User's Manual. Environmental Protection Agency, Athens, Georgia, 106 p..

Bear, J.. 1972. Dynamics of Fluids in Porous Media. American Elsevier Publishing Company, Inc. , New York, N.Y., 764 p..

Davis, G.B. 1983. Mathematical modelling of rate-limiting mechanisms of pyrite oxidation in overburden dumps. Ph.D. Thesis. University of Wollongong. 159 p.

Davis, G.B., and A.I.M. Ritchie. 1986. A model of oxidation in pyritic mine wastes: part 1: equations and approximate solution. Applied Mathematical Modelling, 10, 3 14-322.

Davis, G.B., G. Doherty, and A.I.M. Ritchie. 1986. A model of oxidation in pyritic mine wastes: part 2: comparison of numerical and approximate solutions. Applied Mathematical Modelling, 10, 323-329.

Davis, G.B., and A.I.M. Ritchie. 1987. A model of oxidation in pyritic mine wastes: part 3: import of particle size distribution. Applied Mathematical Modelling, 11, 417-422.

Felmy, A.R., D.C. Girvin, and E.A. Jenne. 1983. MINTEQ: A Computer Program for Calculating Aqueous Geochemical Equilibria. Report, U.S. Environmental Protection Agency, Washington D.C., 62 p..

Leismann, H.M. and E.O. Frind. 1989. A Symmetric- Matrix Time Integration Scheme for the Efficient Solution of Advection-Dispersion Problems. Water Resources research, Vol. 25, No. 6, pp. 1133-l 139.

Levenspiel, 0. 1972. Chemical Reaction Engineering. John Wiley and Sons Inc., New York

Walter, A.L., E.O. Frind, D.W. Blowes. 1992. MINTRAN User's Guide. Waterloo Centre for Groundwater Research.

7. APPENDIX 1 - PYROX SIMULATION

The first example is an input file for PYROX.

Example 1, input file for PYROX model. This style of input file is used when PYROX is run as a stand alone model.

```
1  0  0                                          ;mineral,niwt%,znwt%
0.000070  0.99                                   ; grain radius[m],starting radius(0-1)
.ld-13                                           ; D2 for oxidized coating[m2/s]
l.d-2  10  20                                    ; dt[yr],ptime,end time
 1.500  26                                       ; depth of unsat.[m],# nodes in unsat
0.0108  0.50  0.300  15     1375                 ;fracsulf,por,mois.cont.,temp[C],rhob[kg/m3]
0.0108  0.50  0.300  15     1375
0.0108  0.50  0.300  10     1375
0.0108  0.50  0.320  10     1375
0.0108  0.50  0.330  10     1375
0.0108  0.50  0.340  10     1375
0.0108  0.50  0.350  10     1375
0.0108  0.50  0.360  10     1375
0.0108  0.50  0.375  10     1375
0.0108  0.50  0.382  10     1375
0.0108  0.50  0.386  10     1375
0.0108  0.50  0.390  10     1375
0.0108  0.50  0.400  10     1375
0.0108  0.50  0.405  10     1375
0.0108  0.50  0.410  10     1375
0.0108  0.50  0.415  10     1375
0.0108  0.50  0.419  10     1375
0.0108  0.50  0.423  10     1375
0.0108  0.50  0.427  10     1375
0.0108  0.50  0.430  10     1375
0.0108  0.50  0.432  10     1375
0.0108  0.50  0.434  10     1375
0.0108  0.50  0.436  10     1375
0.0108  0.50  0.438  10     1375
0.0108  0.50  0.439  10     1375
0.0108  0.50  0.440  10     1375
```

The following is the output from simulation 1.

```
sulfide mineral is PYRITE
 input file name is sim2dp.dat

 particle radius a = 0.000070   initial radius rstart = 0.990000

 no. intervals 26 print time 10.00 time step' 0.01000
-------------------------------------------------------------------
 element diff. coef   airfilled porosity   fracsulf

   1    0.8437E-06        0.200000          0.0108
   2    0.83288-06        0.200000          0.0108
   3    0.7309E-06        0.190000          0.0108
   4    0.6028E-06        0.175000          0.0108
   5    0.5231 E-06       0.165000          0.0108
   6    0.4482E-06        0.155000          0.0108
   7    0.3781E-06        0.145000          0.0108
   8    0.2974E-06        0.132500          0.0108
   9    0.2332E-06        0.121500          0.0108
  10    0.2035E-06        0.116000          0.0108
  11    0.1830E-06        0.112000          0.0108
  12    0.1493E-06        0.105000          0.0108
  13    0.1164E-06        0.097500          0.0108
  14    0.963 1E-07       0.092500          0.0108
  15    0.7785E-07        0.087500          0.0108
  I6    0.626%07          0.083000          0.0108
  17    0.5029E-07        0.079000          0.0108
  18    0.3908E-07        0.075000          0.0108
  19    0.3024E-07        0.071500          0.0108
  20    0.2451E-07        0.069000          0.0108
  21    0.2029E-07        0.067000          0.0108
  22    0.16408-07        0.065000          0.0108
  23    0.1286E-07        0.063000          0.0108
  24    0.1044E-07        0.061500          0.0108
  2.5   0.8942E-08        0.060500          0.0108
-------------------------------------------------------------------

 time is 10.000 years
d e p t h   0 2  bdry frac. so4-2  h +  fe+2 ni+2 zn+2
 (m)   conc.  pstn  rxtd  kg   kg   kg   kg   kg
0.030  0.9949 0.4307  0.9201  2.377  0.025  0.691  0.000 0.000
0.0900.9848  0.4393  0.9152  2.364  0.025  0.687  0.000  0.000
0.150  0.9743 0.4478  0.9102  2.350  0.025  0.683  0.000 0.000
0.210  0.9624 0.4572  0.9044  2.335  0.024  0.679  0.000 0.000
0.270  0.9488 0.4676  0.8977  2.317  0.024  0.674  0.000  0.000
0.330  0.9336 0.4787  0.8903  2.297  0.024  0.668  0.000  0.000
0.390  0.9164 0.4908  0.8817  2.274  0.024  0.661  0.000  0.000
0.4500.8961  0.50460.8714  2.247  0.024  0.653  0.000  0.000
0.5100.8715  0.5206  0.8588  2.213  0.023  0.643  0.000 0.000
0.570  0.8434 0.5383  0.8439  2.173  0.023  0.632  0.000  0.000
0.6300.8134  0.5564  0.8276  2.130  0.022  0.619  0.000  0.000
0.690  0.7804 0.5755  0.8092  2.081  0.022  0.605  0.000  0.000
0.7500.7417  0.5971  0.7869  2.021  0.021  0.588  0.000 0.000
0.810  0.6972 0.6209  0.7603  1.950  0.020  0.567  0.000  0.000
0.8700.6473  0.6467  0.7292  1.867  0.020  0.543  0.000 0.000
0.9300.5912  0.6746  0.6925  1.769  0.019  0.514  0.000  0.000
0.990  0.5289 0.7048  0.6494  I.654  0.017  0.481  0.000  0.000
1.050  0.4598 0.7375  0.5982  I.517  0.016  0.441  0.000  0.000
1.110  0.3836 0.77320.5370  1.354  0.014  0.394 0.000  0.000
1.170  0.3039 0.8107  0.4663  1.165  0.012  0.339  0.000  0.000
1.230  0.2265 0.8481  0.3891  0.959  0.010  0.279  0.000 0.000
1.290  0.1555 0.8843  0.3075  0.742  0.008  0.216  0.000  0.000
1.3500.0943  0.9187  0.2240  0.519  0.005 0.151  0.000  0.000
1.4100.0485  0.9484  0.1464  0.31 1  0.003  0.091 0.000  0.000
1.470  0.0242 0.9675  0.0943  0.172  0.002  0.050  0.000  0.000
            so4 produced =    43.159 kg
             fe produced =    12.546 kg
            h+ produced =     0.453 kg
```

ni+2 produced = 0.000 kg
zn+2 produced = 0.000 kg

total so4 from start = 43.159 kg
total fe from start = 12.546 kg
total h+ from start = 0.453 kg
total ni+2 from start = 0.000 kg
total zn+2 from start = 0.000 kg

time is 20.000 years

depth (m)	0 2 conc.	bdry pstn	frac. rxtd	so4-2 kg	h+ kg	fe+2 kg	ni+2 kg	zn+2 kg
0.030	0.998	1	0.0000	1.0000	0.213	0.002	0.062	0.000	0.000
0.090	0.994	1	0.0000	1.0000	0.226	0.002	0.066	0.000	0.000
0.150	0.989	9	0.0000	1.0000	0.240	0.003	0.070	0.000	0.000
0.210	0.984	9	0.0000	1.0000	0.255	0.003	0.074	0.000	0.000
0.270	0.979	1	0.0000	1.0000	0.273	0.003	0.079	0.000	0.000
0.330	0.972	2	0.0000	1.0000	0.293	0.003	0.085	0.000	0.000
0.390	0.964	2	0.0000	1.0000	0.316	0.003	0.092	0.000	0.000
0.450	0.954	4	0.0000	1.0000	0.343	0.004	0.100	0.000	0.000
0.510	0.941	8	0.0000	1.0000	0.377	0.004	0.110	0.000	0.000
0.570	0.926	7	0.0574	0.9992	0.415	0.004	0.121	0.000	0.000
0.630	0.909	8	0.1430	0.9967	0.452	0.005	0.131	0.000	0.000
0.690	0.890	3	0.1958	0.9921	0.488	0.005	0.142	0.000	0.000
0.750	0.866	3	0.2447	0.9849	0.529	0.006	0.154	0.000	0.000
0.810	0.837	5	0.2926	0.9745	0.572	0.006	0.166	0.000	0.000
0.870	0.803	6	0.3399	0.9601	0.616	0.006	0.179	0.000	0.000
0.930	0.763	7	0.3881	0.9408	0.663	0.007	0.193	0.000	0.000
0.990	0.717	0	0.4377	0.9153	0.710	0.007	0.206	0.000	0.000
1.050	0.662	1	0.4897	0.8815	0.756	0.008	0.220	0.000	0.000
1.110	0.597	8	0.5452	0.8366	0.800	0.008	0.232	0.000	0.000
1.170	0.525	8	0.6028	0.7795	0.836	0.009	0.243	0.000	0.000
1.230	0.450	3	0660	0.7109	0.859	0.009	0.250	0.000	0.000
1.290	0.374	4	0.7158	0.6316	0.865	0.009	0.251	0.000	0.000
1.350	0.301	5	0.7694	0.5430	0.852	0.009	0.248	0.000	0.000
1.410	0.240	0	0.8160	0.4557	0.826	0.009	0.240	0.000	0.000
1.470	0.203	2	0.8450	0.3965	0.807	0.008	0.235	0.000	0.000

so4 produced = 13.580 kg
fe produced = 3.948 kg
h+ produced = 0.142 kg
ni+2 produced = 0.000 kg
zn+2 produced = 0.000 kg

total so4 from start = 56.739 kg
total fe from start = 16.494 kg
total h+ from start = 0.595 kg
total ni+2 from start = 0.000 kg
total zn+2 from start = 0.000 kg

****
****

progress of reaction front

depth	time of reaction front arrival
0.000	16.410
0.060	16.670
0.120	16.930
0.180	17.210
0.240	17.530
0.300	17.880
0.360	18.280
0.420	18.730
0.480	19.270
0.540	19.930
0.600	0.000
0.660	0.000
0.720	0.000
0.780	0.000
0.840	0.000
0.900	0.000

0.960	0.000
1.020	0.000
1.080	0.000
1.140	0.000
1.200	0.000
1.260	0.000
1.320	0.000
1.380	0.000
1.440	0.000
1.500	0.000

The following plots show the oxygen concentration profile and the amount of sulfide remaing from this simulation. These plots should be compared to field date to ensure that the results are realistic.

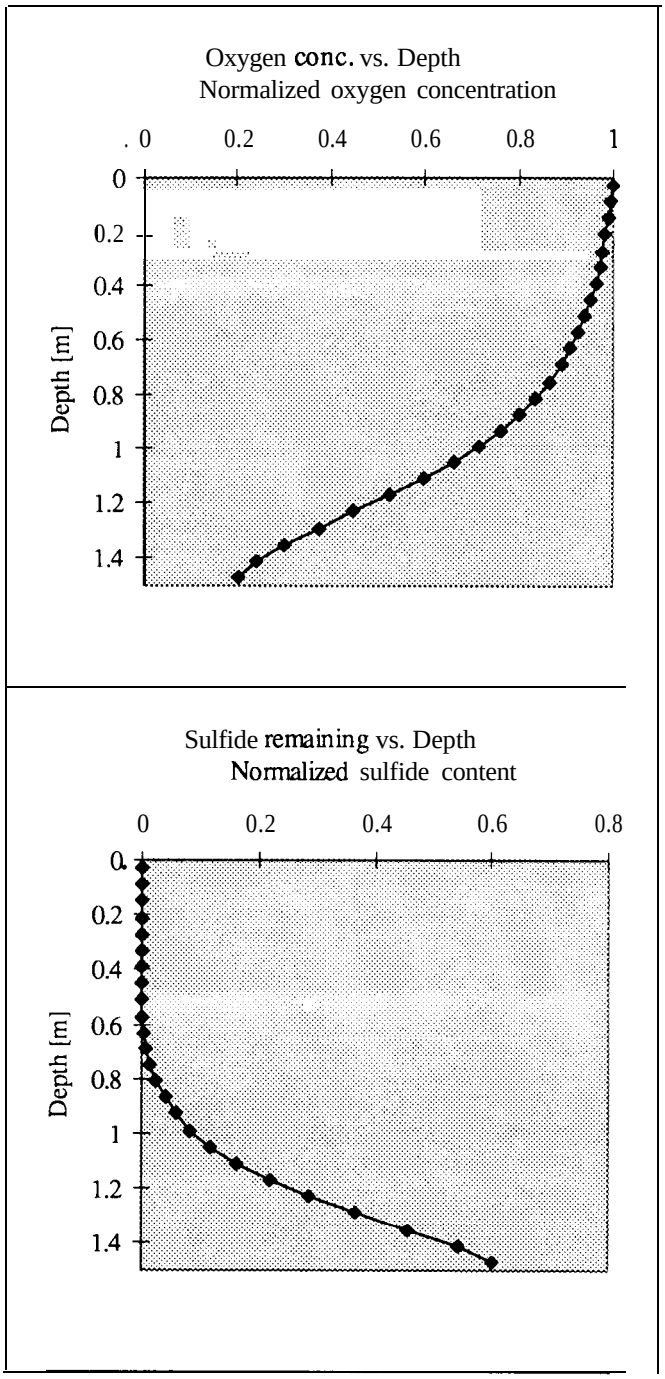

8. APPENDIX 2 - MINTOX 1-D SIMULATION

The following input files are for an Elliot Lake 1-D MINTOX simulation. Example 2a is the diffusion input, and example2b is the reactive transport input.

Example 2a, This style of input file is used to input diffusion /oxidation input into MINTOX. Only the first line needs to be changed when switching from PYROX input to MINTOX input.

```
0.583 1                                  ;fracyear,mineral
0.000030 0.99                            ;grain radius [m],starting radius(0-1)
0.035d- 13                               ;D2 for oxidized coating [m2/s]
l.d-2  1.166  6                          ;dt[yr],ptime,end time
6.00 121                                 ;zl,nxuns
0.0161  0.59  0.30  15    1125           ;fracsulf,por,mois. cont,temp[C],rhob[kg/m3]
0.0161  0.59  0.30  15    1125
0.0161  0.60  0.35  15    1100
0.0161  0.60  0.40  15    1100
0.0161  0.62  0.42  14    1050
0.0161  0.62  0.46  14    1050
0.0161  0.64  0.47  14    1000
0.0161  0.64  0.48  14    1000
0.0161  0.61  0.49  12    1075
0.0161  0.61  0.50  12    1075
0.0161  0.59  0.51  10    1100
0.0161  0.59  0.52  10    1100
0.0161  0.58  0.51  10    1140
0.0161  0.58  0.51  10    1140
0.0161  0.58  0.52  10    1120
0.0161  0.58  0.52  10    1120
0.0161  0.61  0.55  10    1080
0.0161  0.61  0.55  10    1080
0.0161  0.60  0.54  10    1120
0.0161  0.60  0.54  10    1120
0.0161  0.60  0.54  10    1100
0.0161  0.60  0.54  10    1100
0.0161  0.62  0.50  10    1050
0.0161  0.62  0.50  10    1050
0.0161  0.67  0.57  10    900
0.0161  0.67  0.57  10    900
0.0161  0.69  0.57  10    850
0.0161  0.69  0.57  10    850
0.0215  0.73  0.59  10    750
0.0215  0.73  0.59  10    750
0.0205  0.76  0.60  10    650
0.0205  0.76  0.60  10    650
0.0190  0.78  0.56  10    600
0.0190  0.78  0.56  10    600
0.0180  0.73  0.58  10    750
0.0180  0.73  0.58  10    750
0.0170  0.67  0.52  10    900
0.0170  0.67  0.52  10    900
0.0160  0.60  0.45  10    1100
0.0160  0.60  0.45  10    1100
0.0155  0.51  0.40  10    1350
0.0155  0.51  0.40  10    1350
0.0145  0.55  0.33  10    1250
0.0145  0.55  0.33  10    1250
0.0140  0.58  0.32  10    1150
0.0140  0.58  0.32  10    1150
0.0137  0.59  0.37  10    1125
0.0137  0.59  0.37  10    1125
0.0134  0.58  0.39  10    1150
0.0134  0.58  0.39  10    1150
```

0.0161 0.57 0.31 10 1185
0.0161 0.57 0.31 10 1185
0.0161 0.55 0.31 10 1225
0.0161 0.55 0.31 10 1225
0.0161 0.56 0.28 10 1210
0.0161 0.56 0.28 10 1210
0.0161 0.57 0.25 10 1190
0.0161 0.57 0.25 10 1190
0.0161 0.57 0.18 10 1180
0.0161 0.57 0.18 10 1180
0.0161 0.58 0.30 10 1160
0.0161 0.58 0.30 10 1160
0.0215 0.58 0.48 10 1150
0.0215 0.58 0.48 10 1150
0.0215 0.57 0.45 10 1175
0.0215 0.57 0.45 10 1175
0.0215 0.55 0.42 10 1225
0.0215 0.55 0.42 10 1225
0.0215 0.55 0.45 10 1200
0.0215 0.55 0.45 10 1200
0.0215 0.58 0.50 10 1100
0.0215 0.58 0.50 10 1100
0.0215 0.64 0.54 10 1000
0.0215 0.64 0.54 10 1000
0.0215 0.70 0.56 10 825
0.0215 0.70 0.56 10 825
0.0215 0.73 0.58 10 750
0.0215 0.73 0.58 10 750
0.0215 0.75 0.62 10 700
0.0215 0.75 0.62 10 700
0.0215 0.71 0.58 10 800
0.0215 0.71 0.58 10 800
0.0215 0.67 0.56 10 900
0.0215 0.67 0.56 10 900
0.0215 0.64 0.54 10 1000
0.0215 0.64 0.54 10 1000
0.0215 0.62 0.48 10 1050
0.0215 0.62 0.48 10 1050
0.0215 0.60 0.50 10 1100
0.0215 0.60 0.50 10 1100
0.0215 0.64 0.55 10 1100
0.0215 0.64 0.55 10 1100
0.0215 0.67 0.57 10 1100
0.0215 0.67 0.57 10 1100
0.0215 0.71 0.50 10 1100
0.0215 0.71 0.50 10 1100
0.0215 0.60 0.47 10 1100
0.0215 0.60 0.47 10 1100
0.0215 0.60 0.52 10 1100
0.0215 0.60 0.52 10 1100
0.0215 0.60 0.54 10 1100
0.0215 0.60 0.54 10 1100
0.0215 0.60 0.50 10 1100
0.0215 0.60 0.50 10 1100
0.0215 0.60 0.50 10 1100
0.0215 0.60 0.50 10 1100
0.0215 0.60 0.45 10 1100
0.0215 0.60 0.45 10 1100
0.0215 0.60 0.47 10 1105
0.0215 0.60 0.47 10 1105
0.0215 0.60 0.50 10 1100
0.0215 0.60 0.50 10 1100
0.0215 0.60 0.50 10 1100
0.0215 0.60 0.50 10 1100
0.0215 0.60 0.50 10 1100
0.0215 0.60 0.50 10 1100
0.0215 0.60 0.50 10 1100
0.0215 0.60 0.50 10 1100
0.0215 0.60 0.50 10 1100
0.0215 0.60 0.50 10 1100

```
0.0215  0.60    0.50   10     1100
0.0215  0.60    0.50   10     1100
```

Example 2b, Elliot Lake reactive transport input file for 1-D MINTOX simulation.

```
l-d elliot lake simulation          ;problem title
 1.0  0.5  0.0  1.0                 ;wp,wa,wb,leismann weighting terms
 0    1 . 0 0 0 1                   :kmas,ptime,kts,kiter,kbypass
 0    1    5    0    0             ;kprt,nprt,lprt,n1,n2
 12                                 ;pprtt(i),i=1,nprt
 1    1201    1                     ;nex,nez,nytyp,ngtyp
 0.1   6   1000                     ;xl,zl,conf
 0    0    0                       ;is 1,is2,nchs
 0    0    0    3                  ;kb(4), boundary codes
 0.0  -0.62                         ;vxl,vzl(units/yr)
 0.5 0.00 0.0.5 0.05                ;al,at,dd,por,dt(years)
 25.0  0.0  12  10 0                ;temp,fions,nnn,nr,nas
 0 0 3 0 4 0 0 0 0 0 0              ;ifl(11)
 0  0  0                           ;iads,numads,iabq
 1 2 1 121 -1                       ;ix1,ix2,iy1,iy2,more. define background
   150 1.44e-2 0.0 0                ;ca background chemistry idx,t,gx,stad
   460  2.30e-3 0.0  0              ;mg
   410  6.00e-3 0.0  0              ;k
   180  1.14e-3 0.0  0              ;cl
   030 2.59e-8 0.0 0                ;al
   732  3.125e-2 0.0  0             ;so4
   001 0.000e+00 -4.5 0             ;e
   281  1.477e-7  0.00              ;fe3
   140  3.589e-2 0.0 0              ;co3
   330  5.469e-2  -5.9  0           ;h
   280  5.388e-5 0.0 0              ;fe2
   770  1.914e-3  0.00              ;h4sio2
 3  3                               ;lty,lrx, solid & reaction values
2812800   0.0   0.0   0.0           ;fe2/fe3 idys,gks,dhs,cons
 0                                  ;nc,(idd,stoc)*nc
 4  2                               ;lty,lrx
5015001  0.0  0.0      0.070        ;calcite: idys,gks,dhs,cons
 2  150  1.00  140  1.00            ;nc,(idd,stoc)*nc
 4  2                               ;lyt,lrx
2003003  0.0  0.0      .045         ;gibbsite
 2  030  1.00  330  -3.00
 4  2
2077004  0.0   0.0  4.069e+01;amorphous silica
 1 770 1.00
 4  2
5028000   0.0   0.0  2.0e-2        ;siderite
 2 280 1.00 140 1 .OO
 4  2
2028100  0.0  0.0      1 .OOOe-6 ;ferrihydrite
 2281  1.00 330 -3.00
 4  2
6015001   0.0   0.0      .174      ;gypsum
 2 150 1.00 732 1 .00
 5  2
6041002  0.0  0.0      0.0         ; jarosite k
 5 330 -6.0 410 1.0 281 3.0 732 2.0 2 6.0
 4  2
2015000   0.0   0.0   0.10         ;lime
 3  330  -2.0  150  1.0  002  1.0   ;
 6  4
001    0.0     0.0     0.0         ;e
 0
 0                                  ;idnrx
 0                                  ;ntsn
 1 1 1 1 1 1 1 1 2 2 2 2 2 2 2      ;kplt(i), i=1,nnn
 1 2 3 4 5 6 7 8 8 8 8              ;kplts(i), i=1,nr
 0 0 0 0 0 0 0 0 0 1 1 0 0 0 0      ;kpnt, i=1,nnn
 0 1 0 0 1 0 0 0 0 0 0              ;kpnts,i=1,nr
1.000e-03 1.44e-2                   ;ca  tol,same*
```

```
1.000e-03 2.30e-3          ;mg
l.OOOe-03 9.00e-3          ;k
1 .000e-031.14e-3          ;cl
1.000e-03 2.595e-8         ;al
1.000e-03 3.125e-2         ;so4
1.000e-03 1 .000e+00       ;e
1.000e-03 1.400e-7         ;fe3
 1.00%03  3.589e-2         ;co3
1.000e-04 5.469e-2         ;h
1.000e-03 5.318e-5         ;fe2
1 .000e-031.938e-3         ;h4sio2
                           ;ntsc
                           ;ntb cauchy bdry flux, #bdry seg
0.31 1                     ;fbf,nbs (flux in units/yr)
  150 1.25e-2              ;ca cauchy influx idx,uin
  460 1.04e-3              ;mg  (influx  water)
  410 9.0e-3               ;k       "
  180  1.14-4              ;cl      "
  030 1.275-08             ;al      "
  732 7.479~03             ;so4     "
  001 0.000e-00            ;e   "       .
  281 2.317e-08            ;fe3     "
  140 3.936e-03            ;co3     "
  330 4.585e-03            ;h       "
  280 5.358~05             ;fe2     "
  770 1.938e-03            ;h4sio2  "
0.0 0.0 0.0 0.0 0.0        ;breakthrough node numbers
0.0 12.05 0.05 30          ;t0,t1,dt,maxit
                           ;oxflag (1=include oxidation)
0  0 1                     ;npadl,npadr,nec
10                         ;maxskip
```

The following plots are results from the 1-D Elliot lake simulation. The oxidation/diffusion results are not shown and only selected output is plotted. Also the measured field data from the field location modelled is shown as squares where available.

9. APPENDIX 3 - MINTOX 2-D SIMULATION

The following input files are for an Nickel Rim 2-D MINTOX simulation. File 3a is the diffusion input, and file3b is the reactive transport input.

Input tile 3a, Nickel Rim 2-D simulation diffusion input.

```
.5     2                                   ;fracyear,mineral
0.000075  0.99                             ;grain radius,starting radius(0-1)
1.50d-14                                   ;d2 for oxidized coating
1.0d-3      2.5  200                       ;dt,ptime,end time
    1.    51                               ;depth of unsat, number of nodes in unsat
  0.045  0.415  0.02     15  1550  ;       fracsulf,por,moisture cont.,temp,rhob
  0.045  0.415  0.06     14  1550
  0.045  0.415  0.085     13  1550
  0.045  0.415  0.11     12  1550
  0.045  0.415  0.135     11  1550
  0.045  0.415  0.16     10  1550
  0.045  0.415  0.19     10  1550
  0.045  0.415  0.21     10  1550
  0.045  0.415  0.22     10  1550
  0.045  0.415  0.22     10  1550
  0.045  0.415  0.2175     10  1550
  0.045  0.415  0.215     10  1550
  0.045  0.415  0.2125     10  1550
  0.045  0.415  0.21     10  1550
  0.045  0.415  0.215     10  1550
  0.045  0.415  0.236     10  1550
  0.045  0.415  0.26     10  1550
  0.045  0.415  0.29     10  1550
  0.045  0.415  0.32     10  1550
  0.045  0.415  0.323     10  1550
  0.045  0.415  0.328     10       1550      .
  0.045  0.415  0.329     10  1550
  0.045  0.415  0.3295     10  1550
  0.045  0.415  0.33     10  1550
  0.045  0.415  0.32     10  1550
  0.045  0.415  0.29     10  1550
  0.045  0.415  0.27     10  1550
  0.045  0.415  0.2625     10  1550
  0.045  0.415  0.26     10  1550
  0.045  0.415  0.2625     10  1550
  0.045  0.415  0.27     10  1550
  0.045  0.415  0.29     10  1550
  0.045  0.415  0.31     10  1550
  0.045  0.415  0.32     10  1550
  0.045  0.415  0.335     10  1550
  0.045  0.415  0.345     10  1550
  0.045  0.415  0.355     10  1550
  0.045  0.415  0.355     10  1550
  0.045  0.415  0.355     10  1550
  0.045  0.415  0.3555     10  1550
  0.045  0.415  0.355     10  1550
  0.045  0.415  0.353     10  1550
  0.045  0.415  0.351     10  1550
  0.045  0.415  0.35     10  1550
  0.045  0.415  0.353     10  1550
  0.045  0.415  0.355     10  1550
  0.045  0.415  0.355     10  1550
  0.045  0.415  0.355     10  1550
  0.045  0.415  0.3555     10  1550
  0.045  0.415  0.35     10  1550          .
  0.045  0.415  0.35     10  1550
  0.045  0.415  0.35     10  1550
```

Example 3b, Reactive transport input for Nickel Rim 2-D simulation.

```
2D Nickel Rim w/ox..March 17, 1995 - variable background chemistry
 1.0 0.5 0.0                                  ;WP,WA,WB,Leissman terms
 0 50.0 0 0 1                                 ;KMAS,PTIME,KTS,kiter,kbypass
 0 4 2 0 0                                    ;KPRT,NPRT,LPRT,N1,N2
 5.0 10.0 20.0 30.0                           ;PPRTT(I)
  258   100  2  3                            ;NEX,NEZ,NVTYP,NGTYP
3.500e+02 1.400E+01 1 .000e+03                ;XL,ZL,CONF
  0   0   0                                   ;IS1,IS2,NCHS
  0   0   0   3                               ;KB(4),BOUNDARY CODES
  0.  0.                                      ;vx,vz
5.000e+00 2.000E-02 5.046e-03 4.000e-01 0.05        ;AI,At,DD,POR,DT
10.0 0.0 14 10 00                             ;TEMP,FIONS,NNN,NR,NAS
 0 0 3 0 4 0 0 0 0 0 0                        ;IFL(11)
0  0  0                                       ;IADS,NUMADS,IABG
 1 145  1101  +1                              ;ix1,ix2,iy1,iy2 define background
   150 1.446E-02 0.0 0.0                      ;CA BACKGROUND CHEMISTRY IDX,T,GX,STAD
   460 2.067E-02 0.0 0.0                      ;MG          "
   500 1.093E-02 0.0 0.0                      ;NA          "
   410 5.140E-03 0.00.0                       ;K           "
    180 4.252E-04 0.0 0.0                     ;CL          "
    140 1.189E-02 0.0 0.0                     ;CO3         "
    732 2.938E-02 0.0 0.0                     ;SO4         "
    470 4.025E-05 0.0 0.0                     ;MN          "
    770 3.3 14E-04 0.0 0.0                    ;H4SIO4      "
    280 2.468E-05 0.0 0.0                     ;FE2         "
    281 1.249e-08 0.0 0.0                     ;FE3         "
   030 5.711E-09 0.0 0.0                      ;AL          "
    330 1.460E-02 -6.65 0.                    ;H           "
   0010.000E+00 -3.56 0.                      ;E           "
 3  3                                         ;LTY,LRX  SOLID & REACTION VALUES
2812800 0.0 0.0 0.0                           ;FE2/FE3 IDYS,GKS,DHS,CONS
 0                                            ;NC,(IDD,STOC)*NC
 4  2                                         ;LTY,LRX
5015001 0.000E+00 000.00 07.500E-02           ;CALCITE IDYS,GKS,DHS,CONS
 2 0000150 001.00 0000140 001.00              ;NC,(IDD,STOC)*NC
 5  2                                         ;LTY,LRX
2003003 0.000E+00 000.00 OO.OOOE-00           ;GIBSITE
 2   30  1.00   330   -3.00
 5  2
2077004 0.000E+00 000.00 00.000e+00           ;AMORPHOUS SILICA
 1   770   1.00
 5  2
5028000 0.0 0.0          0.000e-00            ;SIDERITE
 2   280   1.00   140   1.00
 5  2
2028100 0.0 0.0          0.000e-00            ;FERRIHYDRITE
 2   281  1.00   330   -3.00
 5  2
6015001 0.0 0.0 0.0                           ;GYPSUM
 2   150   1.00   732   1.00
 5  2
5047000 0.0 0.0 0.0                           ;RHODOCHROSIT
 2   470   1.00   140   1.00
 5  2
5046002 0.0 0.0 0.0                           ;MAGNESITE
 2   460   1.00   140   1.00
 6  4
  001 0.0 0.0 0.0                             ;e-
 0
 0                                            ;idnrx
146 259 1 101 -1                              ;define background
   150 1.446E-02 0.0 0.0                      ;CA BACKGROUND CHEMISTRY IDX,T,GX,STAD
   460 2.067E-02 0.0 0.0                      ;MG          "
   500 1.093E-02 0.0 0.0                      ;NA          "
   410 5.140E-03 0.00.0                       ;K           "
   180 4.252E-04 0.0 0.0                      ;CL          "
```

```
  140 1.189E-02 0.00.0                ;CO3          "
  732 2.938E-02 0.0 0.0               ;SO4          "
  470 4.025E-05 0.0 0.0               ;MN           "
  770 3.3 14E-04 0.0 0.0              ;H4SIO4       "
  280 2.468E-05 0.0 0.0               ;FE2          "
  281 1.249e-08 0.0 0.0               ;FE3          "
  030 5.711E-09 0.0 0.0               ;AL           "
  330 1.460E-02 -6.65 0.              ;H            "
  001 0.000E+00 -3.56 0.              ;E            "
 3  3                                 ;LTY,LRX   SOLID & REACTION VALUES
2812800  0.0  0.0  0.                 ;FE2/FE3 IDYS,GKS,DHS.CONS
 0                                    ;NC,(IDD,STOC)*NC
 4  2                                 ;LTY,LRX
5015001 0.000E+00 000.00 02.530E-02   CALCITE  IDYS,GKS,DHS,CONS
 2 0000150 001.00 0000140 001.00      ;NC,(IDD,STOC)*NC
 5  2                                 ;LTY,LRX
2003003 0.000E+00 000.00 00.000E-00   ;GIBSITE
 2   30   1.00   330   -3.00
 5  2                                 .
2077004 0.000E+00 000.00 00.000e+00   ;AMORPHOUS SILICA
 1   770   1.00
 5  2                                 .
5028000 0.0 0.0         0.000e-00     ;SIDERITE
 2   280   1.00   140   1.00
 5  2
2028100 0.0  0.0         0.000e-00    ;FERRIHYDRITE
 2   281   1.00   330   -3.00         ;.
 5  2
6015001  0.0  0.0  0.0                GYPSUM
 2   150   1.00   732   1.00
 5  2
5047000 0.0 0.0 0.0                   ;RHODOCHROSIT
 2   470   1.00   140   1.00
 5  2
5046002 0.0 0.0 0.0                   ;MAGNESITE
 2   460   1.00   140   1.00
 6  4
  001 0.0  0.0  0.0                   ;e-
 0                                    .
 0                                    ;IDNRX
 0                                    ;ntsn
 1 0 0 0 2 3 4 5 0 6 7 8 8 8 0 0      ;KPLT(I),I=1,NNN
 0 1 2 0 3 4 5 6 7 8 8 0              ;KPLTS(I),I=1,NR
 1 0 0 0 1 1 1 0 0 1 1 1 1 1 0 0      ;KPNT(I),I=1,NNN
 0 1 1 0 1 1 1 1 1 1 1 1 0            ;KPNTS(I),I=1,NR
1 .000E-021.446E-02                   ;CA   TOLERANCE AND RELATIVE VALUES
1.000E-02 2.067E-02                   ;MG           "
1.000E-02 1.093E-02                   ;NA           "
1 .000E-025.140E-03                   ;K            "
1.000E-02 4.252E-04                   ;CL           "
1.000E-02 1.189E-02                   ;CO3          "
1.000E-02 2.938E-02                   ;SO4          "
1.000E-02 4.025E-05                   ;MN           "
1.000E-02 3.314E-04                   ;H4SIO4       "
1.000E-02 2.468E-05                   ;FE2          "
1 .000E-021.249e-08                   ;FE3          "
1.000E-02 5.71 1E-09                  ;AL           "
1 .000E-021.460E-02                   ;H            "
1.000E-02 1 .000E+00                  ;E            "
                                      ;NTSC #OF CONSTANT TJME STEPS
  4                                   ;NTB,CAUCHY BDRY FLUX,#BDY SEG
0.268  101                            flux, NBS(# elements ON BDRY SEGMENT)
  150 1.183E-02                       ;CA CAUCHY  INFLUX  IDX,UIN
  460 1.935E-03                       ;MG       "
  500 1.305E-03                       ;NA       "
  410 6.651E-05                       ;K        "
  180 1.033E-03                       ;CL       "
  140 8.850e-03                       ;C03      "
  732 7.479e-03                       ;SO4      "
  470 4.73 1 E-05                     ;MN       "
  770 1.362E-03                       ;H4SIO4   "
```

```
  280 1.698E-05                    ;FE2      "
  281 1.186E-08                    ;FE3      "
  030 5.080E-09                    ;AL       "
  330 1.1 10E-02                   ;H        "
  001 0.000e-00                    ;E        "
0.000 22                           ;Flux, NBS(# elements ON BDRY SEGMENT)
  150 0.000E-03                    ;CA   CAIJCHY INFLUX IDX,UIN
  460  O.OOOE-03                   ;MG       "
  500 0.000E-03                    ;NA       "
  4 10 0.000E-05                   ;K        "
  180 0.000E-03                    ;CL       "
  140 o.OOOe-03                    ;C03      "
  732 0.000e-03                    ;SO4      "
  470 0.000E-05                    ;MN       "
  770 0.000E-03                    ;H4SIO2   "
  280 0.000E-05                    ;FE2      "
  281 0.000E-08                    ;FE3      "
  030 0.000E-07                    ;AL       "
  330 0.000E-03                    ;H        "
  001 0.000e-00                    ;E        "
0.063 22                           ;Flux,NBS(# elements ON BDRY SEGMENT)
  150 1.183E-02                    ;CA CALJCHY INFLUX IDX,UIN
  460 1.935E-03                    ;MG       "
  500 1.305E-03                    ;NA       "
  410 6.651E-05                    ;K        "
  180 1.033E-03                    ;CL       "
  140 8.850e-03                    ;C03      "
  732 7.479e-03                    ;SO4      "
  470 4.731E-05                    ;MN       "
  770 1.362E-03                    ;H4SIO4   "
  280 1.698E-05                    ;FE2      "
  281 1.186E-08                    ;FE3      "
  030 5.080E-09                    ;AL       "
  330 1.1 IOE-02                   ;H        "
  001 0.000e-00                    ;E        "
0.284 113                          ;NBS
  150 1.183E-02                    ;CA CALJCHY INFLUX IDX,UIN
  460 1.935E-03                    ;MG       "
  500 1.305E-03                    ;NA       "
  410 6.651E-05                    ;K        "
  180 1.033E-03                    ;CL       "
  140 8.850e-03                    ;C03      "
  732 7.479e-03                    ;SO4      "
  470 4.731E-05                    ;MN       "
  770 1.362E-03                    ;H4SIO4   "
  280 1.698E-05                    ;FE2      "
  281 1.186E-08                    ;FE3      "
  030 5.080E-09                    ;AL       "
  330 1.110E-02                    ;H        "
  001 0.000e-00                    ;E        "
 18664 18634 13872 110595060       ;breakthrough node numbers
0.000E+00 30.00E+00  0.05  30      ;T0,T1,DT,MAXIT
1                                  ;oxflag 1=include oxidation
 1460 5                            ;npadl,npadr,nec
25                                 ;maxskip
```

Some of the results from the 2-D simulation are plotted as follows

10. APPENDIX 4 - GEOCHEMICAL DATABASE

The database files used by MINTOX and their analogous MINTEQA2 files are:

MINTOX	MINTEQA2
alk.dbm	alk.dbs
analy.dbm	analyt.dbs
error.dbm	error.dbs
compcp.dbm	comp.dbs
type6cp.dbm	type6.dbs
thermcp.dbm	thermo.dbs

Redox and gas reactions can be included in type6cp.dbm and thermcp.dbm database files within MINTOX and thus do not have their own database files. Modifications to these database files can be made relatively easily. They are in ascii format and the format/unformat routine necessary when modifying MINTEQA2 database files is not needed.

To add a component to the databases edit the compcp.dbm tile and insert the new component in the same format as in the comp.dbs MINTEQA2 file. To add reactions, add the reaction to both the type6cp.dbm and the thermcp.dbm files in the same format as the reaction occurs in the MINTEQA2 database files. The MINTOX program does not need to be recompiled when changes are made to the database files.

1 .l Running PYROX

The PYROX model is relatively easy to use, and runs very quickly. It is however, necessary to have the required input data including: porosity, moisture content, weight percent sulfur as sulfide, bulk density, temperature, particle size, and measurements of O_2 concentrations in the porespace.

Once an input file is set up the program can be run. The input file must have the extension '.dat,' and the output file will have the extension '.out'.

From the directory, that PYROX is stored in, type

PYROX <enter>

The program will then prompt you for the input file name. Enter the filename *without* the '.dat' extension. The program runs, printing out results at the print time interval given in the input file. The program runs until all sulfide minerals have oxidized, or the endtime is reached. For an example run see the Examples Appendix at the end of this manual.

I.*2 Diffusion/oxidation files*

PYROX results must be matched to results seen in the field, or at least checked to see that the rates of oxygen diffusion and sulfide mineral oxidation are realistic. The main reason for this "reality check" is that the oxidation process is extremely sensitive to the moisture content in the unsaturated zone. If the moisture content was measured during an exceptionally dry time, or following a rainfall event, the steady state diffusion results calculated would be completely unrealistic. It is essential that the moisture content profile input is representative of the average moisture content during the months that oxidation occurs.

A summarized PYROX input file is shown below. The filename must have the '.dat' extension. Following the input files, the individual terms in the files are defined. Note that the parameters are free format, so column spacing is not important, as long as there is at least one space between entries.

```
2     0     0                                   ;mineral,fracni,fraczn
0.000075  0.99                                  ;grain radius[m],starting radius(0-1)
1.50d-14                                        ;D2 for oxidized coating[m2/s]
1.Od-2      2.5    200                          ;dt[yr],ptime,end time
1.    51                                        ;depth of unsat.[m],# nodes in unsat
0.025  0.415  0.020     15  1550                ;fracsulf,por,mois.cont.,temp[C],rhob[kg/m3]
0.025  0.415  0.060     14  1550
0.025  0.415  0.085     13  1550
                .
                .
                .
0.025  0.415  0.350     10  1550
```

Definition of terms:

LINE 1.

mineral - defines the sulfide mineral that is oxidizing. l=pyrite, 2=pyrrhotite. Note: any other input here will halt program and print message.

fracni - fraction of nickel present in the sulfide mineral as an impurity. The program calculates how much nickel is released as the sulfide mineral oxidizes. Note: this option not yet available in MINTOX

fraczn - Same as above only for zinc.

LINE2

grain - this is the radius of the sulfide mineral grains in metres.

starting radius- the starting position for the radius of the unreacted cores. The value is normalized such that a value of 1 would mean the particles are completely unreacted and a value of zero would mean completely oxidized. The shrinking core model requires that this value be less that one. Usually 0.99 or greater works fine. In extreme cases the value may have to be reduced to 0.98 or lower.

LINE3

D2 - diffusion coefficient for the oxidized coating forming on the sulfide mineral grains. Since this value cannot be easily measured, it is essentially a fitting parameter. Units are m^2/s.

LINE4

dt - time step in years. l.Od-2 usually works. Should be at least an order of magnitude smaller than the time step used in the reactive transport section.

ptime - print time in years. ie. 5 means output is printed every 5 years.

end time - in years. Program will run until end time is reached or all sulfide minerals have oxidized which ever comes first.

LINE5

depth - depth of unsaturated zone in metres.

#nodes - this is the number of nodes being modelled in the unsaturated zone.

LINE 6 to LINE (6 + # nodes-l)

fracsulf - fraction of bulk density that consists of sulfide in the form of sulfide minerals.

por - porosity of tailings.

mois. cont. - volumetric moisture content of tailings.

Note: Ideally if this value is equal to the porosity the medium is fully saturated. However due to limitations in the empirical formula used to calculate the bulk diffusion coefficient, this value may never be greater that 0.06 less than the porosity or the program will bomb. example - if the porosity of the medium is 0.40, then the maximum allowable moisture content is 0.34, even if the medium is fully saturated. This should not cause problems for the majority of cases.

temp calculated - temperature in degrees Celsius. The diffusion coefficient is a function of temperature.

rhob - bulk density of the tailings in kg/m^3.

2. APPENDIX 1 - PYROX SIMULATION

The first example is an input file for PYROX.

Example 1, input file for PYROX model. This style of input file is used when PYROX is run as a stand alone model.

```
1  0  0                                          ;mineral,fracni,fraczn
0.000070  0.99                                   ; grain radius[m],starting radius(0-1)
.ld-13                                           ; D2 for oxidized coating[m2/s]
l.d-2  10  20                                    ;dt[yr],ptime,end time
1.500  2 6                                       ; depth of unsat.[m],# nodes in unsat
0.0108  0.50  0.300   15    1375                 ;fracsulf,por,mois.cont.,temp[C],rhob[kg/m3]
0.0108  0.50  0.300   15    1375
0.0108  0.50  0.300   10    1375
0.0108  0.50  0.320   10    1375
0.0108  0.50  0.330   10    1375
0.0108  0.50  0.340   10    1375
0.0108  0.50  0.350   10    1375
0.0108  0.50  0.360   10    1375
0.0108  0.50  0.375   10    1375
0.0108  0.50  0.382   10    1375
0.0108  0.50  0.386   10    1375
0.0108  0.50  0.390   10    1375
0.0108  0.50  0.400   10    1375
0.0108  0.50  0.405   10    1375
0.0108  0.50  0.410   10    1375
0.0108  0.50  0.415   10    1375
0.0108  0.50  0.419   10    1375
0.0108  0.50  0.423   10    1375
0.0108  0.50  0.427   10    1375
0.0108  0.50  0.430   10    1375
0.0108  0.50  0.432   10    1375
0.0108  0.50  0.434   10    1375
0.0108  0.50  0.436   10    1375
0.0108  0.50  0.438   10    1375
0.0108  0.50  0.439   10    1375
0.0108  0.50  0.440   10    1375
```

The following is the output from simulation 1.

```
sulfide mineral is PYRITE                    .
 input file name is sim2dp.dat

 particle radius a = 0.000070   initial radius rstart = 0.990000

 no. intervals 26 print time 10.00 time step 0.01000
-------------------------------------------------------------------
 element  diff. coef airfilled porosity   fracsulf

   1     0.8437E-06      0.200000        0.0108
   2     0.8328E-06      0.200000        0.0108
   3     0.7309E-06      0.190000        0.0108
   4     0.6028E-06      0.175000        0.0108
   5     0.5231E-06      0.165000        0.0108
   6     0.4482E-06      0.155000        0.0108
   7     0.3781E-06      0.145000        0.0108
   8     0.2974E-06      0.132500        0.0108
   9     0.2332E-06      0.121500        0.0108
  10     0.2035E-06      0.116000        0.0108
  11     0.1830E-06      0.112000        0.0108
  12     0.1493E-06      0.105000        0.0108
  13     0.1164E-06      0.097500        0.0108
  14     0.9631E-07      0.092500        0.0108
  15     0.7785E-07      0.087500        0.0108
  16     0.6265E-07      0.083000        0.0108
  17     0.5029E-07      0.079000        0.0108
  18     0.3908E-07      0.075000        0.0108
  19     0.3024E-07      0.071500        0.0108
  20     0.2451E-07      0.069000        0.0108
  21     0.2029E-07      0.067000        0.0108
  22     0.1640E-07      0.065000        0.0108
  23     0.1286E-07      0.063000        0.0108
  24     0.1044E-07      0.061500        0.0108
  25     0.8942E-08      0.060500        0.0108
-------------------------------------------------------------------

 time is 10.000 years
depth    o2     bdry   frac.   so4-2   h+     fe+2   ni+2   zn+2
 (m)    conc.  pstn    rxtd     kg     kg      kg     kg     kg
0.030  0.9949 0.4307  0.9201  2.377  0.025  0.691  0.000  0.000
0.090  0.9848 0.4393  0.9152  2.364  0.025  0.687  0.000  0.000
0.150  0.9743 0.4478  0.9102  2.350  0.025  0.683  0.000  0.000
0.210  0.9624 0.4572  0.9044  2.335  0.024  0.679  0.000  0.000
0.270  0.9488 0.4676  0.8977  2.317  0.024  0.674  0.000  0.000
0.330  0.9336 0.4787  0.8903  2.297  0.024  0.668  0.000  0.000
0.390  0.9164 0.4908  0.8817  2.274  0.024  0.661  0.000  0.000
0.450  0.8961 0.5046  0.8714  2.247  0.024  0.653  0.000  0.000
0.510  0.8715 0.5206  0.8588  2.213  0.023  0.643  0.000  0.000
0.570  0.8434 0.5383  0.8439  2.173  0.023  0.632  0.000  0.000
0.630  0.8134 0.5564  0.8276  2.130  0.022  0.619  0.000  0.000
0.690  0.7804 0.5755  0.8092  2.081  0.022  0.605  0.000  0.000
0.750  0.7417 0.5971  0.7869  2.021  0.021  0.588  0.000  0.000
0.810  0.6972 0.6209  0.7603  1.950  0.020  0.567  0.000  0.000
0.870  0.6473 0.6467  0.7292  1.867  0.020  0.543  0.000  0.000
0.930  0.5912 0.6746  0.6925  1.769  0.019  0.514  0.000  0.000
0.990  0.5289 0.7048  0.6494  1.654  0.017  0.481  0.000  0.000
1.050  0.4598 0.7375  0.5982  1.517  0.016  0.441  0.000  0.000
1.110  0.3836 0.7732  0.5370  1.354  0.014  0.394  0.000  0.000
1.170  0.3039 0.8107  0.4663  1.165  0.012  0.339  0.000  0.000
1.230  0.2265 0.8481  0.3891  0.959  0.010  0.279  0.000  0.000
1.290  0.1555 0.8843  0.3075  0.742  0.008  0.216  0.000  0.000
1.350  0.0943 0.9187  0.2240  0.519  0.005  0.151  0.000  0.000
1.410  0.0485 0.9484  0.1464  0.311  0.003  0.091  0.000  0.000
1.470  0.0242 0.9675  0.0943  0.172  0.002  0.050  0.000  0.000
            so4 produced =     43.159 kg
            fe produced =      12.546  kg
            h+ produced =       0.453 kg
```

ni+2 produced = 0.000 kg
zn+2 produced = 0.000 kg

total so4 from start = 43.159 kg
total fe from start = 12.546 kg
total h+ from start = 0.453 kg
total ni+2 from start = 0.000 kg
total zn+2 from start = 0.000 kg

time is 20.000 years

depth (m)	02 conc.	bdry pstn	frac. rxtd	so4-2 kg	h + kg	fe+2 kg	ni+2 kg	zn+2 kg
0.030	0.9981	0.0000	1.0000	0.213	0.002	0.062	0.000	0.000
0.090	0.9941	0.0000	1.0000	0.226	0.002	0.066	0.000	0.000
0.150	0.9899	0.0000	1.0000	0.240	0.003	0.070	0.000	0.000
0.210	0.9849	0.0000	1.0000	0.255	0.003	0.074	0.000	0.000
0.270	0.9791	0.0000	1.0000	0.273	0.003	0.079	0.000	0.000
0.330	0.9722	0.0000	1.0000	0.293	0.003	0.085	0.000	0.000
0.390	0.9642	0.0000	1.0000	0.316	0.003	0.092	0.000	0.000
0.450	0.9544	0.0000	1.0000	0.343	0.004	0.100	0.000	0.000
0.510	0.9418	0.0000	1.0000	0.377	0.004	0.110	0.000	0.000
0.570	0.9267	0.0574	0.9992	0.415	0.004	0.121	0.000	0.000
0.630	0.9098	0.1430	0.9967	0.452	0.005	0.131	0.000	0.000
0.690	0.8903	0.1958	0.9921	0.488	0.005	0.142	0.000	0.000
0.750	0.8663	0.2447	0.9849	0.529	0.006	0.154	0.000	0.000
0.810	0.8375	0.2926	0.9745	0.572	0.006	0.166	0.000	0.000
0.870	0.8036	0.3399	0.9601	0.616	0.006	0.179	0.000	0.000
0.930	0.7637	0.3881	0.9408	0.663	0.007	0.193	0.000	0.000
0.990	0.7170	0.4377	0.9153	0.710	0.007	0.206	0.000	0.000
1.050	0.6621	0.4897	0.8815	0.756	0.008	0.220	0.000	0.000
1.110	0.5978	0.5452	0.8366	0.800	0.008	0.232	0.000	0.000
1.170	0.5258	0.6028	0.7795	0.836	0.009	0.243	0.000	0.000
1.230	0.4503	0.6600	0.7109	0.859	0.009	0.250	0.000	0.000
1.290	0.3744	0.7158	0.6316	0.865	0.009	0.251	0.000	0.000
1.350	0.3015	0.7694	0.5430	0.852	0.009	0.248	0.000	0.000
1.410	0.2400	0.8160	0.4557	0.826	0.009	0.240	0.000	0.000
1.470	0.2032	0.8450	0.3965	0.807	0.008	0.235	0.000	0.000

so4 produced = 13.580 kg
fe produced = 3.948 kg
h+ produced = 0.142 kg
ni+2 produced = 0.000 kg
zn+2 produced = 0.000 kg

total so4 from start = 56.739 kg
total fe from start = 16.494 kg
total h+ from start = 0.595 kg
total ni+2 from start = 0.000 kg
total zn+2 from stan = 0.000 kg

****
**********tt**********

#####progress of reaction front #####

depth	time of reaction front arrival
0.000	16.410
0.060	16.670
0.120	16.930
0.180	17.210
0.240	17.530
0.300	17.880
0.360	18.280
0.420	18.730
0.480	19.270
0.540	19.930
0.600	0.000
0.660	0.000
0.720	0.000
0.780	0.000
0.840	0.000
0.900	0.000

0.960	0.000
1.020	0.000
1.080	0.000
1.140	0.000
1.200	0.000
1.260	0.000
1.320	0.000
1.380	0.000
1.440	0.000
1.500	0.000

The following plots show the oxygen concentration profile and the amount of sulfide remaing from this simulation. These plots should be compared to field date to ensure that the results are realistic.

1.